University of Southern Queensland

Faculty of Engineering and Surveying

Dynamic Characterisation of Cellular Cores and Sandwich Beams

A dissertation submitted by

Haydn O'Leary

in fulfilment of the requirements of

Courses ENG4411 and 4412 Research Project

towards the degree of

Bachelor of Engineering (Civil)

October 2012

University of Southern Queensland

Faculty of Engineering and Surveying

ENG4111 Research Project Part 1 &
ENG4112 Research Project Part 2

Limitations of Use

The Council of the University of Southern Queensland, its Faculty of Engineering and Surveying, and the staff of the University of Southern Queensland, do not accept any responsibility for the truth, accuracy or completeness of material contained within or associated with this dissertation.

Persons using all or any part of this material do so at their own risk, and not at the risk of the Council of the University of Southern Queensland, its Faculty of Engineering and Surveying or the staff of the University of Southern Queensland.

This dissertation reports an educational exercise and has no purpose or validity beyond this exercise. The sole purpose of the course pair entitled "Research Project" is to contribute to the overall education within the student's chosen degree program. This document, the associated hardware, software, drawings, and other material set out in the associated appendices should not be used for any other purpose: if they are so used, it is entirely at the risk of the user.

Professor Frank Bullen

Dean

Faculty of Engineering and Surveying

CERTIFICATION

I certify that the ideas, designs and experimental work, results, analyses and conclusions set out in this dissertation are entirely my own effort, except where otherwise indicated and acknowledged.

I further certify that the work is original and has not been previously submitted for assessment in any other course or institution, except where specifically stated.

Student Name
Student Number:

_____
Signature

_____
Date

Abstract

If the use of sandwich panels in the construction industry is going to continue to increase, it is essential that a low-cost and efficient method of material characterisation is established. This project has investigated using vibration tests to perform dynamic characterisation of sandwich panels and cellular cores. This has involved attempting to identify the natural frequency of the material in order to use the Euler equation for beams to calculate the modulus of elasticity.

The modulus of elasticity and shear modulus have been determined using the four point bending test, in order to compare these with the values calculated from the vibration tests. The values for the modulus of elasticity calculated using the identified natural frequencies are not the values which were expected for the material. These calculated values are considerably less than the expected values which suggest there has been an error in the experimentation.

This error is thought to be caused by the weight of the accelerometer and the attached chord having a large influence on the natural frequency of the system. The modulus of elasticity has been successfully determined for the steel samples which have been used as a benchmark, however these are considerably heavier than the sandwich panels which means the weight of the accelerometer has little effect.

With this in mind it has been found that this experiment using the accelerometer used is not suitable for the dynamic characterisation of sandwich panels and cellular core. Investigation is required to determine if this test can be used for dynamic characterisation of sandwich panels and cellular cores if a non-contact measuring technique, such as a laser vibrometer is used.

Acknowledgements

I would like to take this opportunity to acknowledge my supervisor, Dr Sourish Banerjee for their guidance and wisdom throughout this difficult project. His advice, patience and understanding of the project has been invaluable throughout the course. I am sincerely appreciative of his assistance in completing this project.

I must also thank Dr. Jayantha Epaarachchi for his technical assistance with using the LMS test express program. Also a sincere thankyou must be given to Mr Ernesto Guades for his assistance with the LMS Test Express software and with the hardware used for the measurements.

I must also acknowledge Eris Supeni for his assistance during the testing in the P2 Laboratory. I massive thank you must also be given to Daniel McCallum for providing the results for the four point bending test.

Finally, I must thank Mr Nicholas Keats for manufacturing the frame from which the samples were hung for testing, for which he supplied both the material and labour completely free of charge.

Table of Contents

CERTIFICATION iii

Abstract iv

Acknowledgements v

Table of Figures ix

List of Tables xiii

Nomenclature xiv

1. Introduction 1

1.1 Project Objectives 1

1.2 Environmental Implications 2

1.3 Safety 2

1.4 Resource Analysis 3

2. Background Information 4

3. Related Literature 5

3.1 Sandwich Beams 5

3.2 Young's Modulus 5

3.3 Vibration Theory 6

3.4 Using Timoshenko's Beam Theory to determine materiel properties 6

3.5 Methods for determining material properties 9

3.6 Dynamic characterisation of high damping viscoelastic materials 14

3.7 Euler Equation for Beams 17

3.8 Determining natural frequencies 19

3.9 Fourier Transform Function 21

3.10 Interpreting Frequency Response Diagrams 22

3.11 Determining out-of-plane shear modulus from dynamic test 23

4. Project Methodology 25
4.1 Experimental equipment specifications and setup 25
4.2 Specimen preparation 27
4.3 Experimental Setup 28
4.4 Performing the test 30
4.5 Data Handling 31
4.6 Four point bending test 32
5. Results and Discussion 34
5.1Four Point Bending Test Results 34
5.1.1 40mm Aluminium Skin Samples 34
5.1.2 40mm Fibreglass Skin Samples 36
5.2 Dynamic Characterisation of Steel Samples 38
5.2.1 Long steel sample 38
5.2.2 Short steel sample 43
5.3 Dynamic characterisation of sandwich panels 47
5.3.1 Sandwich panel sample 1 – 20mm with Aluminium skins 47
5.3.2 Sandwich Panel 2 – 20mm with Aluminium Skins 50
5.3.3Sandwich panel sample 3 – 40mm with Aluminium sample 56
5.3.4 Sandwich Panel 4 – 40mm with Aluminium Skins 58
5.3.5 Sandwich Panel Sample 5 – 20mm Sample with Fibreglass skins 61
5.3.6 Sandwich Panel 6 – 20mm sample with fibreglass skins 63
5.3.7 Sandwich Panel 7 – 40mm Sandwich Panel with Fibreglass skins 66
5.3.8 Sample 8 – 40mm Sample with fibreglass skins 68
5.4 Dynamic characterisation of honeycomb cores 71
5.4.1 Sample 9 – 40mm Nida core with no skins 71
5.4.2 Sample 10 – 40mm Nida core with no skins 75
5.5 Alternate method of calculation 77

5.6 Summary of Results 77
6. Conclusion 79
7. Future Work 80
8. References 81
Appendix A 83

Table of Figures

Figure 1 Dynamic test specimen with impact locations and accelerometers (excitation in y) (Schwingshackl et al. 2006).....10
Figure 2 Impulse/response test set-up for cantilever-beam specimen (Gibson, R. F. 2000) 13
Figure 3 Typical frequency/response function for impulse test of composite specimen (Gibson, R. 2000).....14
Figure 4 Modulus and phase of transfer function for metallic beam regarding transverse displacement at the free end.....16
Figure 5 Modulus and phase of transfer functions of CLD beam regarding the transverse direction of the free end (Martinez-Agirre 2011) 17
Figure 6 An element of a beam used to derive the Euler equation for beams (Thompson 1988).....17
Figure 7 Expected force spectrum for impact of stiff steel mass with impact hammer 21
Figure 8 Example of the shape of frequency response function 23
Figure 9 The frontend system used to collect the data. The accelerometer is plugged into channel 1 and the impulse hammer is plugged into channel 2. 25
Figure 10 The PCB086C04 impulse hammer which was used to excite the system .26
Figure 11 A aluminium skinned sandwich panel suspended in the free-free conditions 29
Figure 12 The complete apparatus setup.....30
Figure 13 Set-up of four point bending test (Nakamura 2007).....32
Figure 14 Results from the four point bending test for a 40mm sample with aluminium skins 35
Figure 15 Results from the four point bending test for a 40mm sample with aluminium skin.....35
Figure 16 Results from the four point bending test for a 40mm sample with aluminium skins 36
Figure 17 Results from the four point bending test for a 40mm sample with fibreglass skins 37

Figure 18 Results from the four point bending test for a 40mm sample with fibreglass skins 37
Figure 19 Results from the four point bending test for a 40mm sample with fibreglass skins 38
Figure 20 It can be seen from this graph that all traces have a similar shape, it is very hard to find the first natural frequency, however, the second, third, fourth and fifth can be easily read from the graph. 39
Figure 21 The phase plot of the FRF for the long steel sample using the stainless steel tip 39
Figure 22 The frequency response function for the longer steel sample using the medium hard white plastic tip. The lower natural frequencies were able to be captured better using the white tip. 42
Figure 23 The phase plot of the FRF for the long steel sample using the medium hard white tip 42
Figure 24 Frequency response function for the shorter steel sample when excited with the very hard stainless steel tip. The stainless steel tip tests shows very clearly the two natural frequencies within range. 43
Figure 25 The phase plot for the FRF of the short steel sample using the very hard stainless steel tip 44
Figure 26 The white plastic tip shows the first natural frequency very well, however fails to excite the second natural frequency 45
Figure 27 The phase plot of the FRF for the small steel sample using the medium hard white tip 46
Figure 28 Frequency Response Function for Sandwich Panel 1 over a sample bandwidth of 6400 Hz. The first natural frequency can be seen quite easily at about the 1000 Hz mark. There may also be a natural frequency at the 1700 Hz mark 47
Figure 29 Frequency Response Function for sandwich panel 1 over a sample bandwidth of 3200 Hz 48
Figure 30 The phase plot of the FRF for sample 1 48
Figure 31 Frequency Response Function for sandwich panel 2 over a sample bandwidth of 3200 Hz 51
Figure 32 The phase plot of the FRF for sample 2 51
Figure 33 Alternate Frequency Response Function for sandwich panel 2 over a sample bandwidth of 3200 Hz. 52

Figure 34 The phase plot of the FRF for sample 2 53
Figure 35 The time response for the three tests shown in Figure 31 54
Figure 36 The time response for the three tests shown in Figure 33 55
Figure 37 Frequency Response Function for sandwich panel 3 over a sample bandwidth of 6400 Hz. It is clear from this diagram that there is a natural frequency at around 1300 Hz, it is unclear whether this is the first natural frequency or if there is a lower one around 250 Hz. I think the initial peak is just due to the elasticity of the string. 56
Figure 38 Frequency Response Function for sandwich panel 3 over a sample bandwidth of 3200 Hz. 57
Figure 39 The phase plot of the FRF for sample 3 57
Figure 40 Frequency Response Function for sandwich panel 4 over a sample bandwidth of 3200 Hz 59
Figure 41 The phase plot of the FRF for sample 4 60
Figure 42 Frequency Response Function for sandwich panel 5 over a sample bandwidth of 6400 Hz. The first natural frequency can be easily seen, others not excited at all 61
Figure 43 Frequency Response Function for sandwich panel 5 over a sample bandwidth of 3200 Hz 62
Figure 44 The phase plot of the FRF for sample 5 63
Figure 45 Frequency Response Function for sandwich panel 6 over a sample bandwidth of 3200 Hz. 64
Figure 46 The phase plot of the FRF for sample 6 64
Figure 47 Frequency Response Function of sandwich panel 7 over a sample bandwidth of 6400 Hz. Only one natural frequency can be seen easily. 66
Figure 48 Frequency Response Function for sandwich panel 7 over a sample bandwidth of 3200 Hz. 67
Figure 49 The phase plot of the FRF for sample 7 67
Figure 50 Frequency Response Function for sandwich panel 8 over a sample bandwidth of 3200 Hz. 69
Figure 51 The phase plot of the FRF for sample 8 69
Figure 52 Alternate Frequency Response Function for sandwich panel 8 over a sample bandwidth of 3200 Hz. 70
Figure 53 The phase plot of the FRF for sample 8 70

Figure 54 Frequency Response Function for Nida core sample 9 over a sample bandwidth of 2000 Hz. 72
Figure 55 The phase plot of the FRF for sample 9 72
Figure 56 Frequency Response Function for 0ne trace of Nida core sample 9 over a sample bandwidth of 2000 Hz. 73
Figure 57 Frequency Response Function for Nida core sample 10 over a sample bandwidth of 2000 Hz. 75
Figure 58 The phase plot of the FRF for sample 10 76

List of Tables

Table 1 Values of α_n based on the mode number and boundary conditions 9
Table 2 Values for $\beta_n l^2$ for each of the first five modes of vibration (Young 1989) .19
Table 3 Summary of the steel sample properties 27
Table 4 Summary of the sandwich panel and core properties 28
Table 5 Measured natural frequencies for the long steel sample 40
Table 6 Modulus of Elasticity for first five modes of vibration 41
Table 7 Measured natural frequencies for the short steel sample 44
Table 8 Calculated modulus of elasticity for short steel sample.....46
Table 9 Measured natural frequencies for sample 1 49
Table 10 Calculated modulus of elasticity for sample 1 49
Table 11 Comparison of natural frequencies read from graphs 55
Table 12 The modulus of elasticity (GPa) calculated 55
Table 13 Measured natural frequencies and calculated modulus of elasticity for sample 3 58
Table 14 Measured natural frequencies and calculated modulus of elasticity for sample 4 60
Table 15 Measured natural frequencies and calculated modulus of elasticity for sample 5 63
Table 16 Measured natural frequencies and calculated modulus of elasticity for sample 6 65
Table 17 Identified natural frequencies and calculated modulus of elasticity for sample 7 68
Table 18 Measured natural frequencies and calculated modulus of elasticity for sample 8 71
Table 19 Measured natural frequencies and calculated modulus of elasticity for sample 9 74
Table 20 Measured natural frequencies and calculated modulus of elasticity for sample 10 76
Table 21 Comparison of results using Euler's beam theory and Nilsson's equation.77

Nomenclature

A = Area of cross section

a_c = length of the block

α = rotation of the cross section with respect to x and t

β_n depends on the boundary conditions of the problem

c: Core thickness

D: Bending stiffness

d: Sandwich thickness

$d_{(t,x)}$ = lateral displacement with respect to x and t

Δ: Total beam mid-span deflection

E = Young's Modulus

f_n = frequency of n^{th} mode (Hz)

G = shear modulus

h_C = height of the core

h_m=height of the block

I = moment of inertia of beam about its neutral axis

I_{mx}, I_{my}= Moments of inertia of the block

k = shear factor for the cross section

L = beam length

λ_n = eigenvalue for nth mode, which depends on boundary conditions

m = mass of the block

P: Applied Force

ρ= mass density of beam material

ρ_l is the mass per unit length of the beam

w: sandwich width

ω_n is the n^{th} natural frequency of the system in radians per second

ω_x, ω_y, ω_z= natural frequencies measured in different directions

1. Introduction

The use of sandwich structures is increasing at a rapid rate in the engineering and manufacturing world. There is especially substantial growth in this area, in applications where weight saving is a major advantage. (Mujika et al. 2011) One such example is in aerospace design, where in addition to the light weight, they also possess favourable properties such as higher strength, damage tolerance and thermal resistance. (Sadowski & Bęc 2011) However, whilst the use of these materials is common in the aeronautical industry, they are yet to take off for infrastructure applications. This is largely due the key issue which needs to be resolved, which is the reduction of manufacturing costs.

Sandwich panels are made up of three distinct parts. These are two face sheets, such as aluminium and glass skins, a core material, usually a honeycomb or cellular core, and possibly filling material in the core. (Sadowski & Bęc 2011) The skins are attached to the core using a resin or adhesive. The three different samples used in this experiment will be Nida polymeric honeycomb cores with no skins, and sandwich beams constructed from these cores with aluminium or glass skins.

1.1 Project Objectives

The aim of this project is to determine the natural frequencies for cellular cores and sandwich beams, in an attempt to characterise their dynamic behaviour and calculate their elastic properties.

This project has a number of objectives which will attempt to be met, these include:

1. Research the background information relating to the cellular cores and sandwich beams, and the dynamic characterisation of materials
2. Measure out-of-plane dynamic properties of polymeric honeycomb and foam core materials
3. Measure dynamic characteristics of sandwich beams with various skins
4. Characterise dynamic behaviour and calculate elastic properties
5. Conduct four point bending test on 40mm sandwich panels.
6. Compare results from dynamic test and four point bending test.

1.2 Environmental Implications

This project has no real ethical issues associated with the work being undertaken. The effect that this work may have on safety is also a very tenuous link. However, if successful this project will result in a far more simple and cost effective method to characterise the mechanical properties of sandwich panels.

This may result in more efficient quality control, which will result in a safer end product through greater certainty of the material properties. This will have a positive effect on sustainability, as more accurate values for the material properties will be known, which may prevent structures from being over designed. This work also has a positive sustainable effect as it may promote the use of sandwich panels as an alternative to other finite materials. This work may also mean that large frames currently used for these analyses may not be required which will save the material used to manufacture these.

In order to protect the environment, disposal method of the material once the testing is completed must also be considered. As the dynamic test is non-destructive, the material could be recycled and reused for future testing.

1.3 Safety

There is very little risk of injury when undertaking the project work. All of the materials and apparatus used are lightweight and therefore if dropped will not cause an injury. There will not be any PPE required to undertake the experiment. There is a minor risk that equipment such as the accelerometers or instrument hammer may be damaged if not treated carefully. This will require care to be taken to ensure that this does not happen. Large clamps are being used to hold the frames in place, and these will need to be attached with the extension of these clamps facing down so that someone does not fall and impale themselves on these.

Electricity is also being used to charge the frontend system and the laptop, so care needs to be taken not to be electrocuted. All chords should be kept dry and should be tested and tagged by the universities licensed contractor. Power points should also be turned off when plugging in or unplugging a chord. The Nida core with no skins was cut using a jigsaw, care was taken to ensure that injury was not caused by the blade

coming into contact with any body parts. Steel cap boots should also be warn during testing in case something heavy drops onto your foot.

1.4 Resource Analysis

The materials for testing were the main resource which needed to be organised prior to starting this project. The Sandwich Panels and Nida-Core were obtained by my supervisor Dr. Sourish Banerjee from Auckland. The steel samples which were used as a benchmark were manufactured by a university technician in the university workshop.

The accelerometer, impulse hammer and frontend system were available in the P2 laboratory. The LMS Testxpress program was downloaded onto my personal laptop which was used for all of the testing. The dongle required for the program has been obtained from the P2 laboratory. Limited technical support on the computer software has been available from Dr. Jayantha Epaarachchi and PhD student Ernesto Guades.

The frame to suspend the samples was manufactured by a friend of mine, and I purchased the poly wire from Bowdler English and Wehl. Various other tools were available at the Centre for Excellence in Engineered Fibre Composites as required.

2. Background Information

Knowledge of mechanical properties is not only essential for design, testing of the elastic properties in the manufacturing or construction stage can also be advantageous to the quality control. Gibson found that vibration testing can provide a basis for fast, low-cost characterisation of elastic and viscoelastic properties of composites. (Gibson, R. F. 2000)

This paper will attempt to determine the out-of-plane elastic properties of sandwich beams consisting of Nida Honeycomb Cores by conducting a simple vibration test to characterise the dynamic behaviour of the material. There has been quite a lot of work undertaken in the area of using vibration and static testing to determine elastic properties of materials, and in particular, sandwich panels, and this has been discussed below.

Gibson(2000) estimated that the approximate cost to conduct a complete composite material property characterisation based on the Automotive Composites Consortium manual of test procedures is about $30,000. (Gibson, R. 2000) This is very expensive, and if sandwich beams are to be used in the construction industry, costs such as these will make the use of sandwich panels far less economically viable than more traditional materials. In the automotive or aeronautical industry, the same component is used time and time again, however in the construction industry, each project is completely different and requires completely different components. This means that the cost to characterise sandwich beams will mean that they will only be used on very large projects, as this cost is to greater a percentage of a smaller construction project.

The cost and complexity of the material characterisation test procedures and equipment is such that small and medium sized composite material manufacturers usually must rely on outside testing laboratories to conduct the material characterisation. (Gibson, R. 2000) This creates a problem in the optimisation and control of manufacturing, as the smaller manufacturers cannot monitor the material properties throughout the manufacturing process.

3. Related Literature

3.1 Sandwich Beams

As previously mentioned, sandwich beams consist of two thin face sheets, these face sheets are separated by a core and possibly filler material. The thin face sheets are strong and stiff, and carry the compressive and tensile stresses in the beam. The core on the other hand is light-weight and carries the shear stresses. This concept is similar to an I-beam in where the flange carries the compressive and tensile stresses and the thin web carries the shear stresses. This makes sandwich beams a light-weight yet very stiff building material.

The sandwich beams to be used in this project have Nida-core lightweight honeycomb cores which have been obtained from Auckland in New Zealand. Nida-core polypropylene honeycomb cores are light-weight, quiet tough and resilient and are considerably cheaper than PVC and SAN foam core material. (Nidacore 2008)These cores have the advantage of being able to have exceptional bond and peel strength, due to the cell walls being fused into the non-woven polyester scrim as well as the scrims to bond well with virtually any resin or adhesive system. The polypropylene used for manufacture of these cores has a natural harmonic of 125 to 150 Hz, which makes this material excellent for noise attenuation and vibration damping. While these are favourable characteristics for the core's use as a construction material, the fact that Nida-core is a highly damped material may make it hard to determine the natural frequencies by experimentation. (Nidacore 2008) There are two types of skins being used in this experiment. The first is an aluminium skin, and the other is a unidirectional fibre glass skin.

3.2 Young's Modulus

The Young's Modulus, or Modulus of Elasticity, is a measure of a materials resistance to elastically deform under an applied load, or in other words the stiffness of the material. The Young's Modulus can be calculated by the elastic stress divide by the strain for this stress. This is shown in Equation 1.

$$E = \frac{\sigma}{\varepsilon} \qquad 1$$

As stress has the units of Newtons per square metre (N/m^2) and strain has no units, the unit of the modulus elasticity is Newtons per square metre.

The modulus of elasticity for aluminium is approximately 70 GPa and the modulus of elasticity for steel is approximately 200 GPa.

3.3 Vibration Theory

Vibration is the term given to the oscillatory motion of a system when subjected to a force. There are two types of vibration, and these are free vibration and forced vibration.

Free vibration occurs due to the action of forces in-built in the system itself. In the case of free vibration there are no external forces acting on the system. The system which is acting under free vibration will oscillate at one or more of the systems natural frequencies.

Forced vibration on the other hand is the term given to the vibration which occurs when the system is excited by external forces. If a system is excited at a frequency which coincides with one of the system's natural frequencies, a condition known as resonance will occur, this may result in very large oscillations. (Thompson 1988)

3.4 Using Timoshenko's Beam Theory to determine materiel properties

Larsson (1991) completed a study on the determination of Young's and shear moduli from flexural vibrations of beams based on the Timoshenko Beam Theory. Beams which are considered anisotropic material, the flexural vibration is affected by shear deformation and rotational inertia. This means that there is a possibility to determine the shear modulus of the beam by measuring the natural frequencies of the beam. (Larsson 1991)

A prerequisite to accurately determine the shear modulus is that the influence of shear deformation on the flexural vibration is large enough. This shows that if the ratio of the shear modulus to the Young's modulus is low the accuracy of determining the shear modulus is usually very low. The theory behind the method presented by Larrson (1991) is based on the Timoshenko beam theory. (Larsson 1991)

The determination of the Young's and shear moduli was undertaken by accurately measuring the natural frequencies of the material and estimating the moduli until the theoretical frequencies were close to the measured frequencies. Larsson's study found that the accuracy of the Timoshenko theory allowed an accurate determination of the absolute values of the shear modulus and Young's Modulus. The outcome of this work was that Larsson produced a series of diagrams which could be used to determine the shear modulus and Young's modulus when the natural frequency of the system is known. (Larsson 1991)

The Timoshenko Beam Theory assumes that each cross-section of the beam remains flat. This theory results in an intermediate solution which gives two partial derivatives. These are:

$$\left[kGA\left(\alpha - \mathrm{d}_{(t,x)}{}'\right)\right]' + \rho A\ddot{w} = 0, \qquad kGA\left(\alpha - \mathrm{d}_{(t,x)}{}'\right) - (EI\alpha')' + \rho I\ddot{\alpha} \tag{2}$$

The equation for the natural frequencies can then be determined based on the boundary conditions of the system. Larsson found that the for a beam of length (L) and thickness (h) can be easily written by introducing two dimensionless parameters which are G/E and L/h and the dimensionless eigenfrequencies:

$$\underset{\sim}{\omega_n} = \frac{\omega_n}{\omega_0} \tag{3}$$

Where:

$$\omega_0 = \sqrt{\frac{E}{\rho L^2}} \tag{4}$$

The natural frequencies can then be written by:

$$\omega_n = \sqrt{\frac{E}{\rho L^2}}\,\underset{\sim}{\omega_n}\left(\frac{G}{E}, \frac{L}{h}\right) \tag{5}$$

Where $\underset{\sim}{\omega_n}$ is dependent only on G/E and L/h, both of which are dimensionless and need to be solved numerically. Larsson then proposed that estimates for G and E be made and substituted into the equation. As the values of L and h for the material are known, these substitutions can be made iteratively for various modes of vibration until the natural frequency given by the formula is reasonably close to the natural frequency measured during the experiment. (Larsson 1991)

An extension of this work was completed by Nilsson and Nilsson (2002), and they were able to develop a six order differential equation which governs the apparent bending of sandwich beams using Hamilton's principle. This found that the bending stiffness of sandwich beams is dependent on the natural frequency and boundary conditions of the structure. Their work included an experiment in which they were able to determine the bending stiffness of the entire structure, the bending stiffness of the skins as well as the shear stiffness of the core. (Nilsson 2002)

This study found that in the low frequency range the bending stiffness can be determined by pure bending. As the frequency becomes higher, the laminates are assumed to vibrate in phase, and therefore the bending stiffness of the whole beam is equal to the sum of the bending stiffness of the laminates. The apparent bending stiffness for the mode n of the beam can be found by the expression in Equation 6, where f_n is the natural frequency for mode n, L is the length of the beam and μ is the mass per unit area of the beam.

$$D_{xn} = \frac{4\pi^2 f_n^2 \mu L^4}{\alpha_n^2} \qquad 6$$

The parameter α_n is dependent on the boundary conditions of the beam and the mode number and can be taken from Table 1.

Table 1 Values of α_n based on the mode number and boundary conditions

Boundary Conditions	n	1	2	3	4	5
Free-free and clamped-clamped	α_n	4.73	7.85	11.00	14.14	17.28
Free-clamped	α_n	1.88	4.69	7.85	11.0	14.14

The results obtained by Nilsson and Nilsson (2002) were quite accurate with the measured results closely matching the calculated values. It is interesting to note that 1.2m samples are used in the experiment, and at least 10 bending modes were successfully identified. Due to the low mass of the sandwich beams which was less than 3kg/m a laser vibrometer was used to measure the vibrations achieving non-contact measurements. This is expected to work considerably better than the method being used in this experiment.

3.5 Methods for determining material properties

Schwingshackl et al (2006) examined several available analytic and experimental methods to determine orthotropic material properties of honeycomb, and reviewed fifteen published sets of equations for a specific honey comb material. The analysis of the reviewed theories found that the three major out of plane material properties E_z, G_{yz} and G_{xz} derived from the ASTM methods generally correspond quite closely to the majority of the analytical values. However, it is also noted that in general the theories seem to overestimate the out-of-plane Young's modulus, underestimate the shear modulus G_{xz}, and is quite close to the shear modulus G_{yz}. (Schwingshackl et al. 2006)

Their work led them to a simple technique to measure the main dynamic properties of honeycomb, in an attempt to reduce time and cost for experimental characterisation.

Schwingshackl et al (2006) presented a method which involved using a single specimen with multiple degrees of freedom to determine the equivalent dynamic properties. The experiment involves exciting a spring-mass system and measuring the resonance response frequencies. The equations of motion were then used to determine the unknown material properties.

The experimental set-up involved sandwiching an 80mm x 80mm honeycomb core of 20mm thickness between a large steel base and a steel mass of 3.752kg.The honeycomb was glued to a massive engine foundation using Araldyte. An impact hammer was used to excite the system at impact locations for effective excitations of the predicted mode shapes. The dynamic response of the system in the direction of excitation was captured by four accelerometers. Any possible out-of-plane movement of the steel mass was monitored by two additional accelerometers.

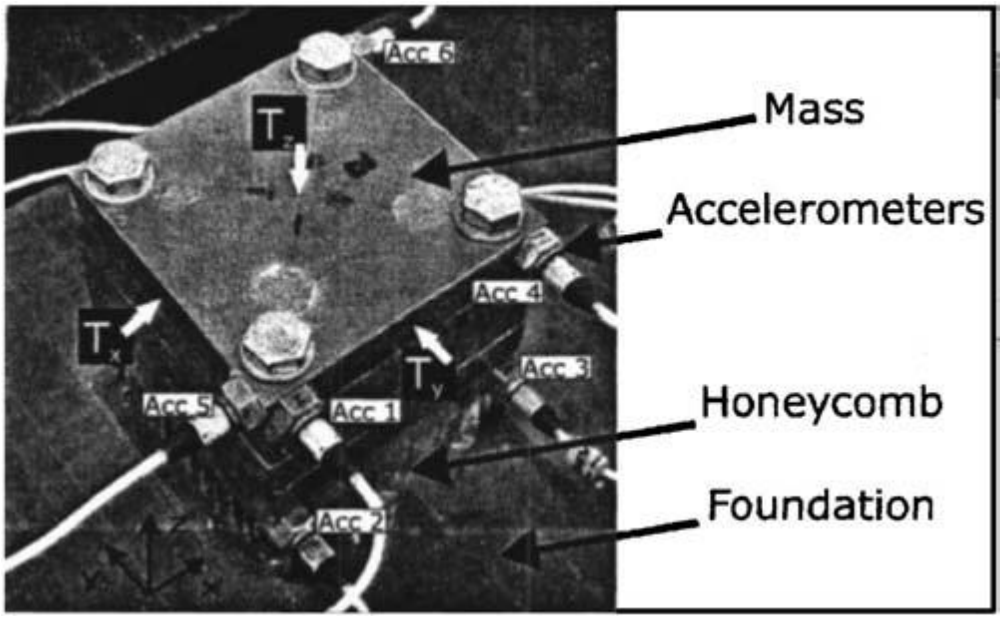

Figure 1 Dynamic test specimen with impact locations and accelerometers (excitation in y) (Schwingshackl et al. 2006)

After performing a numerical analysis and using Lagrange's theory, an expression for the unknown out-of-plane Young's Modulus E_z and the Shear Modulus G_{yz} can be calculated from the known resonance response frequencies that are found in the experiment. (Schwingshackl et al. 2006) The Young's Modulus can be found by:

$$E_z = \frac{h_C m}{a_C^2}\omega^2 \qquad 7$$

This experiment was only able to clearly see the first two captured responses, which created an underdetermined system consisting of two known frequencies for three unknown material properties. This resulted in Schwingshackl et al using a theoretical approach to calculate Young's modulus which was then used to calculate the unknown shear moduli. (Schwingshackl et al. 2006)

Mujika et al (2011) used a similar dynamic method to calculate the out of plane properties as Schwingshackl et al and found that there is good agreement in the results between this dynamic test, the static three point bending test, a finite element analysis model and the analytical approach presented by Gibson and Ashby.

Mujika et al (2011) used a three point bending test, a compression test and a dynamic test to determine the shear modulus of the core. This paper found that the problem of obtaining shear modulus by bending tests is that due to the great influence of shear, large spans are required to avoid this effect. (Mujika et al. 2011)

For the three point bending test the displacement of the mid-point of the specimen is found by:

$$\Delta = \frac{PL^3}{48D} + \frac{PL}{4D} \qquad 8$$

Where :

$$D = \frac{E(d^3 - C^3)w}{12} \qquad 9$$

And:

$$U = \frac{G(d + c)^2 w}{4c} \qquad 10$$

The shear stress distribution in a sandwich beam with a soft core is not considered to be parabolic like material with a regular rectangular, homogenous cross-section, but is considered to be uniform through the core. (Mujika et al. 2011)

Sadowski and Bec (2011) investigated the eigenvibration of honeycomb sandwich panels reinforced by polymeric foam, and found that the mechanical response has a high dependency on the internal structure and properties of the core. This investigation involved using a sandwich plate with a honeycomb core. The first ten natural frequencies were found for the sandwich panel filled with H100 polymeric foam, H200 polymeric foam, and a sample with no filling foam at all. There were three different apparatus setups used and these were two opposite edges simply supported, one edge clamped, and all four edges clamped. (Sadowski & Bęc 2011)

Sadowski and Bec (2011) found that in general local vibrations of the aluminium foil constituting honeycomb core occurred in the samples which had no foam filler. While the sandwich panels that had the filled core, the plate tended to vibrate as a whole structure. The samples which had no filling of the honeycomb structure also had remarkably higher natural frequencies. However this trend may be reversed or the difference in values may be closer in the high frequency range due to the local vibration modes occurrence. (Sadowski & Bęc 2011)

Sadowski and Bec (2011) performed a modal analysis of three different samples which included the sandwich plate with honeycomb core and polymeric foam filler, the core (without face sheets), and the sandwich plate without the honeycomb aluminium foil core but instead containing the polymeric foam core. The results of this analysis found that most of the shear capacity is due to the core. The values of Kirchoff's moduli for the full sandwich structure are not that much greater than the values for the core without face sheets. The values of Gxy and Gyz were greatly reduced when the core consisted only of polymeric foam with no aluminium foil honeycomb structure in the core with values of about 70 MPa as opposed to 850 to 1300 MPa when the honeycomb aluminium foil was used. Sadowski and Bec (2011) concluded that the use of foam filler in the honeycomb core improved both static and dynamic properties especially by reducing local modes of vibrations and improving stiffness. (Sadowski & Bęc 2011)

Gibson (2000) proposed a method for dynamic characterisation which used modal testing in a single mode of vibration. This involved the free excitation of a cantilever structure, and analysing the first natural frequency to determine the material properties. (Gibson, R. F. 2000)The experiment setup is shown below:

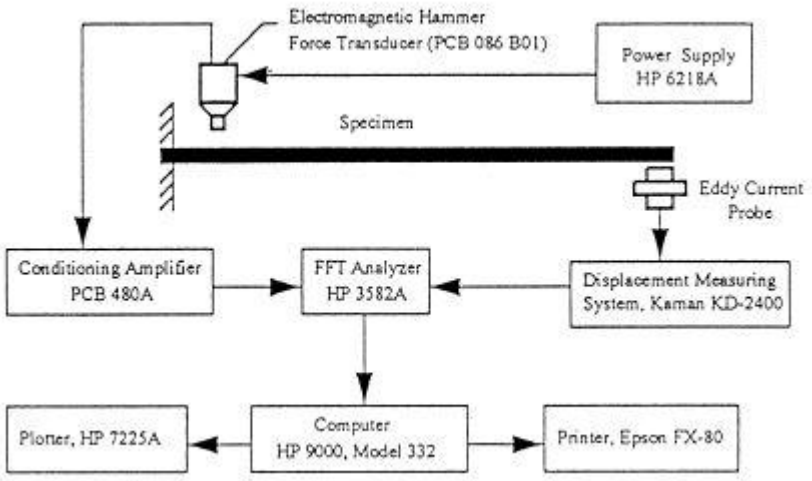

Figure 2 Impulse/response test set-up for cantilever-beam specimen (Gibson, R. F. 2000)

When the cantilever beam is excited using an Electromagnetic Hammer Force Transducer the vibration is measured by a displacement measuring system. The measured response is then digitised and can be analysed both in the time domain or can be transformed to the frequency domain using fast Fourier transform (FFT) analysers in the computer. This allows the responses to be presented in the frequency response spectrum, where when graphed the peaks in the frequency/response function (FRF) correspond to the natural frequencies of the system. (Gibson, R. F. 2000) It can be seen in Figure 3 below that the peaks in the graph correspond to the natural frequencies of the system. This is the typical FRF when the specimen is excited at the opposite end of the beam to where the measurements are being taken.

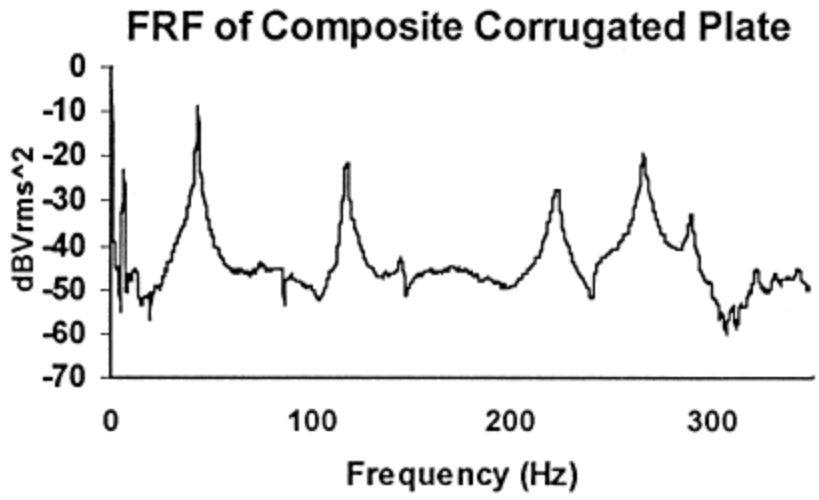

Figure 3 Typical frequency/response function for impulse test of composite specimen (Gibson, R. 2000)

The appropriate frequency equation can be derived from the equation of motion for the specimen, and by substituting the natural frequency obtained along with the specimen dimensions and density, the effective modulus can be found. For the cantilever beam shown in figure 2 the frequency equation can be expressed by:

$$f_n = \frac{(\lambda_n L)^2}{2\pi^2}\left(\frac{EI}{\rho A}\right)^{\frac{1}{2}} \qquad 11$$

(Gibson, R. F. 2000)

Equation 11 is based on the Euler equation for beams which is explained later in the report.

3.6 Dynamic characterisation of high damping viscoelastic materials

Martinez-Agirre and Elejabarrieta (2011) presented a new inverse method for the dynamic characterisation of high-damping materials from vibration test data. This method used forced vibration tests with resonance and without resonance to determine the mechanical properties. (Martinez-Agirre 2011)

The forced vibration test without resonance enables the determination of the material properties of bulk viscoelastic materials. The vibration test with resonance allows the

determination of the mechanical properties of those bonded to the elastic components in the constrained layer dampening and the free layer dampening configurations as well. This study uses the standard ASTM E756-05 which describes a procedure to find the modulus of elasticity of homogenous materials. (Martinez-Agirre 2011)

However using this procedure, a large number of tests with different free lengths need to be undertaken to obtain a sufficient number of points to fit the viscoelastic model with certainty. The assumptions which are required to be made for this type of analysis, results in limitations for characterising high damping materials, which drastically reduces the frequency range where the modulus can be accurately determined.

Figure 4 shows the measured response recorded by Martinez-Agirre and Elejabarrieta for a metallic beam, the first graph is the modulus and the second graph is the phase plot. This response has been produced using a forced vibration test, and it shows that the peaks corresponding to the natural frequencies are easy to identify. Also there is a change in phase corresponding with each of the resonant frequencies. This is a similar graph to what we will be trying to achieve through our testing. The only difference will be that we will be using a driving point impact test.

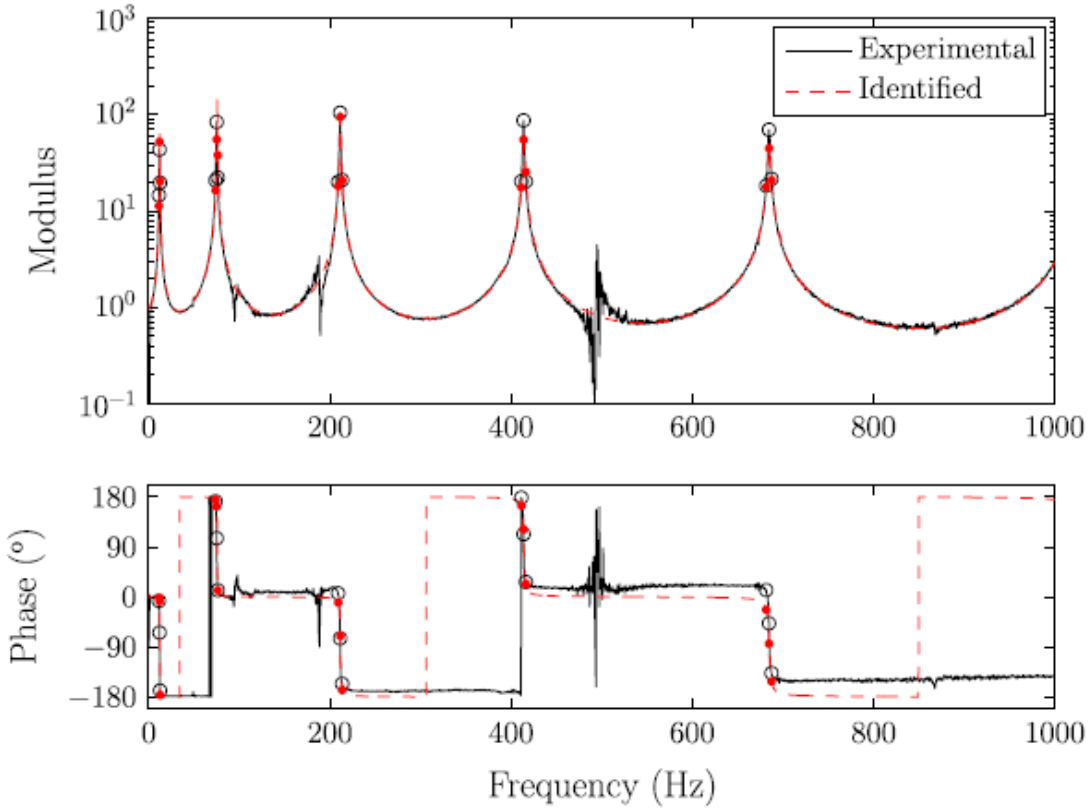

Figure 4 Modulus and phase of transfer function for metallic beam regarding transverse displacement at the free end.

To show the difference between a metallic beam and a viscoelastic core the modulus and phase frequency response plots for the constrained layer dampening system, which is similar to a sandwich panel, have been shown in Figure 5. It can be seen from Figure 5 that it is considerably harder to excite the higher natural frequencies in the highly damped material. The first two peaks are quite distinct, however as the mode number gets higher the peaks become less distinct.

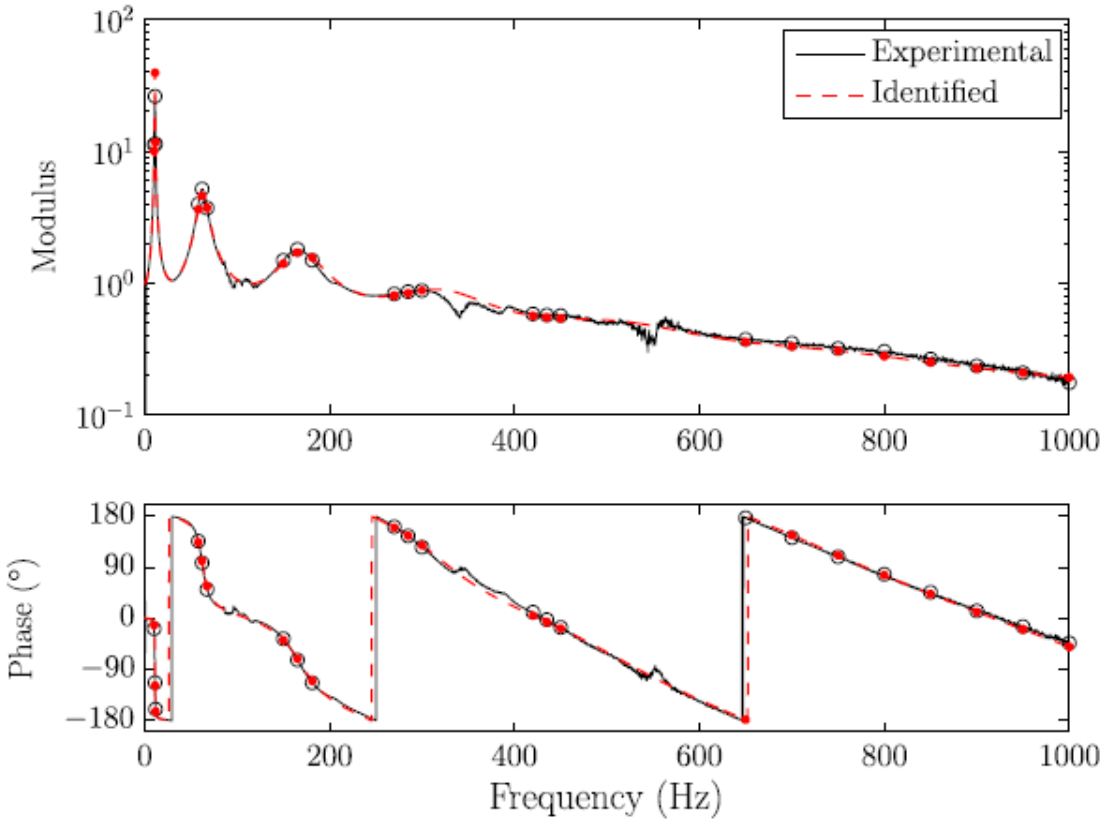

Figure 5 Modulus and phase of transfer functions of CLD beam regarding the transverse direction of the free end (Martinez-Agirre 2011)

3.7 Euler Equation for Beams

The differential equation for the lateral vibration of beams can be formulated by considering the forces and moments acting on an element of the beam presented in Figure 6. (Thompson 1988)

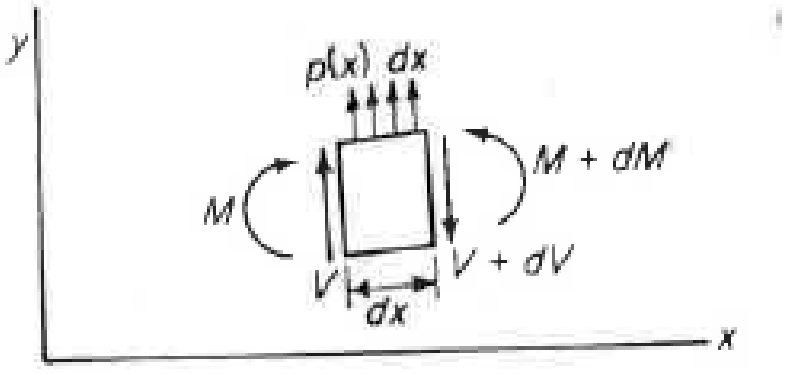

Figure 6 An element of a beam used to derive the Euler equation for beams (Thompson 1988)

V is the shear force and M is the bending moment and p(x) represents the loading per unit length of the beam. By summing the forces in the y-direction

$$dV - p(x)dx = 0 \tag{12}$$

If the moments about any face on the right face of the element, this leaves:

$$dM - Vdx - \frac{1}{2}p(x)(dx)^2 = 0 \tag{13}$$

When the limits are taken, the following important relationships are created:

$$\frac{dV}{dx} = p(x), \quad \frac{dM}{dx} = V \tag{14}$$

This relationship says that the rate of change of shear along the length of the beam is equal to the load per unit length of the beam. The second equation states that the rate of change of the bending moment along the length of the beam is equal to the shear in the beam. From this equation we can obtain:

$$\frac{d^2M}{dx^2} = \frac{dV}{dx} = p(x) \tag{15}$$

From this the Euler Equation states that the natural frequency of vibration for the uniform beam can be found by Equation 16.

$$\omega_n = (\beta_n l)^2 \sqrt{\frac{EI}{\rho_l l^4}} \tag{16}$$

The natural frequency in Hz can be found by dividing this equation by 2π which gives:

$$\omega_n = \frac{(\beta_n l)^2}{2\pi}\sqrt{\frac{EI}{\rho_l l^4}} \quad (17)$$

The values for $(\beta_n l)^2$ have been determined for various boundary conditions. The values of $(\beta_n l)^2$ for the first five natural frequencies with free-free boundary conditions have been presented in the following table (Young 1989):

Table 2 Values for $\beta_n l^2$ for each of the first five modes of vibration (Young 1989)

Mode	$\beta_n l^2$
1	22.4
2	61.7
3	121
4	200
5	299

If the length of the beam, mass per unit length of the beam and second moment of area of the beam are accurately measured, and the natural frequency of the beam can be determined through experimentation, the modulus of elasticity of the material can be calculated.

3.8 Determining natural frequencies

For this project, a similar method to determine the natural frequency of the beam will be used as that used by Gibson in his paper on "Modal vibration response measurements for characterisation of composite materials and structures". (Gibson, R. 2000)

The program being used to record the vibrations of the beam, and compute the frequency response functions is LMS Test Express. LMS have an article called "Advanced FRF based determination of structural inertia properties" which gives a description on a possible way to perform the analysis.

It describes that the modal test can use either impact hammer or shaker excitation on the structure in free-free conditions. It also recommends using 6 excitation locations in a single direction and 8-12 response locations in 3 directions. ('Advanced FRF

based determination of structural inertia properties')This test requires limited measurement effort and no special equipment. The LMS test express program is capable of performing operations such as Fast Fourier Transform (FFT) and Frequency Response Function (FRF) on the data which is collected in the time domain.

While this article recommends that a shaker can be used to excite the beam, however the development of technology such as microprocessor based Fast Fourier Transform processors and PC based virtual instruments has made it more attractive to use impulsive excitation and use frequency-domain analysis or time domain analysis to extract the natural frequencies. (Gibson, R. 2000)

By using the impulse hammer it results in a nearly constant force over a broad frequency range, which means that all of the resonant frequencies in the frequency range can be excited. (*Model 086C04 SPECS 086C04 SERIES Installation and Operating Manual* 2010) There are a number of different tips which come with the impact hammer which vary in hardness. The impact cap material determines the energy content imparted on the beam. (*Model 086C04 SPECS 086C04 SERIES Installation and Operating Manual* 2010)

The caps which can be used include red (super soft impact cap), black (soft impact cap), white plastic (medium impact cap), and the stainless steel (hard impact cap). Figure 7 below shows the force spectrum for an impact of a stiff steel mass using the different tips available. This shows that in order to excite the higher frequencies the harder tip needs to be used. This figure also shows the shape which the force spectrum of the impact should take when performing the experiment.

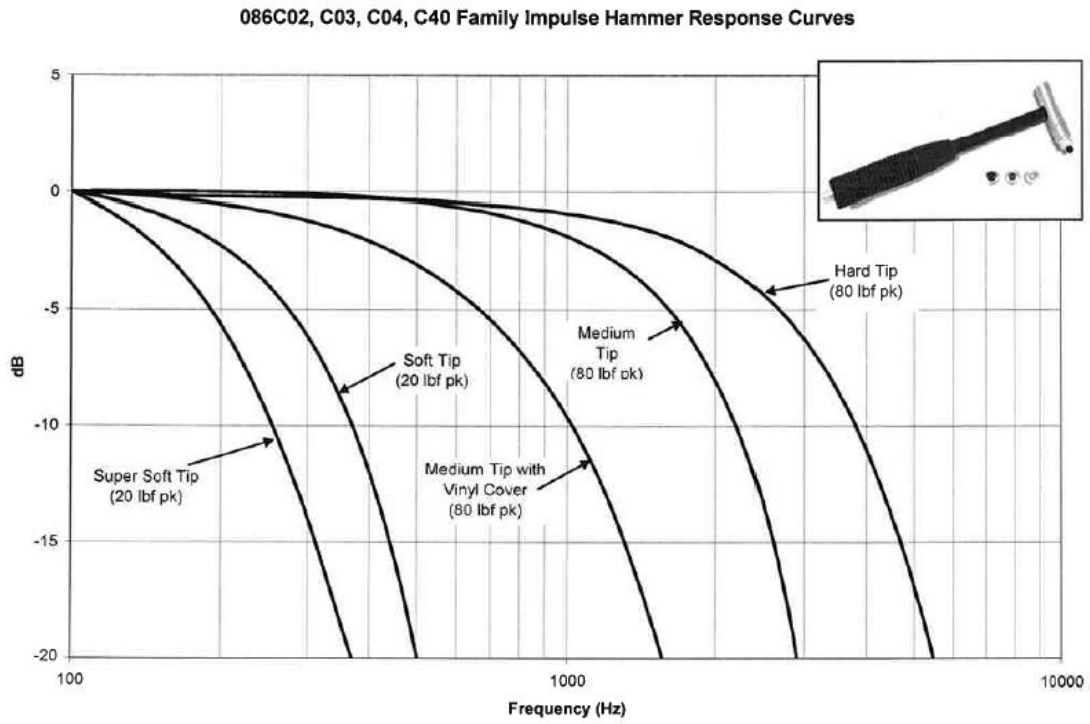

Figure 7 Expected force spectrum for impact of stiff steel mass with impact hammer

3.9 Fourier Transform Function

The data from the accelerometer on the beam and the force transducer in the impulse hammer is collected in the time domain. This is done by the movement of the accelerometer being measured, being fed through an analogue to digital converter, and is then presented as a position for each time interval. (Newland 1993) The vibration of the beam is therefore able to be graphed as a continuous function of time.

However, in order to find the natural frequencies of the system, the data needs to be transferred to the frequency domain. This is done using the Fast Fourier Transform (FFT). The Fast Fourier Transform is used to calculate the Discrete Fourier Transform (DFT) by using a computer algorithm. The Discrete Fourier Transform is used to find the spectra from the measured time data.

The advent of the FFT in 1965 has provided a quicker method for calculating the DFT based on calculating the DFT of the original discrete time series directly and

then manipulate this transformed sequence to produce the spectral estimates as required.

Renault et al defined the Frequency Response Function (FRF) input mobility as:

$$\widetilde{FRF} = \frac{\check{W}}{\check{F}} \qquad 18$$

where $\check{F}$ is the injected force complex amplitude in Newtons, and $\widetilde{W}$ is the velocity in metres per second at the excitation point. (Renault 2011) The FRF is a complex number and therefore consists of a graph of the real data, called the FRF, and a phase plot of the imaginary data. The peaks in the FRF correspond to a resonant frequency, and this can be checked using the phase plot. A resonant frequency should have a corresponding change of phase in the phase plot.

3.10 Interpreting Frequency Response Diagrams

Renault et al (2011) conducted a study on the "Characterisation of elastic parameters of acoustical porous materials from bending beam vibrations" in which the elastic parameters of soft, highly damped porous materials were analysed. To give an example of the results that may be expected from our analysis, Figure 8 was taken from Renault et al's report (2011). This figure shows the difference in the resonant frequencies between an aluminium base beam and a base beam with double sided tape on it. This is a driving point test, which means that the beam has been excited in the same position as where the response is being measured. A driving point test will be used in the experimentation for this report, so the shapes of the frequency response functions are expected to be similar to Figure 8. (Renault 2011)

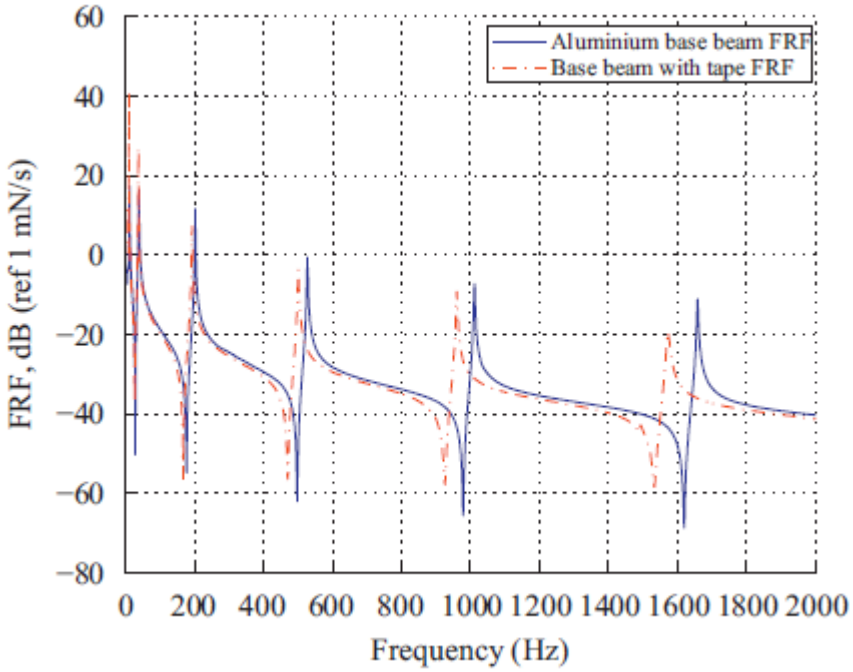

Figure 8 Example of the shape of frequency response function

3.11 Determining out-of-plane shear modulus from dynamic test

The characterisation of the shear modulus of sandwich beams is currently covered in two American Society for Testing and Materials (ASTM) standards, which are C393 and C273. It is also considered in the equivalent International Organisation for Standardisation standard, ISO1922:2001. (Mujika et al. 2011) The ASTM C393 standard covers flexural tests on flat sandwich constructions to determine the flexural stiffness, core shear modulus, core shear strength and the facings compressive or tensile strengths. (*ASTM C393 / C393M - 11e1* 2012) However if the bare core can be obtained it is better to determine the core shear strength and shear modulus using ASTM C273. (*ASTM C393 / C393M - 11e1* 2012)

ASTM C273 covers the determination of the shear properties of sandwich construction core materials. The test may be conducted both on sandwich panels bonded to the plates and on bare core materials bonded directly to the loading plates. This test may be used on continuous core materials such as foams as well as on discontinuous core materials such as the honeycomb structure of Nida-core. (ASTM 2011)

This test consists of subjecting a sandwich panel or core material monotonically increasing shear force parallel to the plane of its faces. This shear force is applied through the loading plates, and the core's shear modulus, shear strength and shear stress can be determined using the core's nominal area. In order to determine these, the failure mode must be the shear failure of the core material, and must not be de-bonding of the core from the face sheet or loading plate. (ASTM 2011)

There are a number of interferences which may affect the results of the ASTM C273 test, especially when testing a honeycomb core. For example when testing a honeycomb core, the core shear modulus and shear strength can be affected by the thickness of the adhesive bond to the honeycomb core. This test method also requires specialised apparatus including micrometres, a tensile or compressive test fixture, the testing machine, a conditioning chamber, and an environmental testing chamber.

Schwingshackl et al (2006) and Mujika et al (2011)proposed are far simpler and more cost effective method to determine the shear modulus of sandwich materials, as described previously in this section. (Mujika et al. 2011) This involved finding the shear modulus using Equation 19.

$$G_{yz} = -\frac{\left(-12I_{m_x}\omega_{hy}^2 h_C + a_C^4 E_z\right) m\omega_{hy}^2 h_C}{(3\omega_{hy}^2 h_m^2 h_C m + 12I_{m_x}\omega_{hy}^2 h_C - a_C^2 E_z)a^2} \qquad 19$$

4. Project Methodology

4.1 Experimental equipment specifications and setup

An LMS VB8 Frontend system was used for data acquisition and is capable of achieving a maximum rate of 25 kHz. A picture of the frontend system has been presented in Figure 9. LMS Testxpress© software was used to post process the data. A new project was set up in the program for each type of sample to be tested. The setup of this system involved setting the various parameters in the program to the same values which had been used for similar testing in the P2 laboratory. These parameters were taken from the reference file called USQ_Wagners_Beam_Testing, which was a file used by Dr. Jayantha Epaarachchi to perform a similar test.

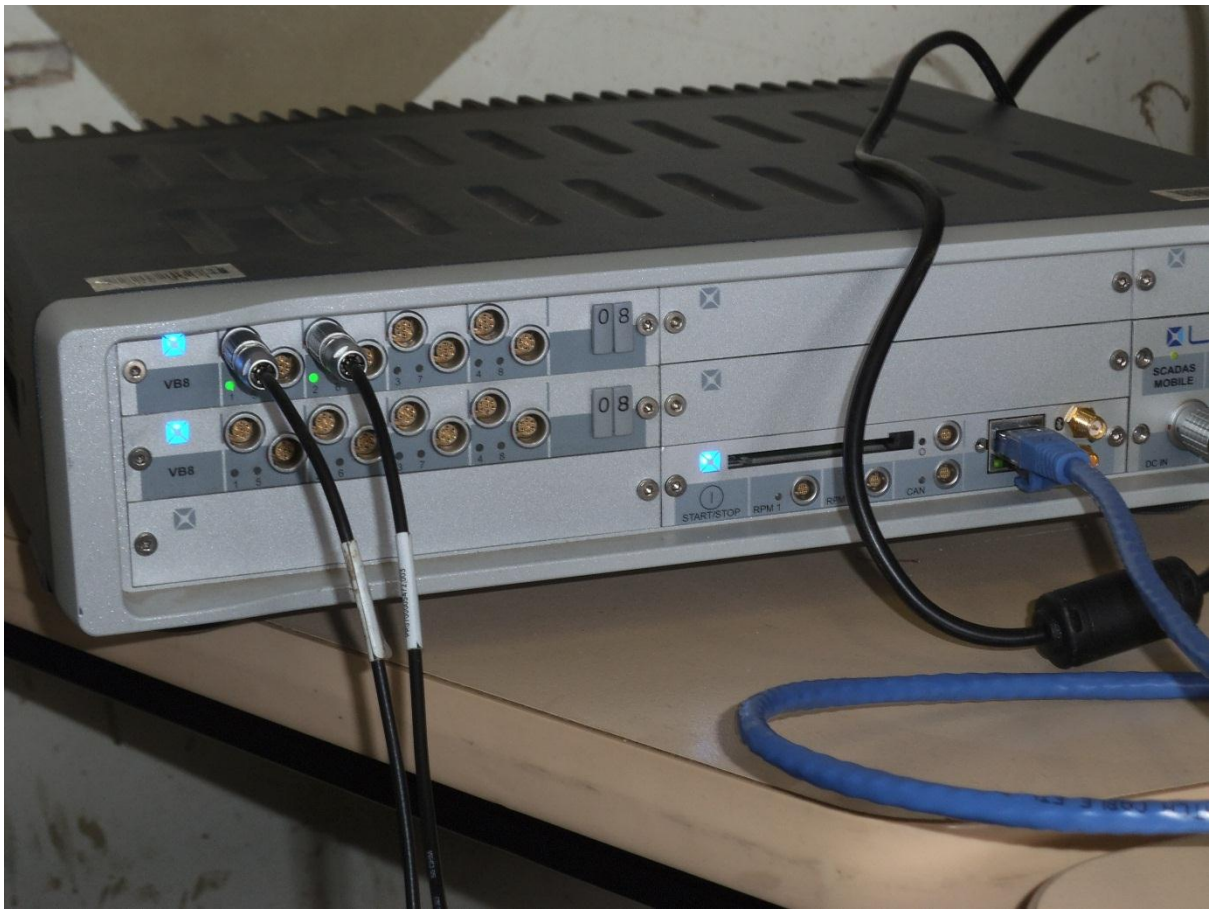

Figure 9 The frontend system used to collect the data. The accelerometer is plugged into channel 1 and the impulse hammer is plugged into channel 2.

The calibration value for the accelerometer was set to 0.0001008 and the unit to g's in accordance with the calibration certificate that goes with the accelerometer. The

Electrical unit was set to milliVolts. The calibration value for the impact hammer was 1.14 and the unit was Newtons, as per the calibration certificate for the hammer. The sample rate was set as 2048 Hz. The ICP was set to off.

Each channel being used, in this case channel 1 and channel 2, were turned on. The coupling setting was set to alternating current. The bridge type used was no bridge. The shunt value was set to 1 with a shunt tolerance of 2. The balance tolerance was also set to 2. Calibrate was set to on. The input range was 3.16 Volts, 10 decibels, or the input range (unit) was 2771.93. The external gain in decibels was 0. The high pass was set to 0.5 Hz.

A PCB086C04 impulse hammer was used to excite the system. This hammer has an accelerometer in the tip which is capable of measuring the force imparted on the beam. The type of tip used was changed depending on the material being tested, ranging from the very hard stainless steel tip being used for the steel samples to the super soft red tip which was used for the nida core with no skins.

Figure 10 The PCB086C04 impulse hammer which was used to excite the system

4.2 Specimen preparation

Initially two metal samples of different dimensions will be tested to ensure the results being obtained are correct before going on to testing the sandwich panels. These metal beams have been constructed by the university staff in the Z4 lab. The sandwich panels which contain Nida honeycomb cores have been manufactured in Auckland.

Prior to testing the dimensions and weight per unit length of each beam needs to be accurately measured for input into the equations to determine the natural frequency. The dimensions of the beams were measured using the digital vernier callipers. The total mass of the beam was measured in the P11 laboratory and was converted to weight per metre by the following equation:

$$mass\ per\ metre = \frac{mass\ of\ beam}{length\ of\ beam} \qquad 20$$

The dimensions and masses for the steel beams, sandwich panels and core samples used in the experimentation have been summarised in the following table:

Table 3 Summary of the steel sample properties

Sample No.	Beam Type	Length (mm)	Width (mm)	Depth (mm)	Mass (g)	Mass/metre (g/m)
S1	Steel	252	49.33	19.93	1910.9	9568
S2	Steel	627	49.89	24.84	5998.99	7583

Table 4 Summary of the sandwich panel and core properties

Sample No.	Beam Type	Length (mm)	Width (mm)	Depth (mm)	Skin thickness (mm)	Mass (g)	Mass/metre (g/m)
1	Aluminium skin sandwich panel	250	74.82	20.73	0.45	79	316
2	Aluminium skin sandwich panel	250	74.5	20.55	0.45	83.2	332.8
3	Aluminium skin sandwich panel	250	84.73	40.25	0.45	119.3	477.2
4	Aluminium skin sandwich panel	250	84.91	40.31	0.45	118.5	474
5	Fibreglass skin sandwich panel	250	75.4	20.9	0.76	82.1	328.4
6	Fibreglass skin sandwich panel	250	75.77	20.77	0.76	80.2	320.8
7	Fibreglass skin sandwich panel	250	85.4	40.85	0.76	122.5	490
8	Fibreglass skin sandwich panel	250	85.4	40.62	0.76	126.2	504.8
9	H8HP Nida core sample	252	81	39.94	0	61.9	247.6
10	H8HP Nida core sample	252	81	39.94	0	61.9	247.6

4.3 Experimental Setup

In order to imitate free-free conditions the sample will be hung from two frames by poly wire. Poly wire has been used as this is more flexible than steel wire, yet strong enough to carry the weight of the samples.

Figure 11 A aluminium skinned sandwich panel suspended in the free-free conditions

The two frames have been constructed of metal, and are of sufficient height that the beams can be suspended on the string underneath them without hitting the table. Any length beam can be tested as the frames are separated and can be moved apart to accommodate any length of beam. The frames are both clamped to the table to restrict excessive movement and to prevent the frames from toppling over under the weight of the specimens being tested.

The accelerometer is attached to the underside of one end of the beam using bees wax. A very small amount of bee's wax which will keep the accelerometer in place needs to be used, so that the vibrations of the beam will be accurately transferred to the accelerometer. It must be placed as close to the free end as possible, however the accelerometer must not protrude past the end of the beam.

The accelerometer is connected by a chord to Channel 1 of the frontend system. The impulse hammer is connected by a chord to Channel 2 of the frontend system. The

frontend system is connected by a local area network chord to a laptop computer containing the LMS Testxpress software, which is used to check and record the data.

Figure 12 The complete apparatus setup

4.4 Performing the test

The beam needs to be as flat and as stationary as possible prior to starting the test. A graph of Channel 1 is put on to a 2D plot in the LMS Test Express window and the scope button is pressed to allow the movement of the accelerometer to be viewed. Test hits are conducted on the specimen and these can be viewed on the screen to check that everything is working.

The technique of hitting is the most important part to getting good results in this experiment. The maximum amount of force must be imparted on the beam as possible, however double hitting needs to be avoided. Double hitting occurs when after the beam is hit by the hammer it rebounds and again comes into contact with

the hammer, causing a double spike on the time plot of Channel 2 which shows the impact hammer data.

The technique to be used is therefore hitting the beam as hard as possible and then pulling the hammer away quickly before the beam can rebound and again hit the impact hammer. Double hitting can be checked for by looking at the scope for Channel 2 to ensure that there is only one peak. The Fast Fourier Transform (FFT) plot of the impact hammer force impulse output can also be used to determine if it was a double hit or not.

In addition to this the beam needs to be struck as close to the position of the accelerometer as possible when carrying out a driving point test. This means that the beam must be struck as close to the free end of the beam as possible. This is where a greater degree of difficulty presents itself in the dynamic test in comparison with the static test. The number of things that can go wrong with hitting the beam to affect the measured results makes this test difficult to get accurate results.

Once the experimenter is happy with the hitting technique, the tests can be recorded by clicking on the record button just prior to exciting the beam with the impulse hammer. The program will record for 10 seconds, so this is the time within which the beam must be struck.

There are a number of different tips which can be substituted on to the impact hammer depending on the rebound of the beam. The harder tips can usually excite the higher frequencies of the material, while the softer tips are ideal for exciting the lower frequencies. For this reason the experimenter must perform a number of tests with the different tips to ensure with which tip the best frequency response can be achieved.

4.5 Data Handling

The Frequency Response Function is calculated for time periods of 0.08 seconds when the sample width is 6400 Hz which was used for most of the tests. For this reason the time when the beam was struck must be found by zooming in on the time domain graph showing the movement of the accelerometer. This time must be noted and the Frequency Response Function plot for the time period which contains the excitation of the beam can then be chosen to analyse.

In order to derive the natural frequency of the specimen, the better Frequency Response Function plots are chosen to be plotted on the same graph. This should give a clear indication of the natural frequency for the system, as multiple tests should have corresponding peaks in the same location. The LMS Test Express program is capable of outputting the data to a text file, which can allow graphing in Matlab. However this was found to be quite labour intensive, and so it was decided to determine the natural frequency using the graphs in the LMS Test Express program.

4.6 Four point bending test

A four point bending test was undertaken on some 40mm sandwich beams similar to those used in the dynamic analysis. The test was carried out in accordance with ISO14125 and involved loading the beams at the quarter points of the beam. Figure 13 shows an example of the apparatus set-up for the four point bending test, however the length of the span was 200mm instead of the 3000mm as shown in the image.

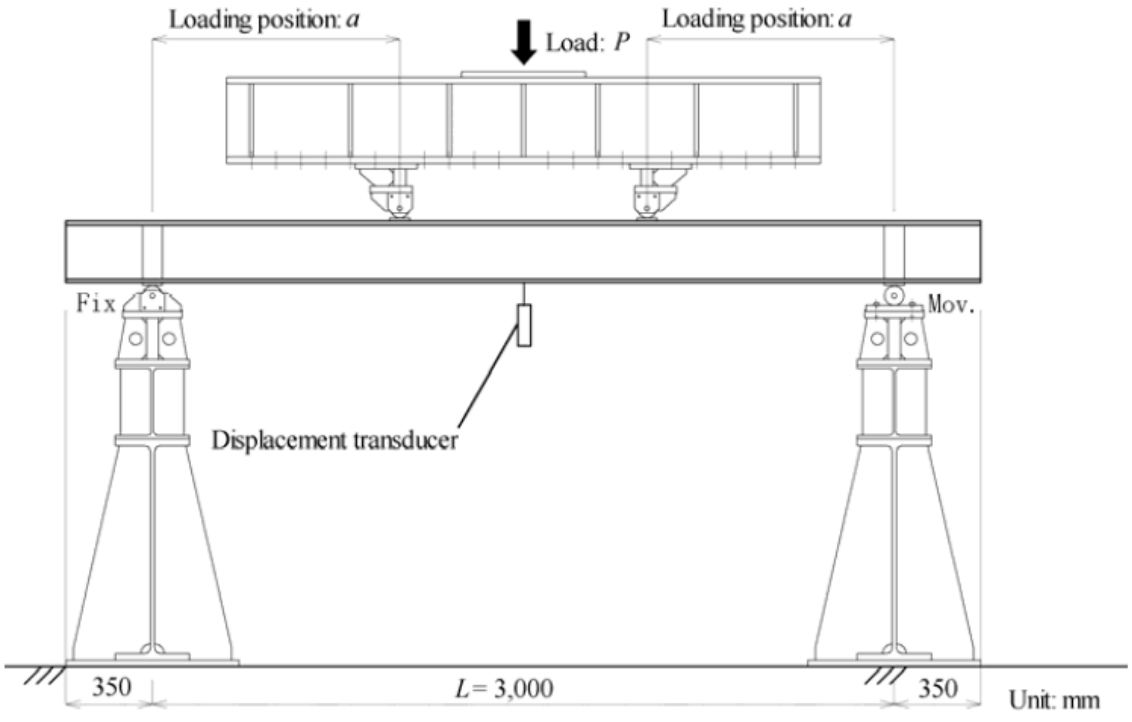

Figure 13 Set-up of four point bending test (Nakamura 2007)

The results from this test can be used to calculate the modulus of elasticity and shear modulus of the beam. The equation for the deflection of the beam can be found using Equation 21(Nakamura 2007).

$$\Delta = \frac{PL^2 a}{48EI}\left(3 - 4\frac{a^2}{L^2}\right) + \frac{P}{2GA}a \qquad 21$$

The values for E and G can be found by selecting two different values for the applied load and measured deflection and then solving the two simultaneous equations to find E and G. Here the distance to the loading point (a) is 50mm. The skins are considered to carry all of the bending stress so the Moment of Inertia (I) has been calculated for the skins only using the parallel axis theorem. The area (A) has been calculated as the area of the honeycomb core only as it has been assumed that the core carries all of the shear stress.

5. Results and Discussion

5.1Four Point Bending Test Results

5.1.1 40mm Aluminium Skin Samples

The results from the four point bending tests can be used to calculate the modulus of elasticity and shear modulus of the sandwich panels. Figure 14, Figure 15 and Figure 16 are the load verse displacement plots for the four point bending test of three different 40mm samples with aluminium skins. The Modulus of Elasticity for each of the samples can be found by substituting values for the load and deflection of the beam prior to yielding, which is the linear portion of the graph, into an equation to describe the deflection of the beam. To do this the two different values for load and displacement have been substituted into equation 21 and the modulus of elasticity and shear modulus has been calculated by solving the two simultaneous equations.

For this calculation it has been assumed that the aluminium skins carry all of the bending and the Nida core carries the shear. Therefore the moment of inertia has been calculated using the parallel axis theorem to find the moment of inertia for the skins only. The modulus of elasticity and shear modulus of the average value of the three graphs based on a load close to 500 N and a load close to 1000 N has been calculated and the Young's Modulus was found to be 73 GPa with a shear modulus of about 13 MPa. This is fairly close to the results that are expected. Aluminium has a modulus of elasticity of about 70 GPa, so this value is quite close. The technical document for H8HP Nida core honeycomb polymeric core states that the shear modulus of the core is 9 MPa. (Nidacore 2010)The measured 13 MPa is therefore fairly close to this value, however the difference may be due to an underestimation of the shear properties by the manufacturer or there is a chance that the aluminium skin is also carrying some of the shear stress.

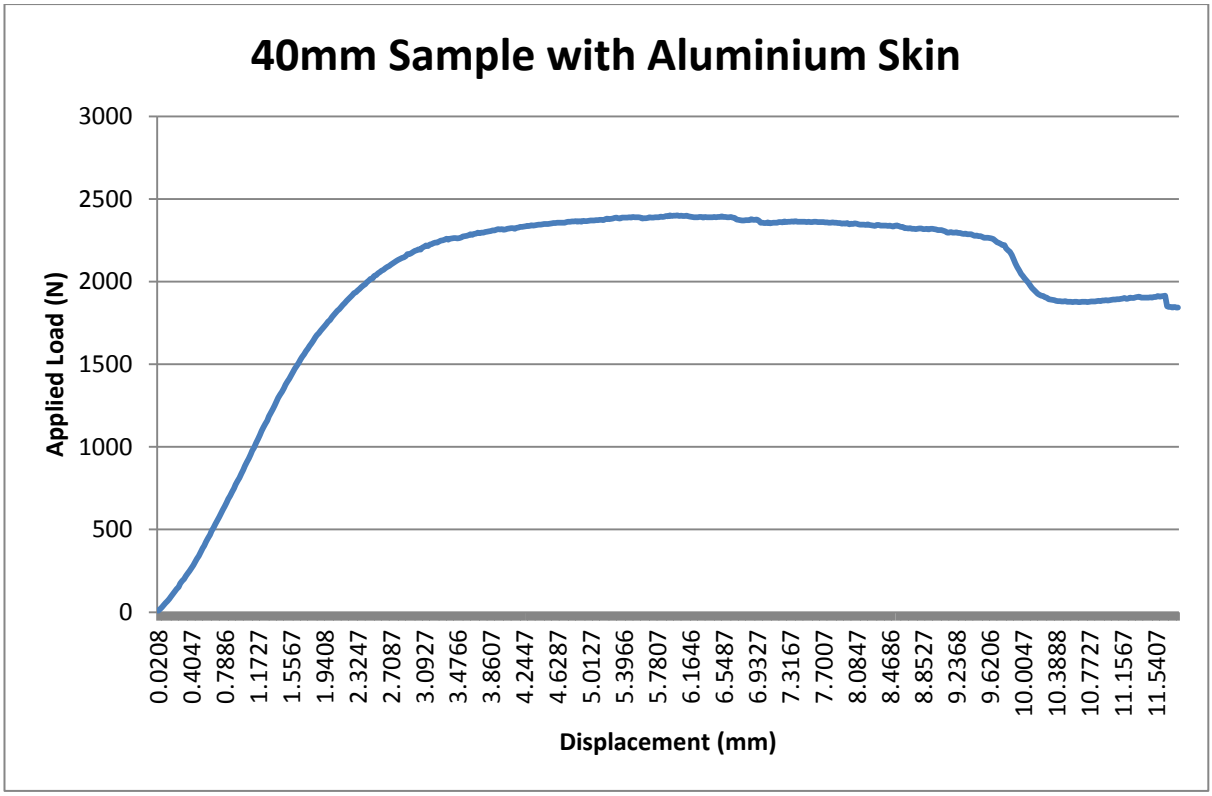

Figure 14 Results from the four point bending test for a 40mm sample with aluminium skins

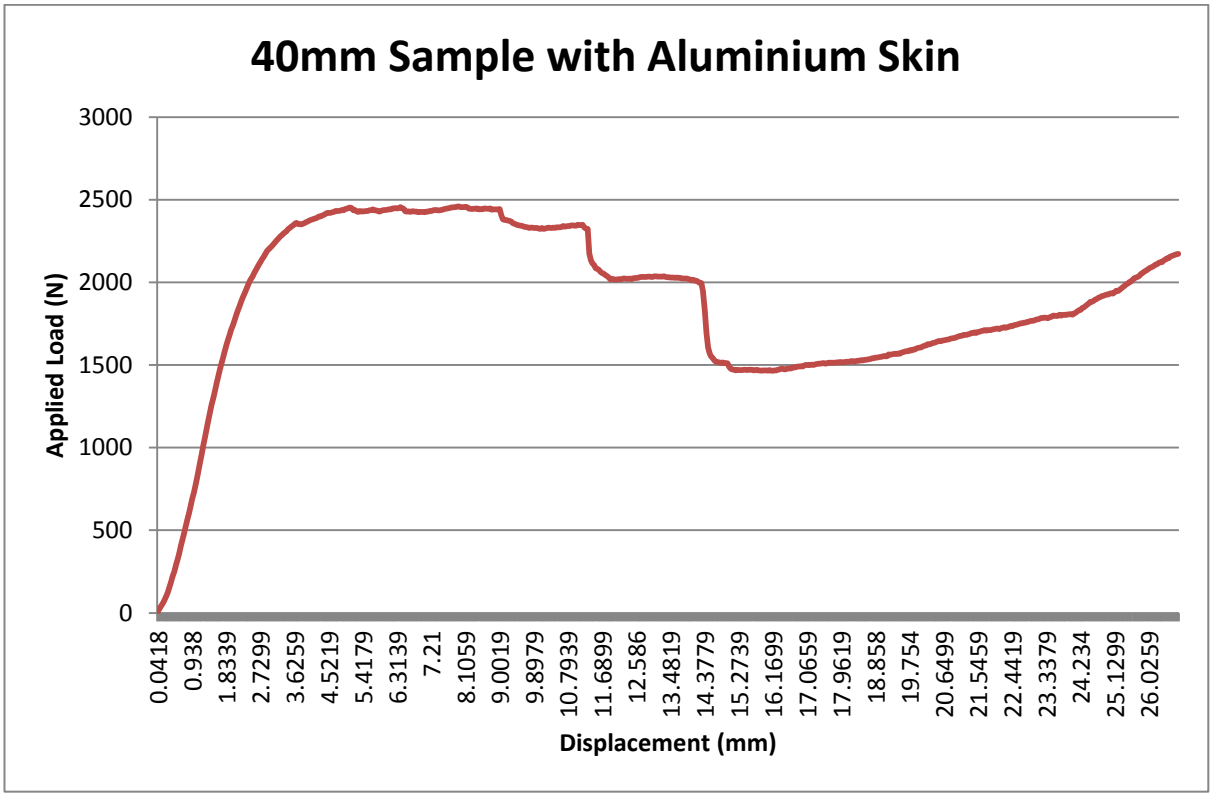

Figure 15 Results from the four point bending test for a 40mm sample with aluminium skin

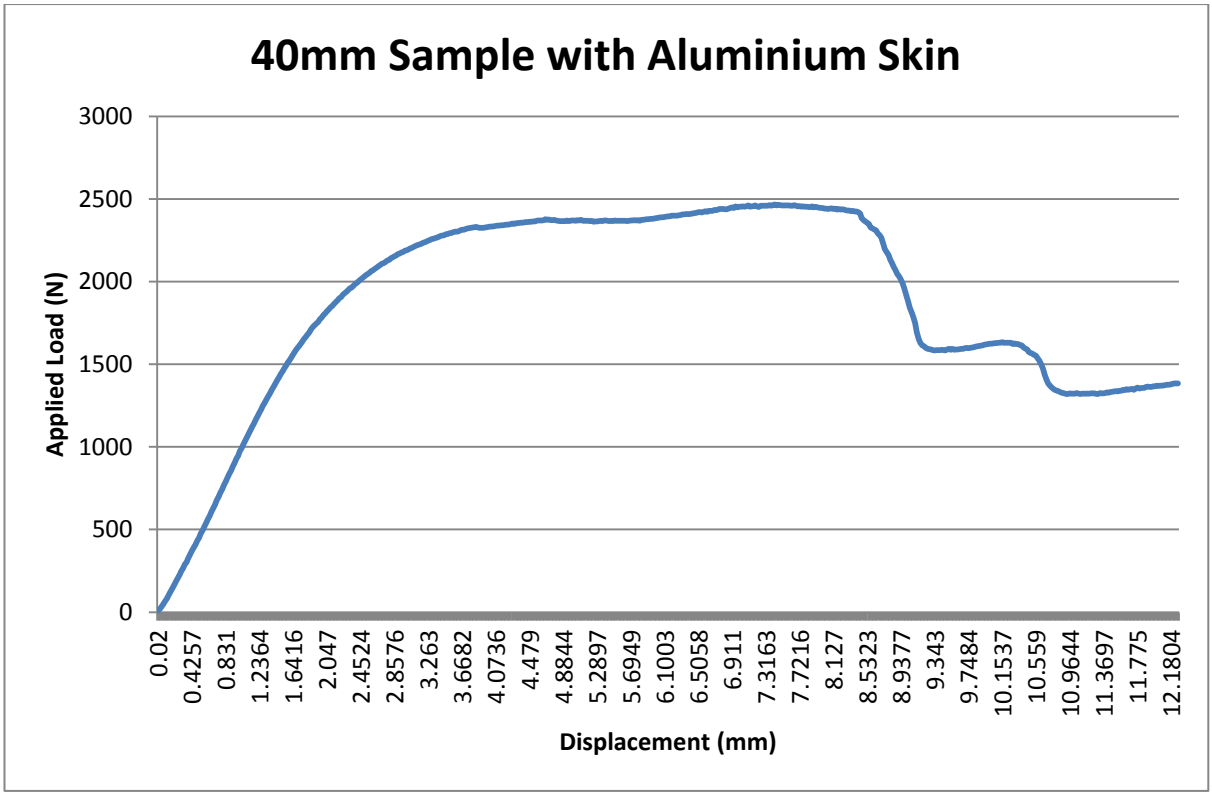

Figure 16 Results from the four point bending test for a 40mm sample with aluminium skins

5.1.2 40mm Fibreglass Skin Samples

Figure 17, Figure 18 and Figure 19 are the load verse displacement plots for the four point bending test of three different 40mm samples with fibreglass skins. Using Equation 21and substituting in two different values of the applied load and the measured deflection the modulus of elasticity and shear modulus has been found by solving the simultaneous equation. The calculated shear modulus was found to be 13 MPa again. This is the same as the shear modulus which was calculated for the samples with the aluminium skins. This shows that these tests are accurate and that the difference between theses calculated values and the values listed in the manufacturers technical document are probably due to an under estimation of the shear properties by the manufacturer. This is probably because the lower percentile is usually used for specifications to ensure that the material is safe. The modulus for elasticity for the fibreglass skin has been found to be 39 MPa. There is nothing that we can really compare this value with due to the variations in modulus of elasticity for fiberglass laminates, however this value is very close to other values in the literature. (Zenkert 1997)

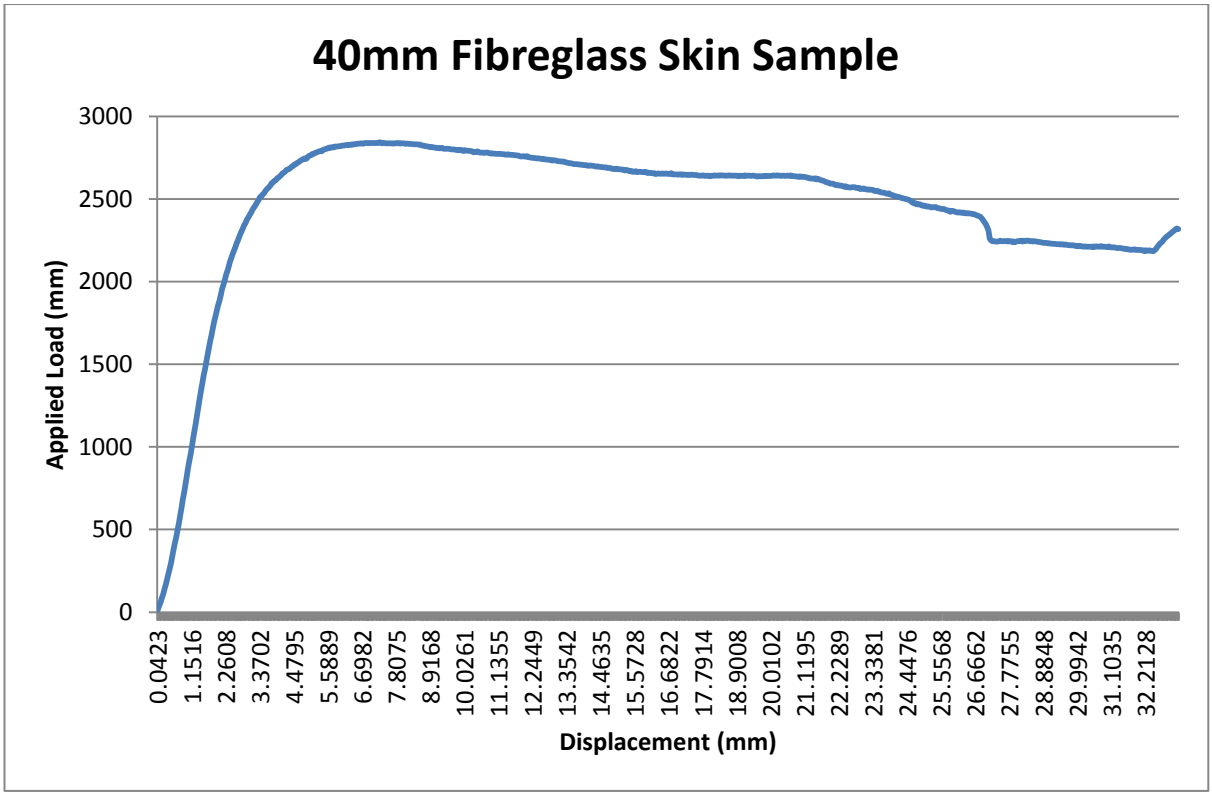

Figure 17 Results from the four point bending test for a 40mm sample with fibreglass skins

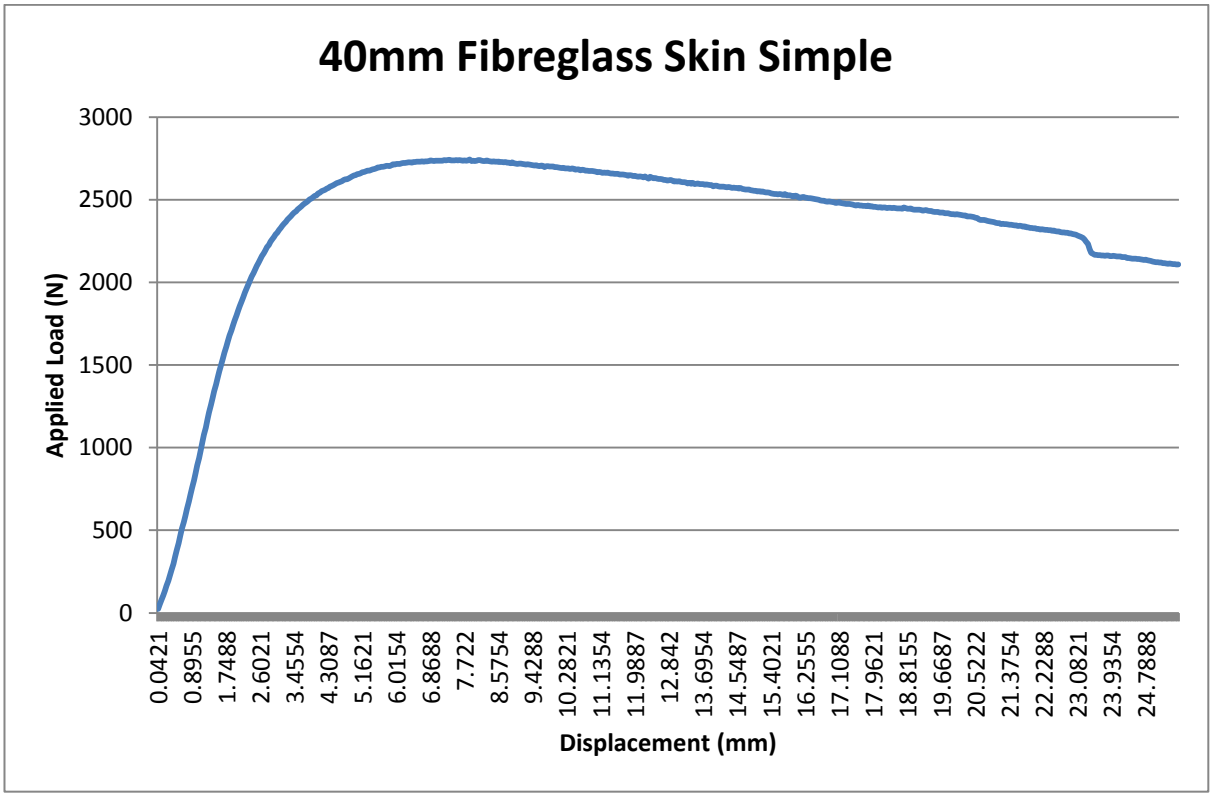

Figure 18 Results from the four point bending test for a 40mm sample with fibreglass skins

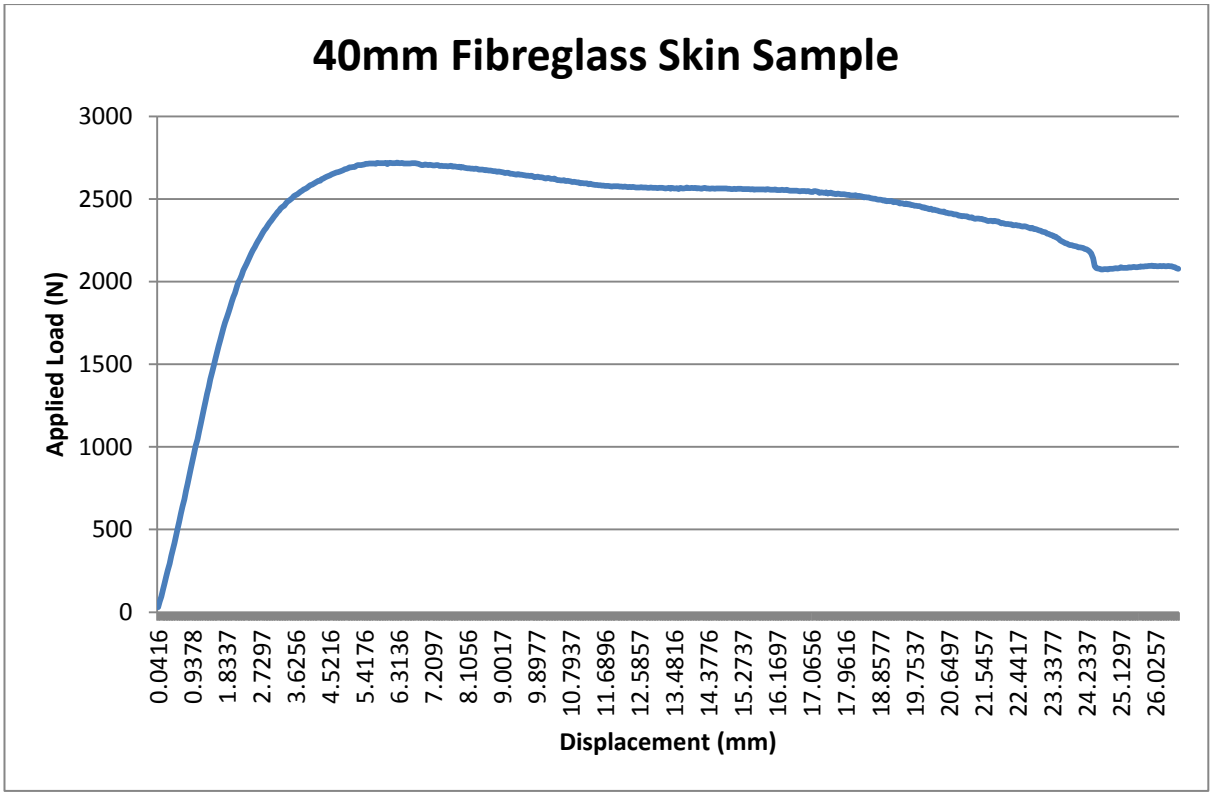

Figure 19 Results from the four point bending test for a 40mm sample with fibreglass skins

5.2 Dynamic Characterisation of Steel Samples

5.2.1 Long steel sample

A fairly good response has been achieved using the very hard stainless steel tip. It can be seen in Figure 20 that the first natural frequency being recorded is at 900 Hz. We know from the test using the medium hard white plastic tip that there is a natural frequency lower than this at 325 Hz. The reason that the first natural frequency has not been excited in this test is because the Frequency Response Function is only calculated for a 0.08 second time interval. As the steel sample is not very well damped, the vibration carries on passed the cut off for the function. This is why the medium hard white plastic tip has also been used for the steel sample to accurately determine the lower natural frequencies.

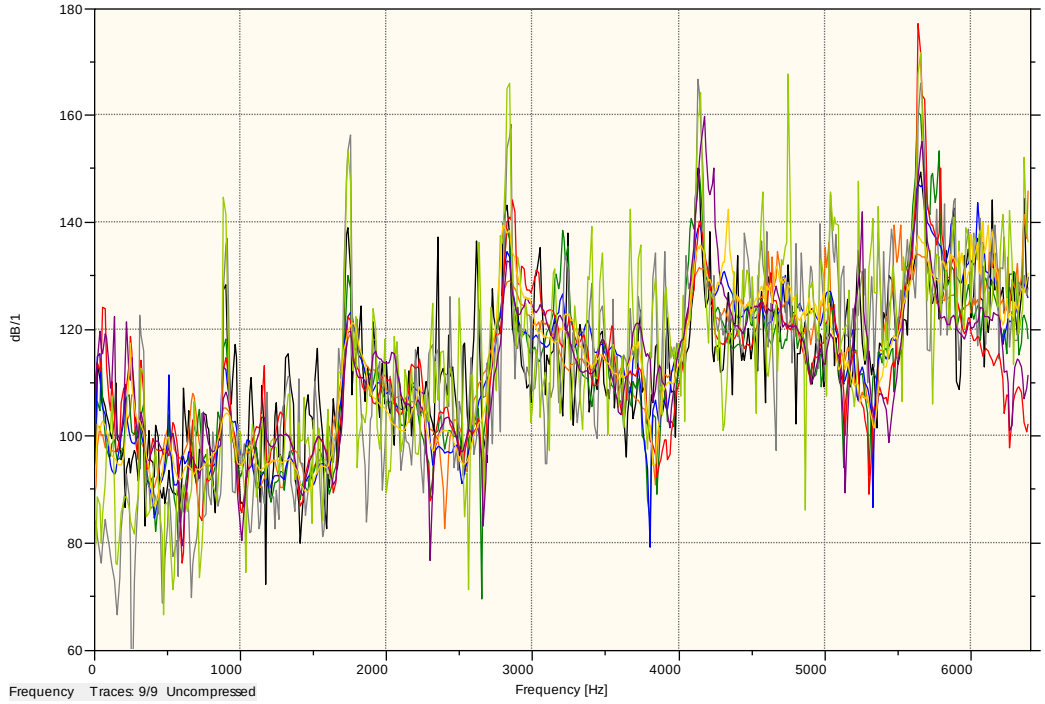

Figure 20 It can be seen from this graph that all traces have a similar shape, it is very hard to find the first natural frequency, however, the second, third, fourth and fifth can be easily read from the graph.

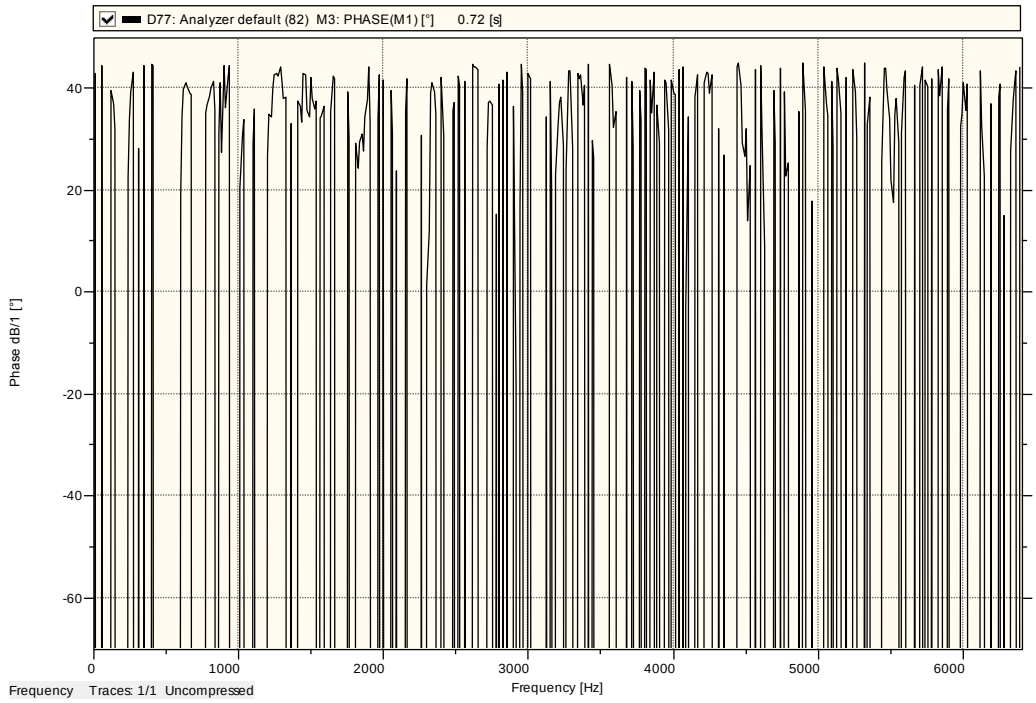

Figure 21 The phase plot of the FRF for the long steel sample using the stainless steel tip

Figure 20 clearly shows the second, third, fourth, fifth and sixth natural frequencies. The shape of this graph is also consistent with the shape expected when conducting a driving point test. This shape is where an anti-peak occurs just prior to a peak, which

corresponds to the natural frequency of the system. After a peak the graph then gradually declines to an anti-peak before rising suddenly to another peak, which represents another natural frequency.

The green trace shown in Figure 20 has the most notable peaks out of all the other traces, however it is also the noisiest of the traces. This trace also has a peak at about 4700 Hz which is not in any other of the traces. For this reason this has not been assumed to be a peak associated with a resonant frequency.

Figure 21 shows the phase plot of the frequency response for the long steel sample. It is expected that a change in phase in this graph will occur correspond to the natural frequencies. The phase plot usually goes from -180 to +180, however the phase plots produced by the LMS Program have not been able to produce this. Figure 21 does have a phase change corresponding to the peaks which were identified from the frequency response graph, however this graph also has a number of phase changes which do not correspond to any peaks. The phase changes are far too close together to be even considered as a natural frequency. For this reason this phase plot can't really be used to identify natural frequencies. The natural frequencies read from this graph have been presented in Table 5.

Table 5 Measured natural frequencies for the long steel sample

Mode number	Natural frequency (Hz)
1	325
2	900
3	1737
4	2825
5	4138

The Euler equation for beams can then be used to calculate the modulus of elasticity for the steel sample:

$$\omega_n = \frac{(\beta_n l)^2}{2\pi}\sqrt{\frac{EI}{\rho_l l^4}} \qquad 22$$

In order to find the natural frequency this equation is transformed to give:

$$E = \frac{\left(\frac{2\pi\omega_n}{(\beta_n l)^2}\right)^2 \rho_l l^4}{I} \qquad 23$$

When the first five natural frequencies are substituted into the equation, the modulus of elasticity for each mode has been found.

Table 6 Modulus of Elasticity for first five modes of vibration

Mode Number	Modulus of Elasticity (GPa)
1	193
2	195
3	189
4	183
5	175

The modulus of elasticity for steel is normally 200 GPa, and the values in Table 6 are fairly close to this value. As the mode number increases the value of the modulus of elasticity becomes less accurate and decreases. This is also expected because as the mode of vibration increases there is more influence of torsion and rotation which should be taken into account.

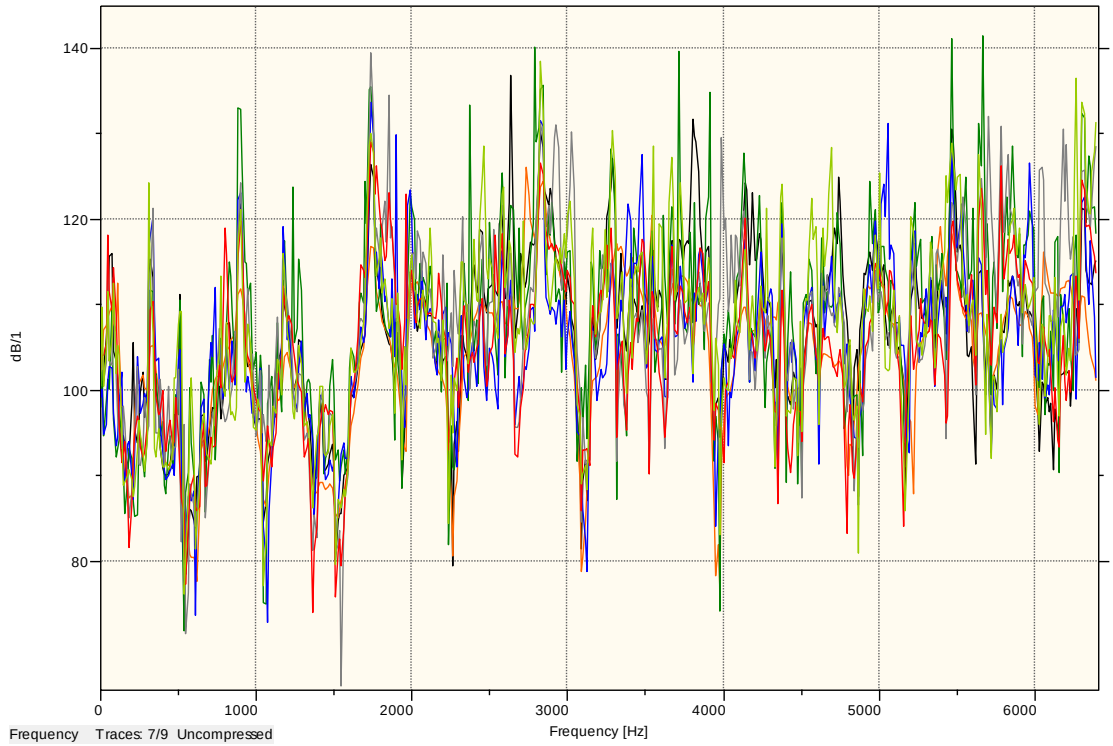

Figure 22 The frequency response function for the longer steel sample using the medium hard white plastic tip. The lower natural frequencies were able to be captured better using the white tip.

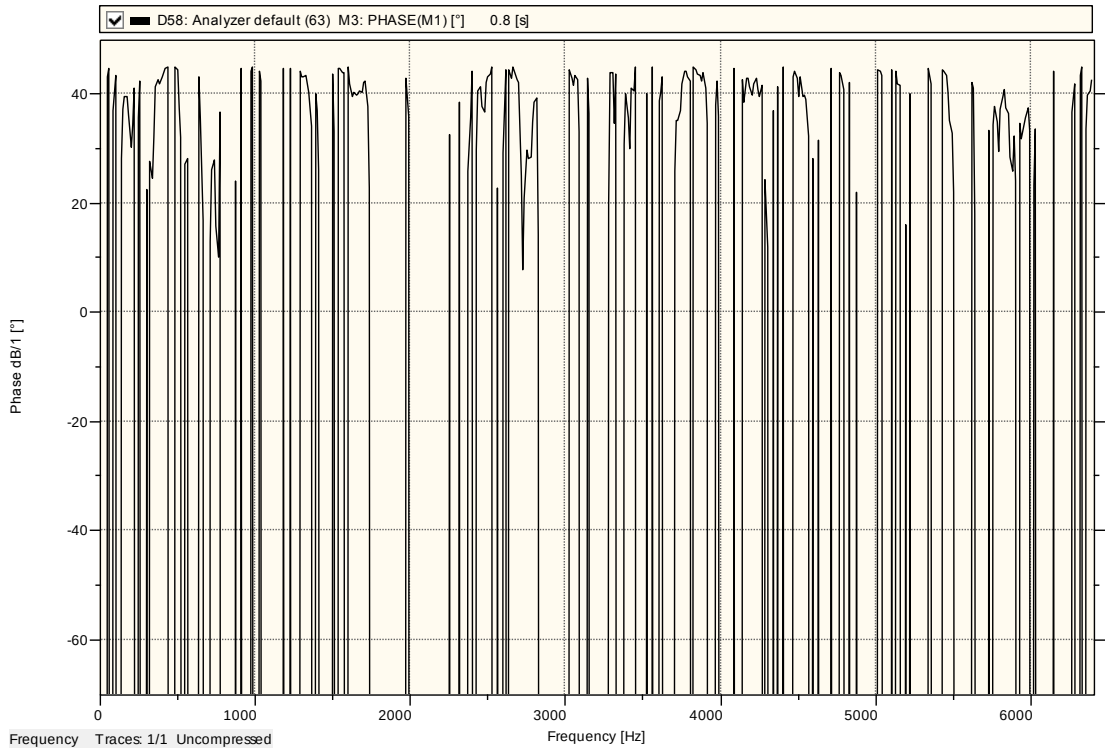

Figure 23 The phase plot of the FRF for the long steel sample using the medium hard white tip

5.2.2 Short steel sample

Both the stainless steel tip and the white plastic tip were again used for the shorter steel sample in order to ensure that both the higher and lower natural frequencies were excited well. Using the stainless steel tip there are two distinct peaks on the frequency domain graph which correspond with natural frequencies. The first of these is at about 1600 Hz and the second occurs at about 4300 Hz as can be seen in Figure 24.

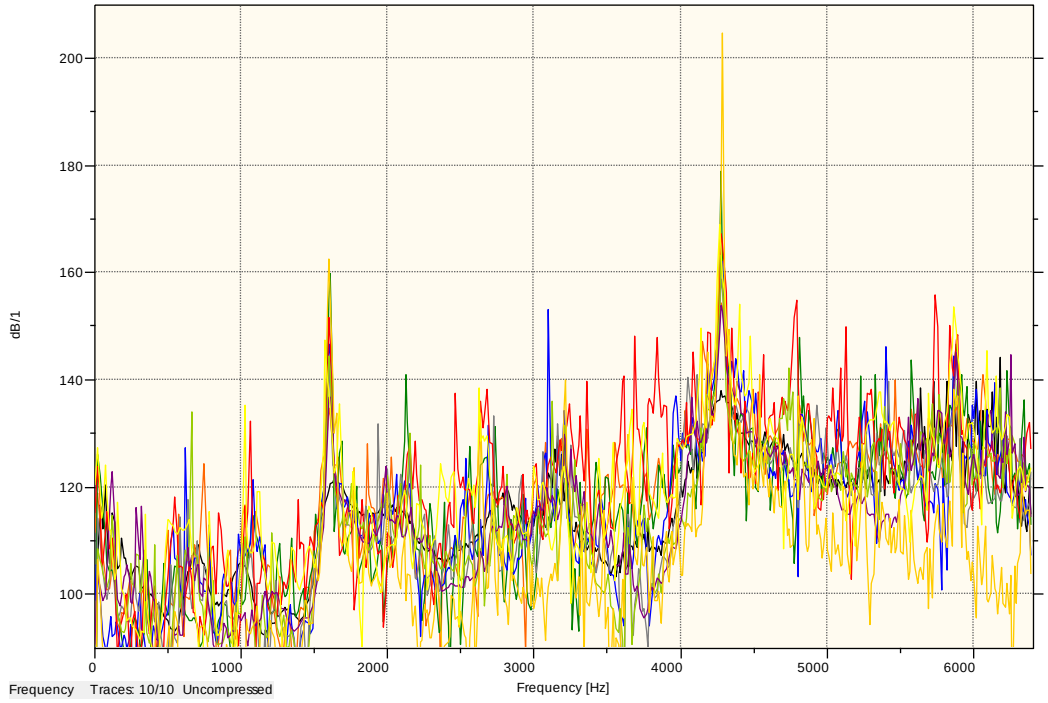

Figure 24 Frequency response function for the shorter steel sample when excited with the very hard stainless steel tip. The stainless steel tip tests shows very clearly the two natural frequencies within range.

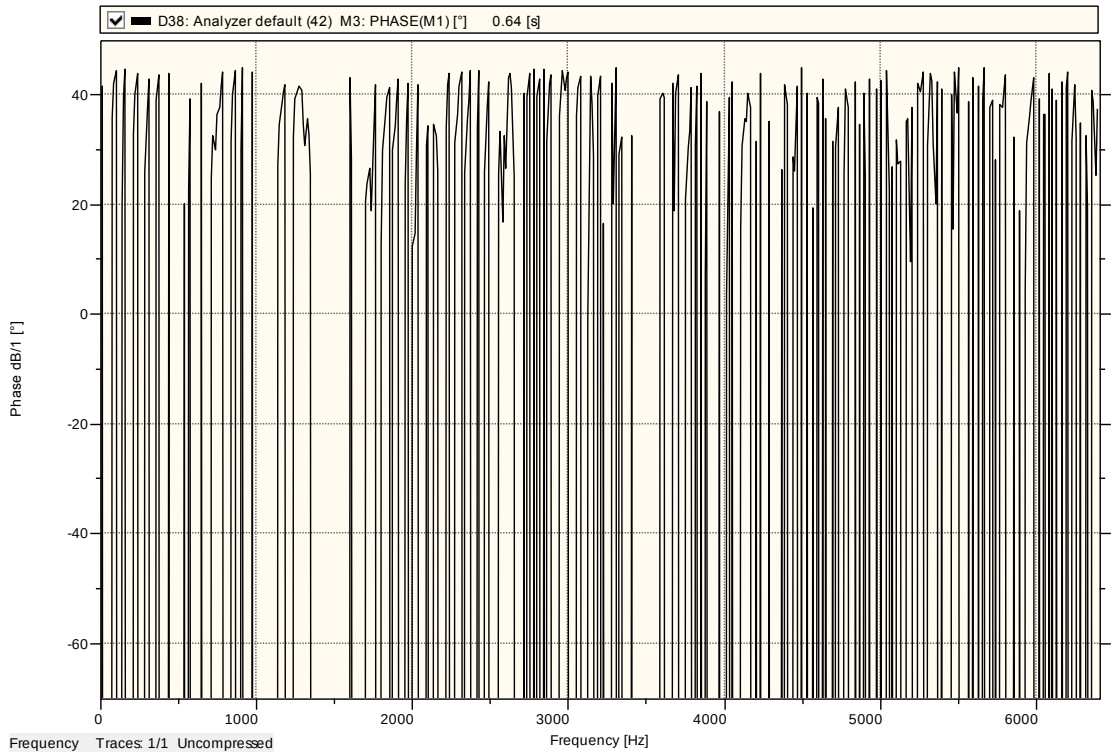

Figure 25 The phase plot for the FRF of the short steel sample using the very hard stainless steel tip.

Using the medium hard white plastic tip, only the first natural frequency is visible as a distinct peak. On this graph the second natural frequency does not appear to be excited at all. Some of the tests have peaks in the same area as the peaks when using the stainless steel tip, however they are still not very accurate.

For this reason, the average of the Figure 24 and Figure 26 was used to determine the first natural frequency, however the second natural frequency was determined from Figure 24 only when the stainless steel tip was used. The phase plots are not very clear again, and have not been used to identify the natural frequencies. They have however been included in the report for completeness.

Table 7 Measured natural frequencies for the short steel sample

Mode number	Natural frequency (Hz)
1	1605
2	4275

The natural frequencies for the first two modes have been presented in Table 7. Unfortunately due to the sampling bandwidth only the first two natural frequencies

could be determined for the steel sample. However due to the good response that was achieved for these natural frequencies, this should be enough to determine that the results are plausible.

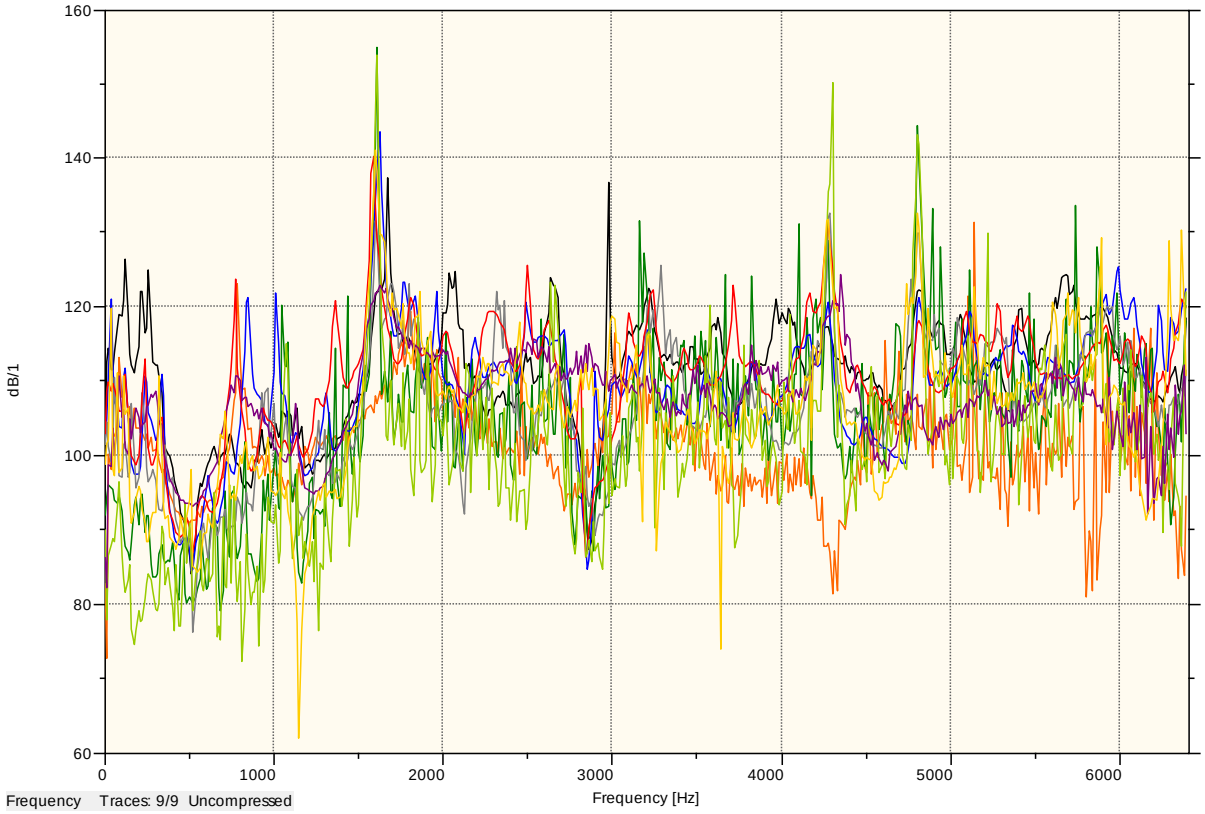

Figure 26 The white plastic tip shows the first natural frequency very well, however fails to excite the second natural frequency

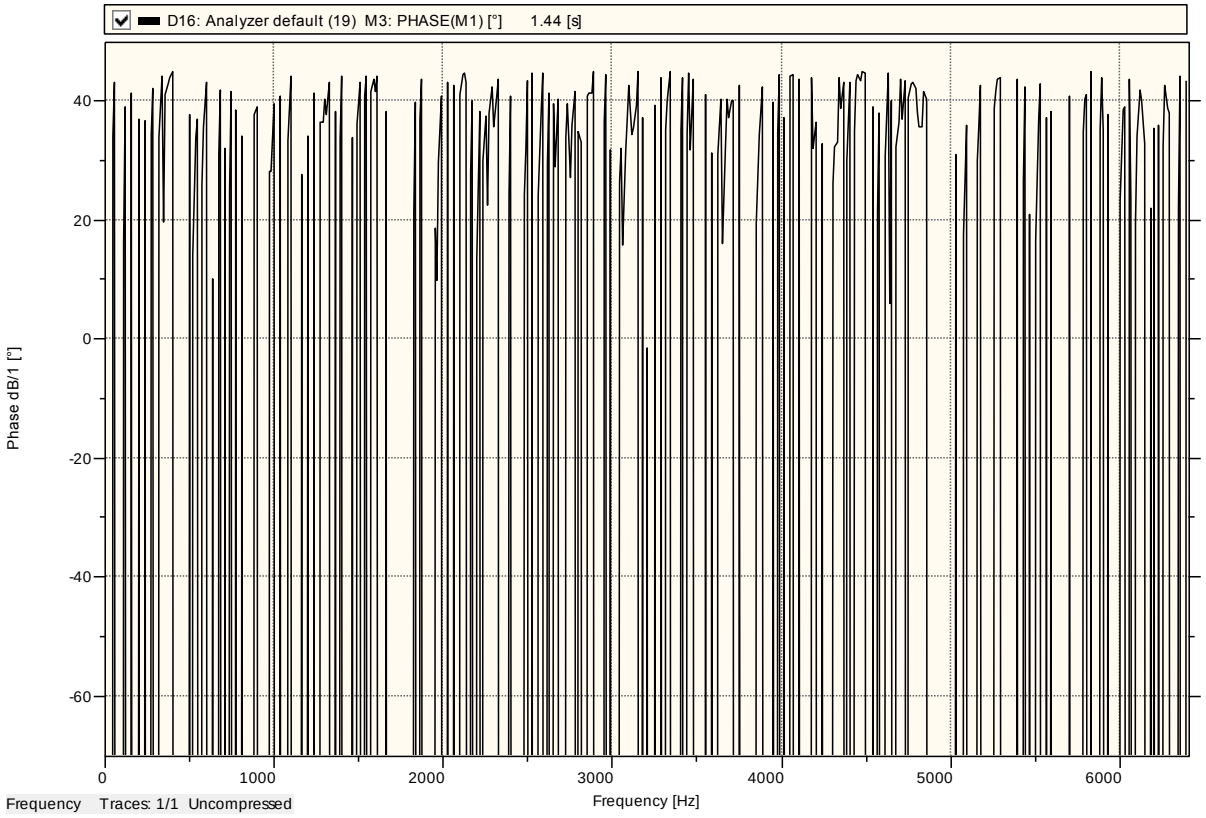

Figure 27 The phase plot of the FRF for the small steel sample using the medium hard white tip

The modulus of elasticity has once again been determined using the Euler equation for beams and the results for this have been presented in

Table 8 Calculated modulus of elasticity for short steel sample

Mode Number	Modulus of Elasticity (GPa)
1	190
2	178

These are once again fairly close to the theoretical modulus of elasticity for steel of 200 GPa, and once again the results become less accurate as the mode number increases. This shows that the method being used can accurately determine the modulus of elasticity for a homogenous material such as steel.

5.3 Dynamic characterisation of sandwich panels

5.3.1 Sandwich panel sample 1 – 20mm with Aluminium skins

It has proven to be considerably harder to obtain a good response when exciting the sandwich panels due to the high damping properties of the polypropylene honeycomb core. The very hard stainless steel tip has proven to provide the best response when testing the sandwich panels with aluminium skins. Figure 28 shows the response for the first sample with a sample bandwidth of 6400 Hz. As can be seen by the poor response, this sampling bandwidth was not suitable for this material. The sampling bandwidth was therefore changed to 3200 Hz and the sample was retested.

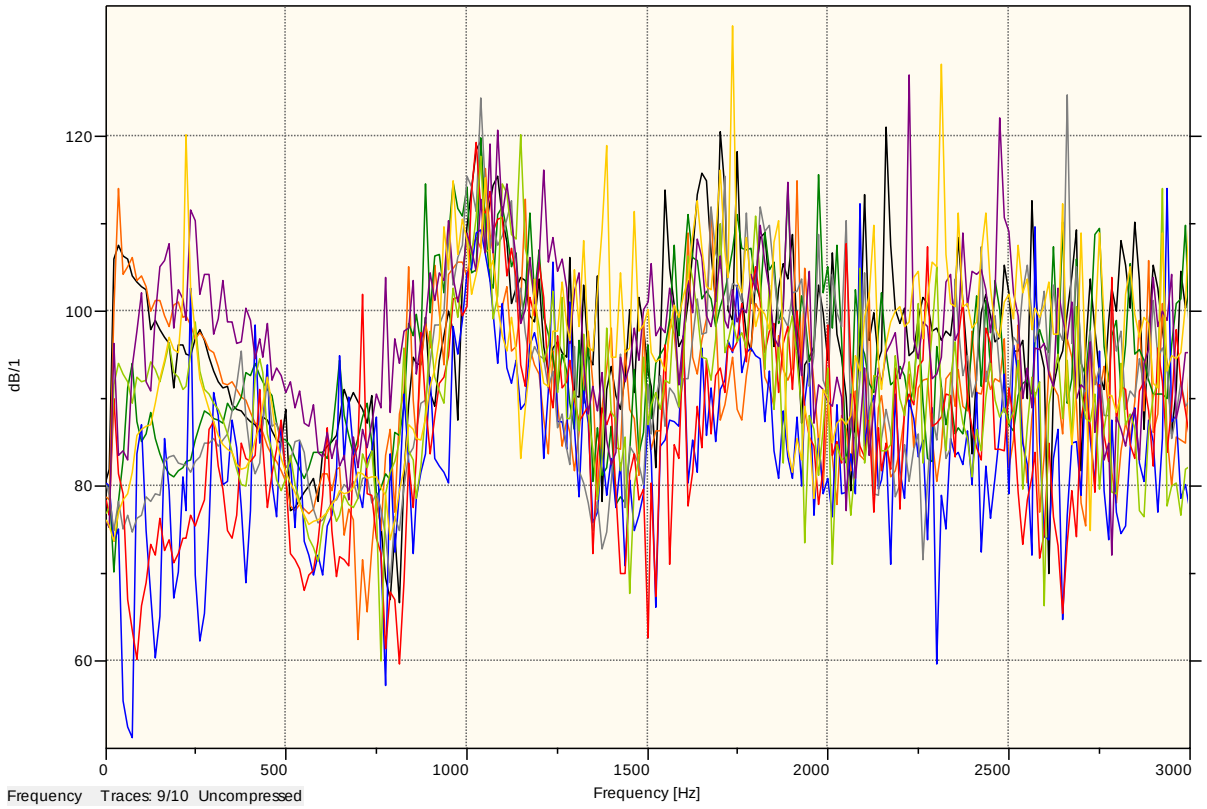

Figure 28 Frequency Response Function for Sandwich Panel 1 over a sample bandwidth of 6400 Hz. The first natural frequency can be seen quite easily at about the 1000 Hz mark. There may also be a natural frequency at the 1700 Hz mark

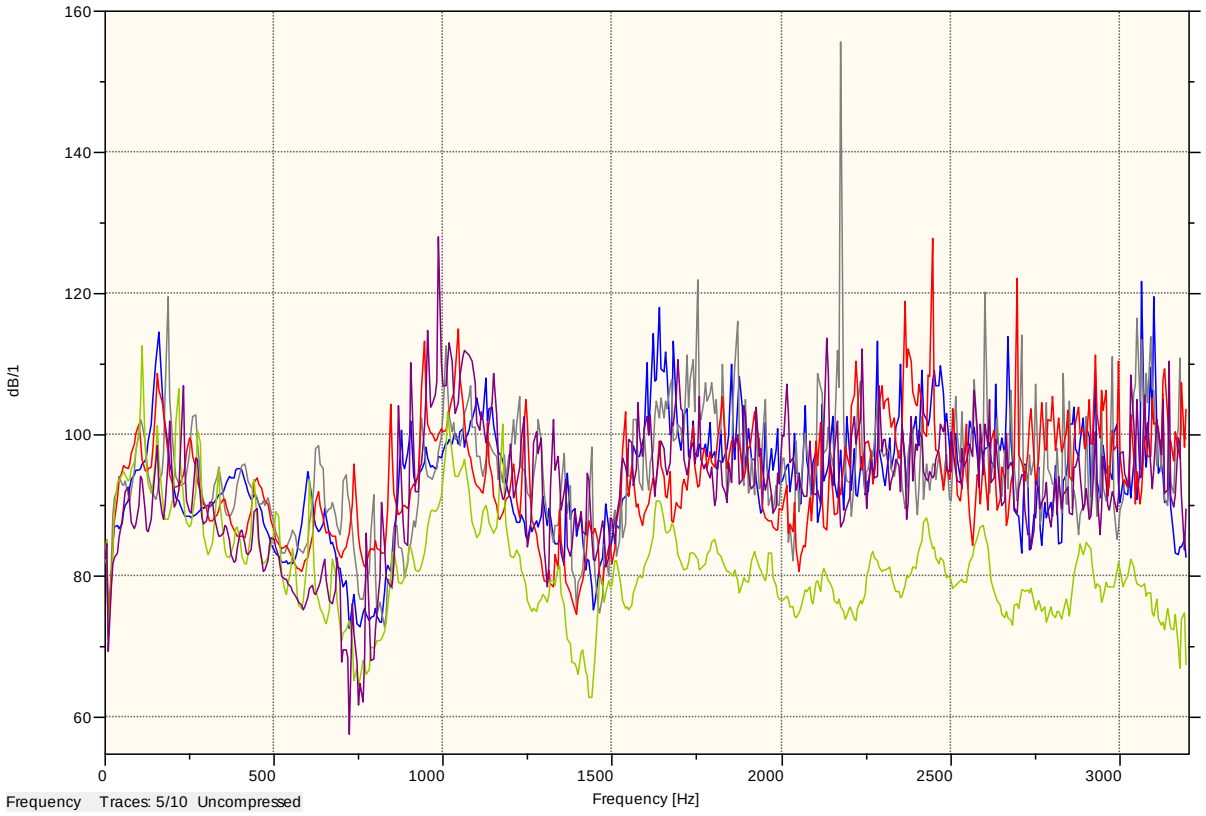

Figure 29 Frequency Response Function for sandwich panel 1 over a sample bandwidth of 3200 Hz

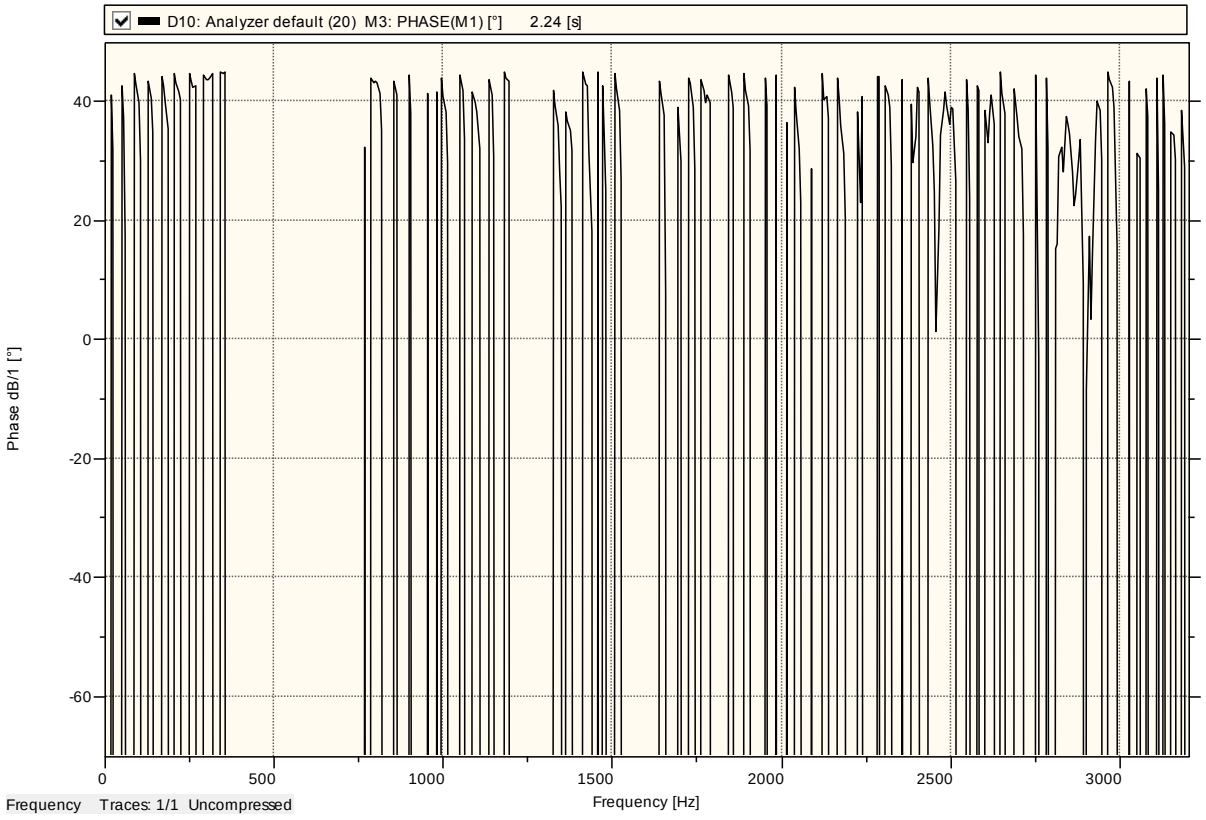

Figure 30 The phase plot of the FRF for sample 1

Figure 29 shows the frequency response function measured when a sample of 40mm aluminium skinned sandwich panel is excited over a sampling bandwidth of 3200 Hz. It can be seen from Figure 29 that the first natural frequency has been excited at around 200 Hz. A second peak, corresponding to a natural frequency, has been excited quite well at about 1000 Hz. After this the plot becomes quite noisy, however the shape of the graph suggests that there is a third natural frequency at around 1650 Hz. This third peak is not as defined as the first two, however it is fairly certain that there is a peak located somewhere in this area. It is interesting to note that the second and third natural frequencies identified in Figure 29 can also be identified in Figure 28, however the peaks in Figure 28 are not as distinct. Figure 30 shows the phase plot of the FRF, however this is once again a very poor phase plot and is not what is expected for modal testing of materials. The natural frequencies read from Figure 29 are shown in Table 9.

Table 9 Measured natural frequencies for sample 1

Mode Number	Natural Frequency (Hz)
1	215
2	1000
3	1640

These natural frequencies were substituted into Equation 23, and the modulus of elasticity for each mode has been identified. Assuming that the skins carry all of the bending, the moment of inertia has been calculated using the parallel axis theorem in order to calculate the moment of inertia for the skins only. These have been presented in Table 10.

Table 10 Calculated modulus of elasticity for sample 1

Mode Number	Modulus of Elasticity (GPa)
1	0.7
2	1.9
3	1.3

The results presented in Table 10 vary greatly with a range from 0.7GPa to 1.9GPa, which shows that the results for this sample have not been very accurate. One of the reasons that these results vary so greatly may be due to the weight of the accelerometer and the tension in the chord attached to the accelerometer. As the sandwich panel is so light the weight of the accelerometer may have a big effect on the recorded response. As it has been assumed that the aluminium skins carry all of the bending, it is expected that the modulus of elasticity for this beam will be the same as the modulus of elasticity for aluminium which is 70 GPa. The calculated modulus of elasticity is considerably lower than this which shows that something has gone wrong with the test.

5.3.2 Sandwich Panel 2 – 20mm with Aluminium Skins

To ensure the results being obtained were accurate, a second 20mm aluminium skin sandwich panel was tested. A sample bandwidth of 3200 Hz was used and the measured response for a number of tests can be seen in Figure 31. Figure 32 shows the phase plot of the FRF for this sample, this is a much better phase plot. It shows that there is a phase change corresponding to the second peak which confirms that this is a natural frequency. This phase plot is still not the correct plot which is expected as it should have a range of +180 to -180.

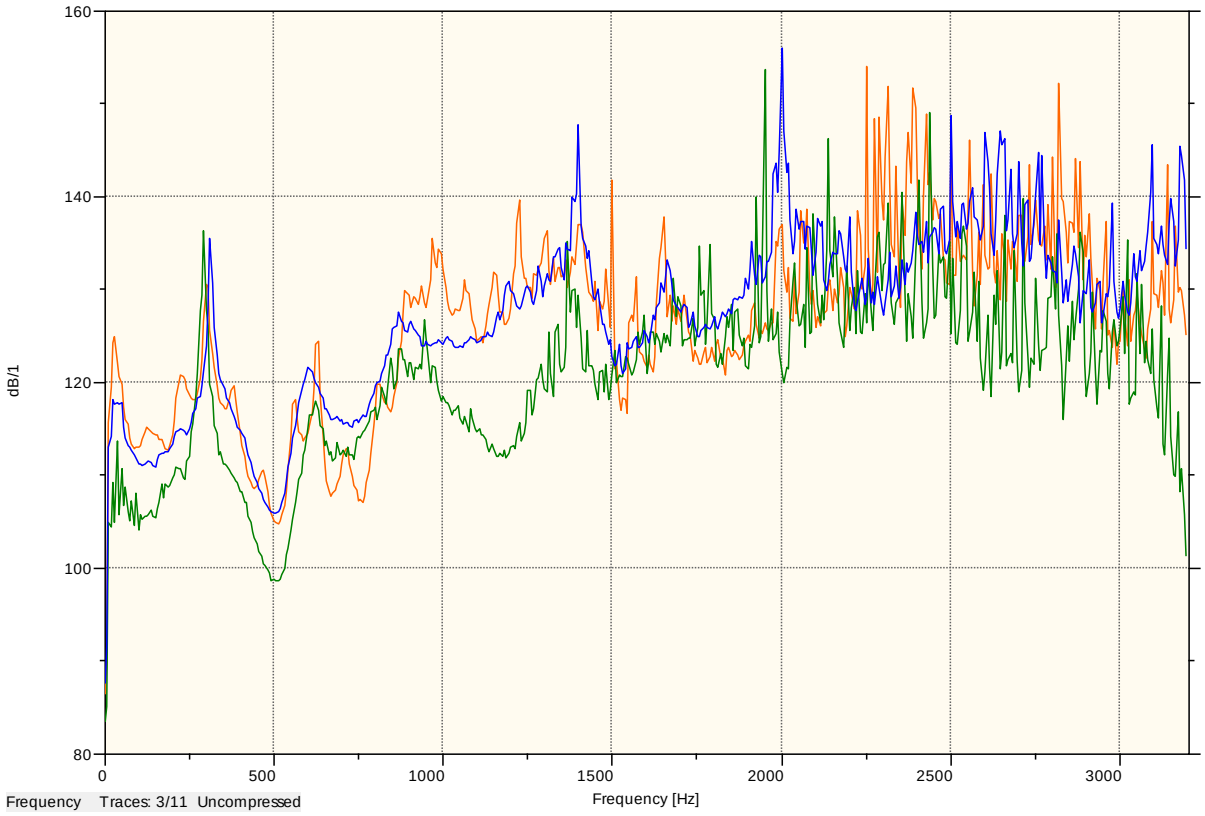

Figure 31 Frequency Response Function for sandwich panel 2 over a sample bandwidth of 3200 Hz

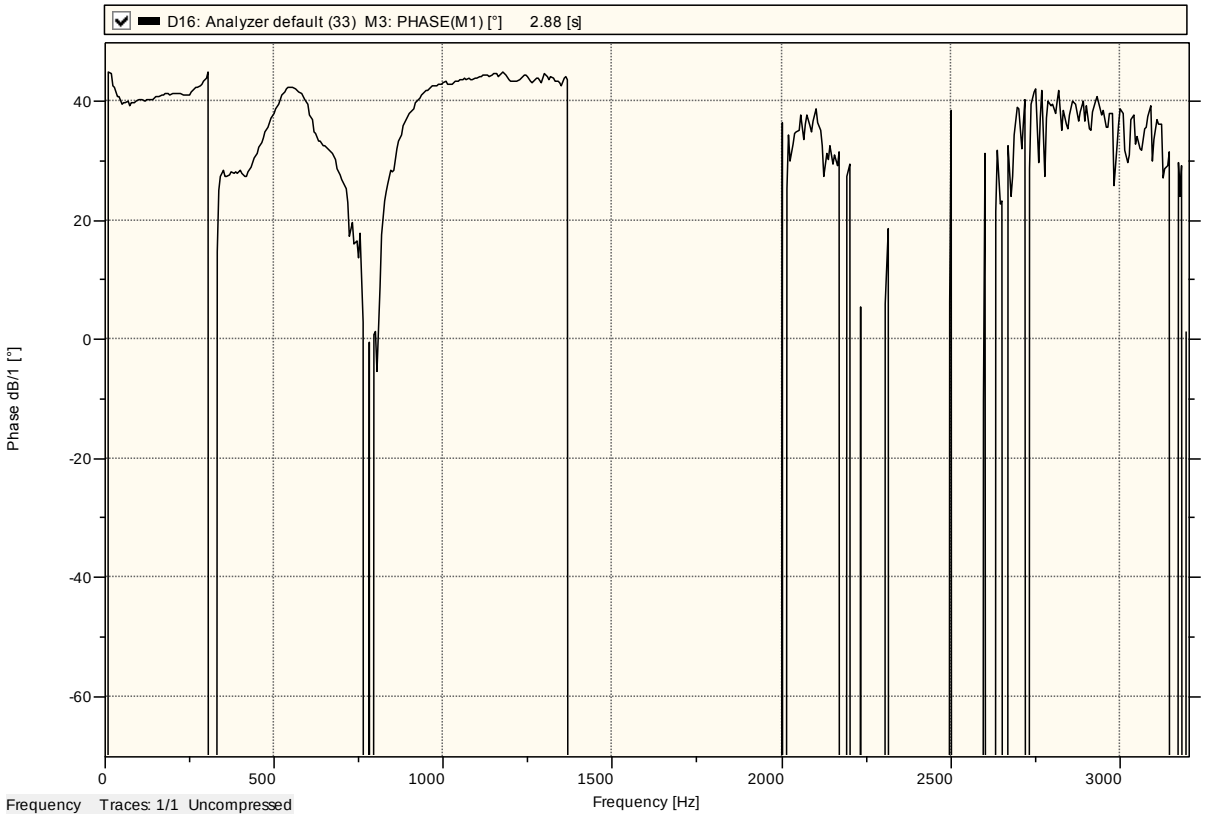

Figure 32 The phase plot of the FRF for sample 2

The first peak identified in Figure 31, was at about the 300 Hz mark. This mode had been excited very well with all of the tests displaying this peak quite distinctively. There is a small peak at around 600 Hz, however this has not been assumed to be corresponding to a bending natural frequency. This peak may be present due to the excitation of a torsional or axial natural frequency. The second mode which has been excited has been interpreted as being at about the 950 Hz mark. The three different tests show this peak in different positions, so the average of the three tests was taken. There is a third peak which has been identified at around the 1450 Hz mark. Again this peak varies between the three tests, however the three peaks are in roughly the same area, and the average has again been taken. There is also a peak which has been excited at about 2000 Hz. This peak has been fairly well excited in all three tests, so this is probably another natural frequency, if not a bending natural frequency, it may be an axial or torsional natural frequency.

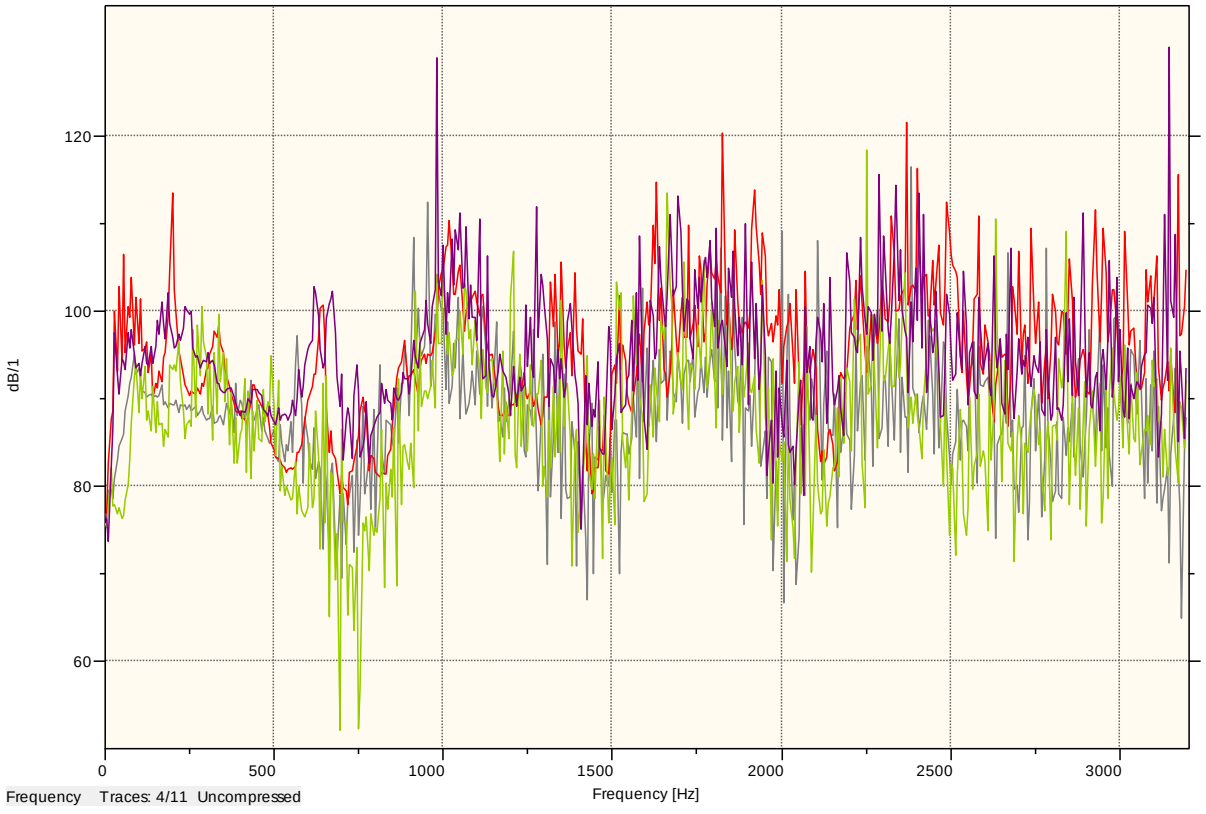

Figure 33 Alternate Frequency Response Function for sandwich panel 2 over a sample bandwidth of 3200 Hz.

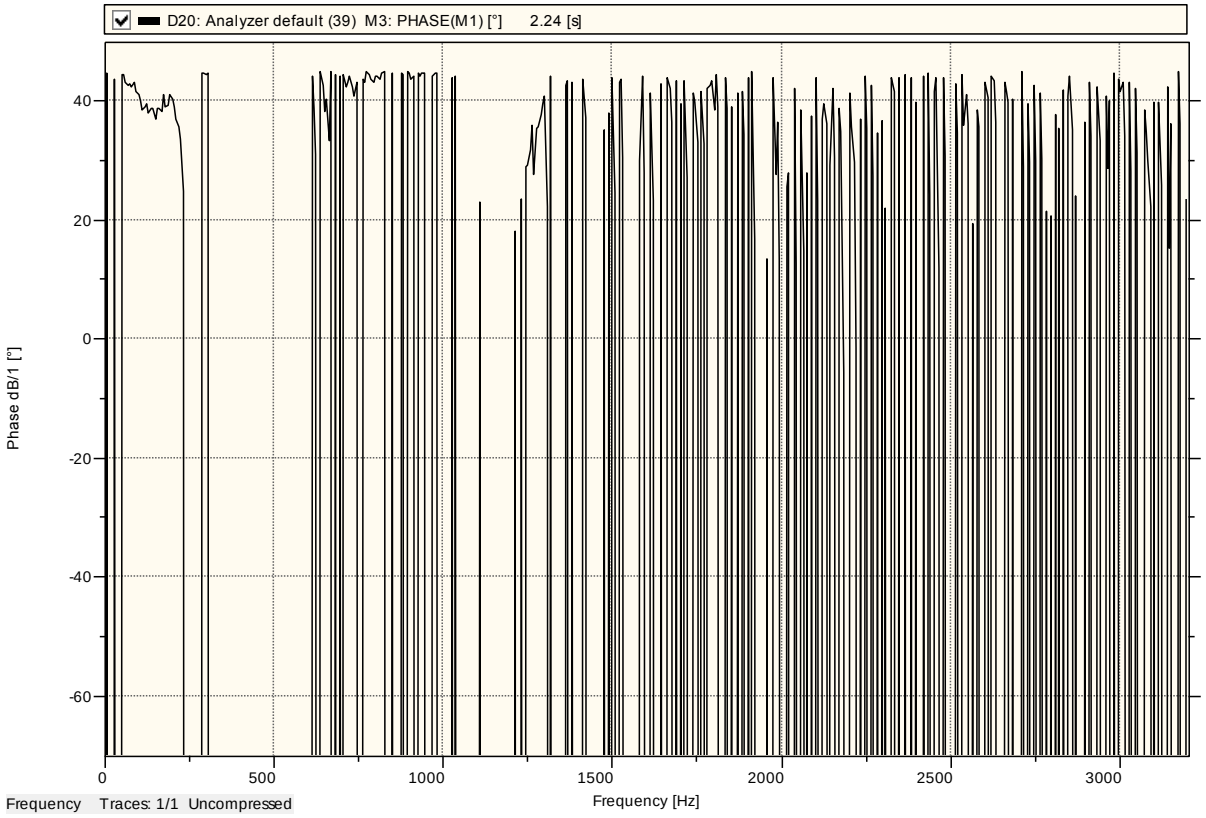

Figure 34 The phase plot of the FRF for sample 2

There were another four tests taken which corresponded fairly closely to the natural frequencies achieved with the first sample. Figure 33 shows another set of recorded responses with sample 2, and it can be seen that the location of the peaks for these tests vary substantially from the measured responses in Figure 31. This shows the complexity of performing a dynamic test where there are so many factors affecting the results. There has been a change in the parameters to produce another grouping of the frequency response. The first natural frequency in Figure 33 has not been excited very well, however it appears to be evident at around the 200 Hz mark. There is once again a peak at the 650 Hz mark which has been assumed not to correspond with a bending natural frequency. The second mode is quite distinct and can be seen at about the 1000 Hz mark. There also looks to be a peak at around the 1750 Hz mark however this peak is too noisy to accurately obtain a value for the natural frequency. One thing that may have caused a change in this frequency response may have been the hitting technique or the force imparted on the sample. To investigate this Figure 35 and Figure 36 show the time domain response for the two tests. It can be seen that the amplitude of Figure 35 ranges from 2000 to 6000, which is a lot greater than the amplitude of the traces in Figure 36 which ranges from 0 to 100.

This clearly shows that the results can be greatly affected by the amount of energy which is imparted on the sample. In this instance the test with the greater amplitude would be thought to give the better results as more natural frequencies should have been excited.

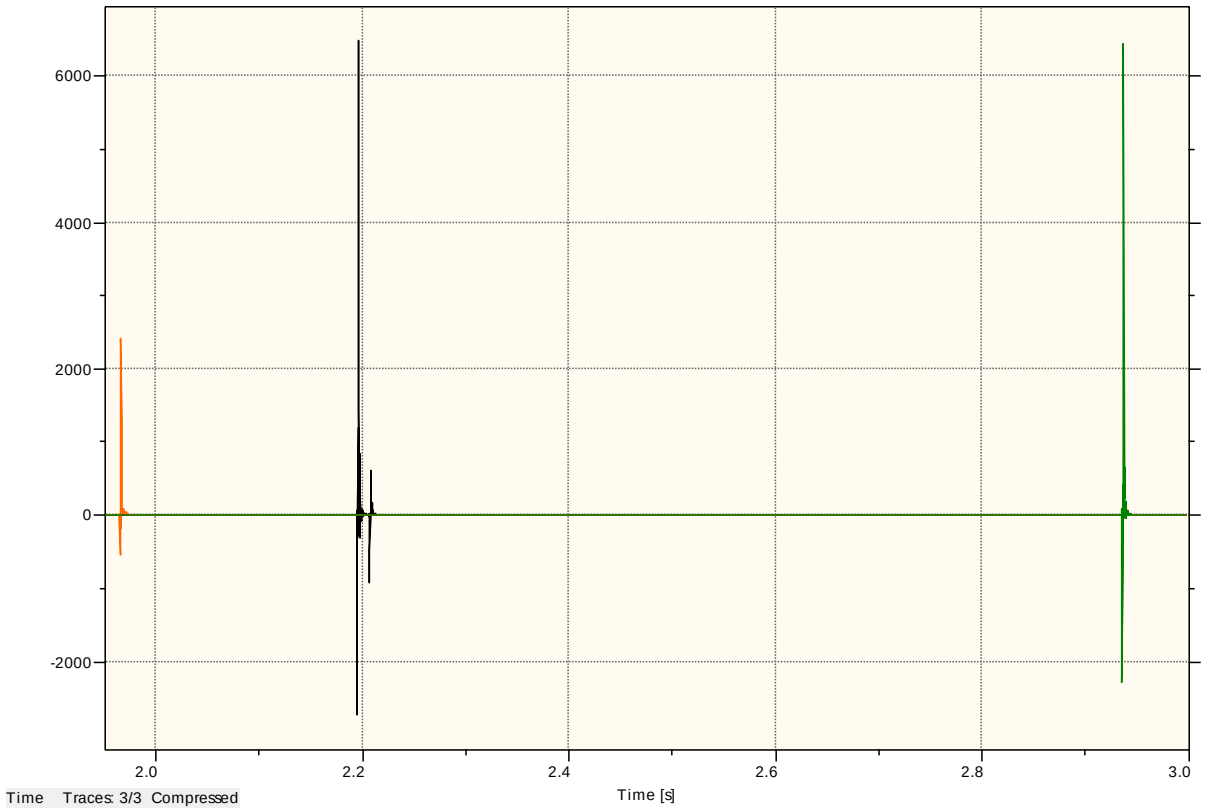

Figure 35 The time response for the three tests shown in Figure 31

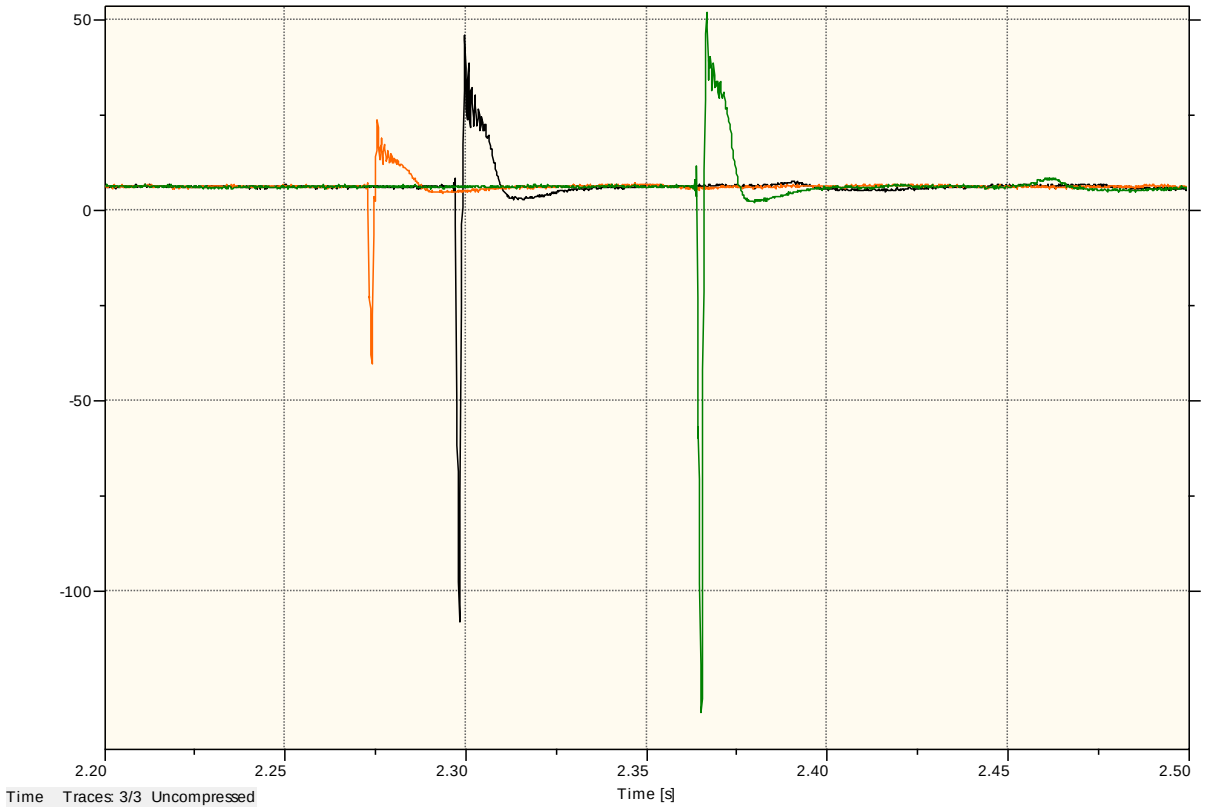

Figure 36 The time response for the three tests shown in Figure 33

Table 11 Comparison of natural frequencies read from graphs

Mode	Figure 31	Figure 33
1	300	200
2	950	1000
3	1400	

The figures in Table 11 show that the main variance between the 2 lots of results is between the first natural frequencies, with the second natural frequency being a lot closer between the two.

Table 12 The modulus of elasticity (GPa) calculated

Mode	Figure 31	Figure 33
1	1.36	0.6
2	1.8	1.99
3	1.01	

Once again these recorded results are considerably different for different modes. Even the highest of the calculated results is still considerably lower than the expected value of 70 GPa. One thing which may be causing these low values is the wrongful identification of the peaks as natural frequencies. This was checked by substituting some of the higher natural frequencies in as the first mode, however they still did not correspond with the expected modulus of elasticity. The main factor causing these poor results is thought to be the weight of the accelerometer compared to the low weight of the sandwich panel.

5.3.3Sandwich panel sample 3 – 40mm with Aluminium sample

Similarly to sample 1, sample 3 was initially tested using a sample bandwidth of 6400 Hz. The response using this bandwidth has been presented in Figure 37. Once again this did not give a very clear frequency response graph, however it can be seen that the first peak on the graph is around the 250 Hz mark. There is also a small peak at around 750 Hz. A third peak can be identified at around 1350 Hz.

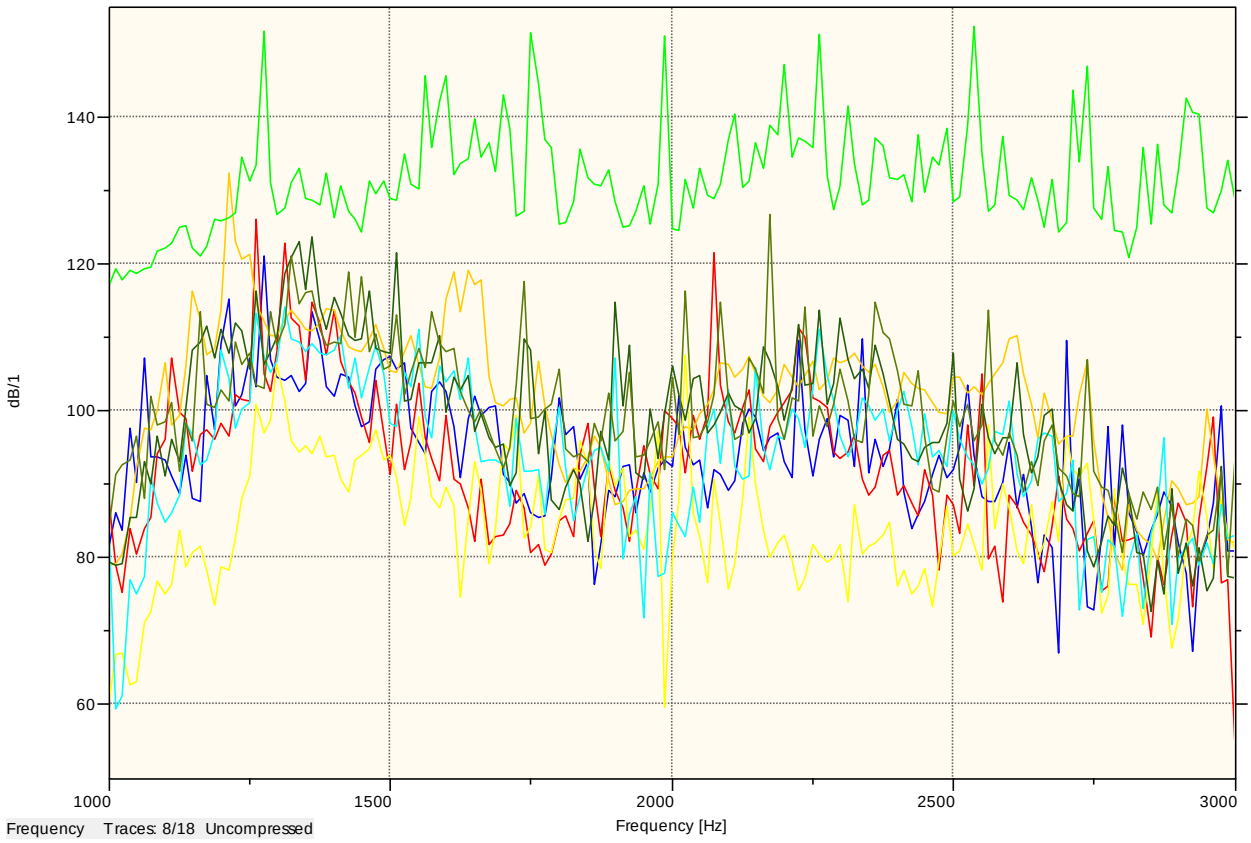

Figure 37 Frequency Response Function for sandwich panel 3 over a sample bandwidth of 6400 Hz. It is clear from this diagram that there is a natural frequency at around 1300 Hz, it is unclear whether this is the first natural frequency or if there is a lower one around 250 Hz. I think the initial peak is just due to the elasticity of the string.

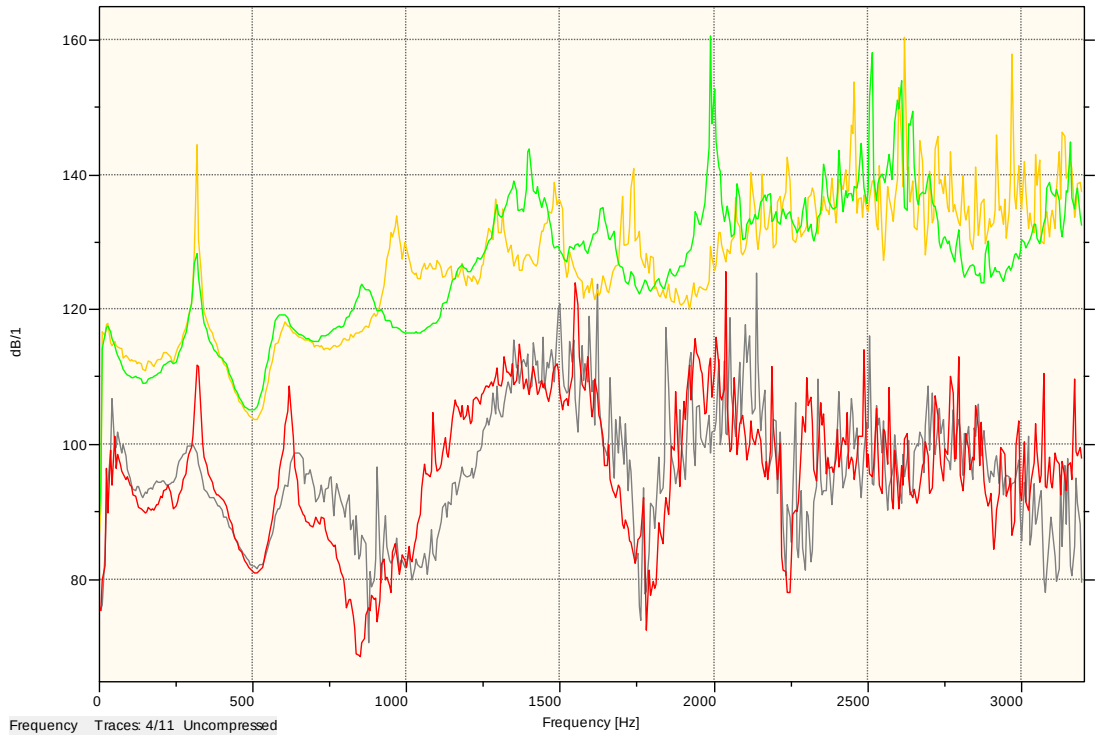

Figure 38 Frequency Response Function for sandwich panel 3 over a sample bandwidth of 3200 Hz.

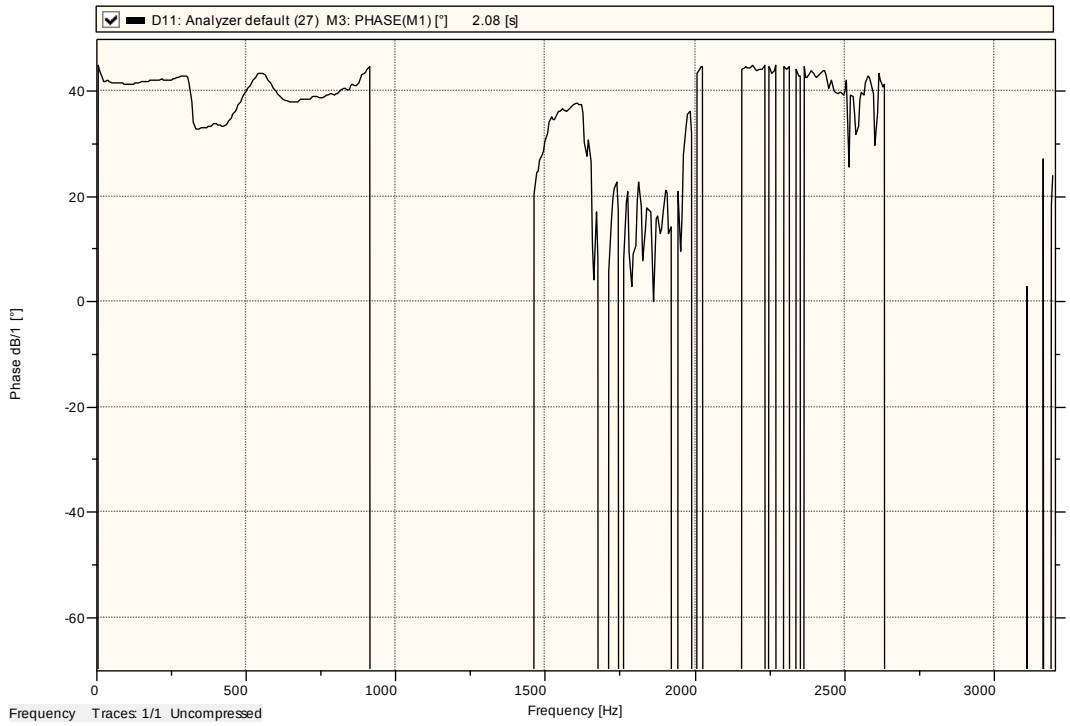

Figure 39 The phase plot of the FRF for sample 3

Sample 3 was then tested using a sample bandwidth of 3200 Hz. The measured frequency response for these tests can be seen in Figure 38. The initial very low peak is assumed to be due to the elasticity of the poly wire which was used to simulate free-free boundary conditions. The first natural frequency in this graph is quite distinct and shows up in all of the recorded tests. This peak occurs at about 300 Hz. There is then a quite distinct peak which occurs at a frequency of about 600 Hz. There is also a peak which occurs somewhere between 1400 Hz and 1600 Hz, which is distinct, but varies between different tests. Finally it looks as though there is a peak which occurs at around 2000 Hz. The phase plot has also been shown in Figure 39, however this does not really correspond with the FRF at all. There is a phase change at around 900 Hz however, this does not correspond with any distinct peaks in the FRF. For this reason the phase plot has again not been used to calculate the natural frequency.

Table 13 Measured natural frequencies and calculated modulus of elasticity for sample 3

Mode	Natural Frequency (Hz)	Modulus of Elasticity (GPa)
1	300	0.29
2	600	0.15
3	1450	0.24

The calculated modulus of elasticity for sample 3 is very low when compared to the expected value of 70 GPa. The calculated modulus of elasticity based on the four point bending test was calculated as 73 GPa which confirms that this result should be around the 70 GPa mark. This result strengthens the conclusions that are already being made from the previous two samples that this method is unsuitable for calculating the modulus of elasticity for these types of sandwich panels.

5.3.4 Sandwich Panel 4 – 40mm with Aluminium Skins

Another sample of 40mm aluminium skin sandwich panel was tested, and the measured frequency response can be seen in Figure 40. A sample bandwidth of 3200 Hz was used, and a fairly consistent response was achieved. The peak below 100 Hz

has been assumed to be due to the elasticity of the poly wire and has not been analysed as a natural frequency. The first mode has been identified at a frequency of 310 Hz, where there is a very distinct peak which has been excited in all of the tests shown on the graph. There is a second peak at around 600 Hz, however this has not been excited very well, and therefore is probably not a bending natural frequency. For this reason the second natural frequency which has been excited has been assumed to be at about 940 Hz. This has been successfully excited in the majority of the tests, however it has failed to be excited in a few of the traces. There is a third peak in the graph somewhere between the frequency of 1250 Hz and 1500 Hz. It is obvious that the is a natural frequency somewhere in this range, however the different tests show the peaks in different positions across this range. An average of these tests has been taken and the third natural frequency has been adopted as 1375 Hz. The phase plot has again been shown in Figure 41, and once again the first phase change occurs at the second identified natural frequency. If this is taken as the first natural frequency then the modulus of elasticity is taken as 4 GPa which is slightly better, however it is still considerably lower than the expected value of 70 GPa.

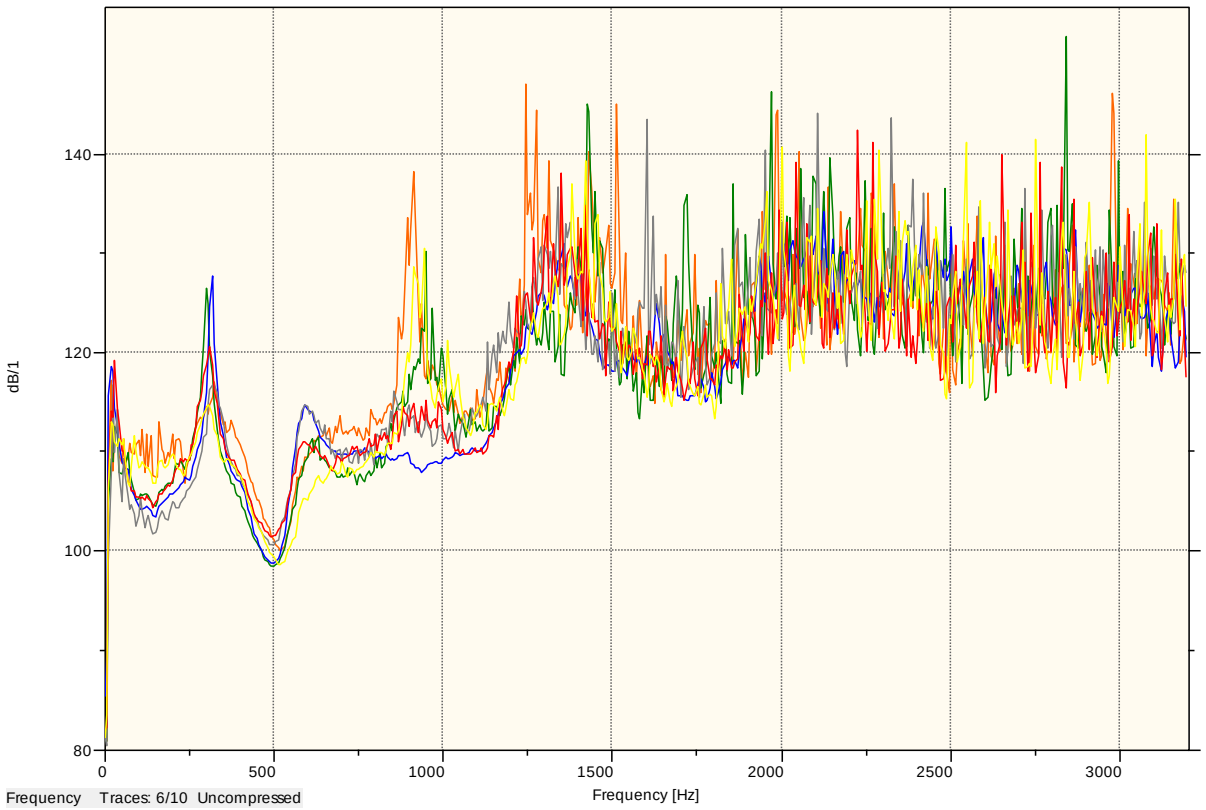

Figure 40 Frequency Response Function for sandwich panel 4 over a sample bandwidth of 3200 Hz

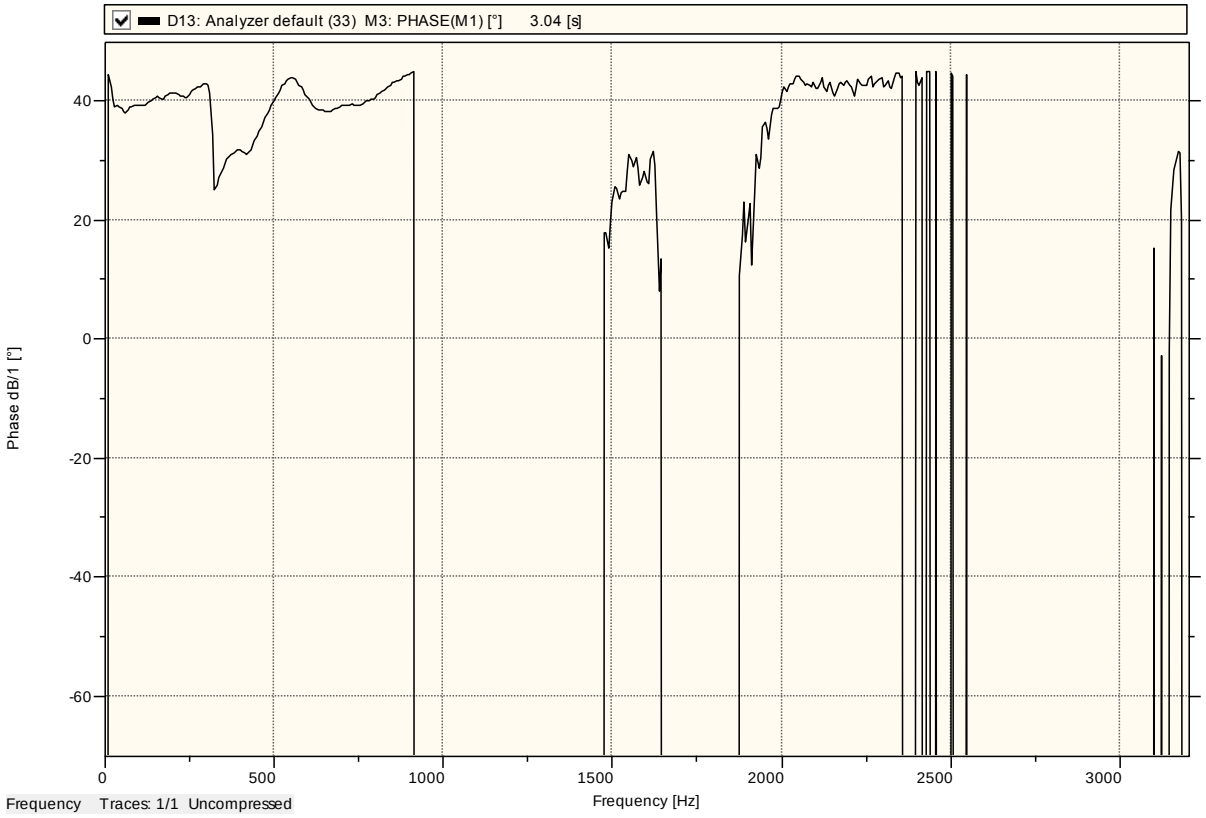

Figure 41 The phase plot of the FRF for sample 4

These calculated natural frequencies have been used to calculate the modulus of elasticity for the sample. The calculated modulus of elasticity for each mode has been presented in Table 14.

Table 14 Measured natural frequencies and calculated modulus of elasticity for sample 4

Mode	Natural Frequency (Hz)	Modulus of Elasticity (GPa)
1	310	0.46
2	940	0.56
3	1375	0.31

These results presented in Table 14 are similar to the calculated results for sample 3. While this shows that the expected results are not being obtained, it also suggests that the same problem exists in both of these two tests. This gives weight to the theory that the errors in the testing are being caused by the weight of the accelerometer and the chord on the sandwich panel having a large effect on the natural frequency being recorded and are not due to poor hitting.

5.3.5 Sandwich Panel Sample 5 – 20mm Sample with Fibreglass skins

Figure 42 shows the measured frequency response for a number of tests using a sample bandwidth of 6400 Hz. Similar to previous tests a few of the initial natural frequencies can be identified, however the majority of the graph is too noisy to identify any natural frequencies.

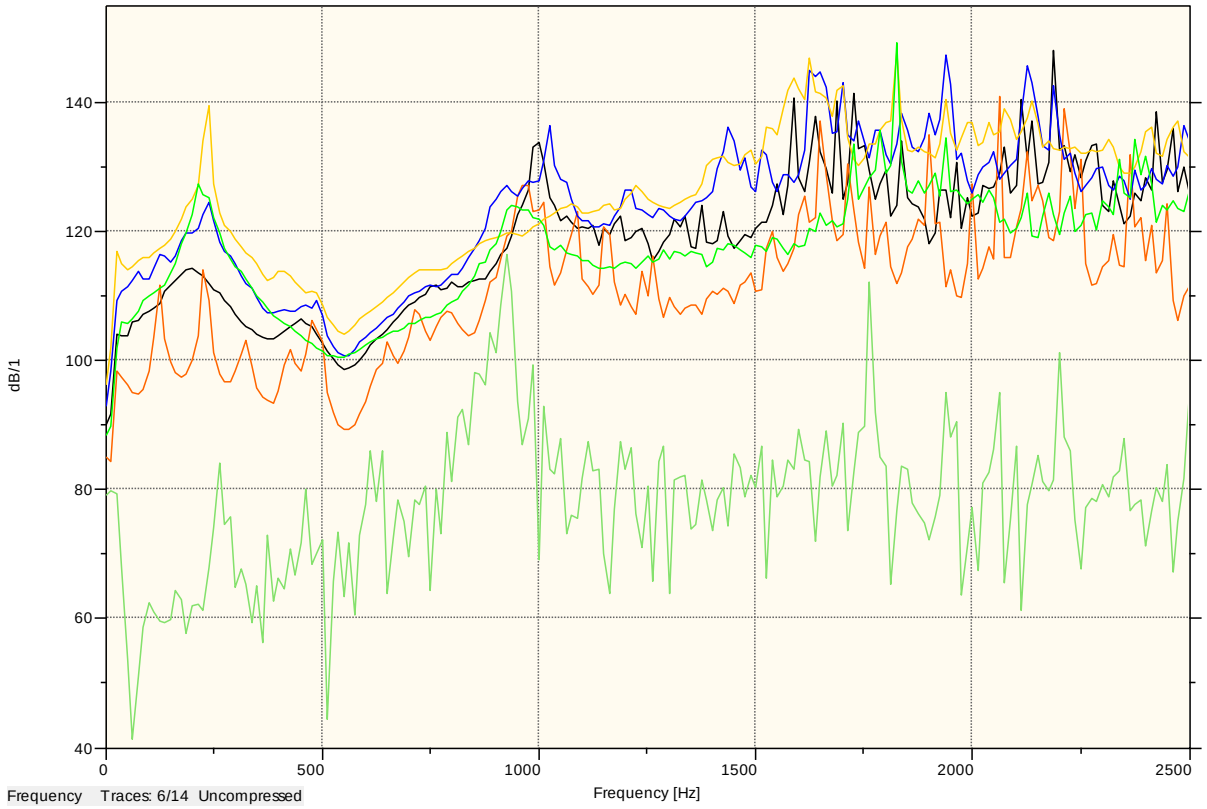

Figure 42 Frequency Response Function for sandwich panel 5 over a sample bandwidth of 6400 Hz. The first natural frequency can be easily seen, others not excited at all

The sample bandwidth was then changed to 3200 Hz and a number of tests were performed. The results of these tests have been presented in the frequency response function in Figure 43. The first natural frequency is not very well defined but occurs somewhere around the 325 Hz mark. The second natural frequency is quite distinct in all of the traces and occurs at approximately 925 Hz. The blue trace then shows a distinct peak fairly close to this second natural frequency at around 1200 Hz. This has been assumed to be a natural frequency corresponding to a torsional mode of vibration. After these two initial peaks, the function becomes very noisy and it becomes difficult to identify any more natural frequencies. Only the blue trace shows another distinct peak at around 1500 Hz which may correspond to a natural frequency of the material, but is not expected to be a bending natural frequency. The

phase plot has changes in phase corresponding to the identified peaks, which adds to the certainty that these are natural frequencies of the system, however once again the phase plot does not have the expected shape.

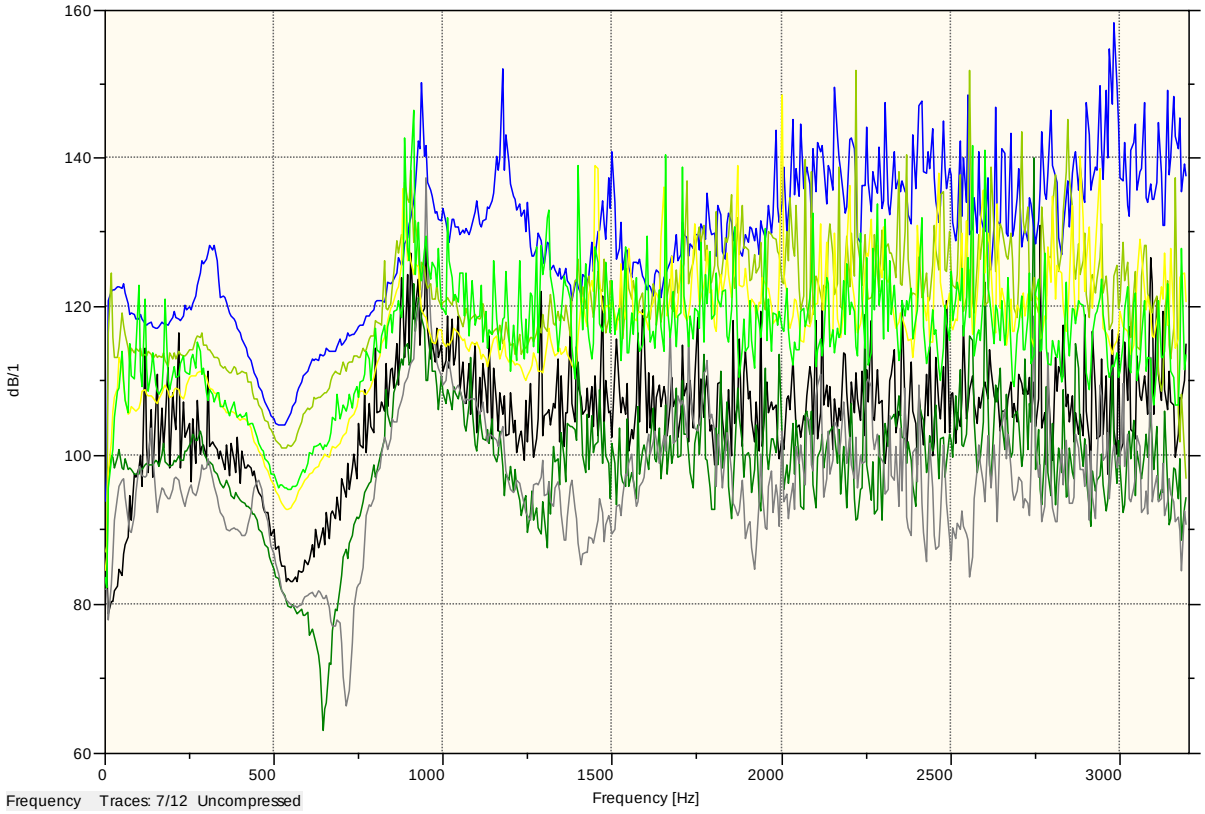

Figure 43 Frequency Response Function for sandwich panel 5 over a sample bandwidth of 3200 Hz

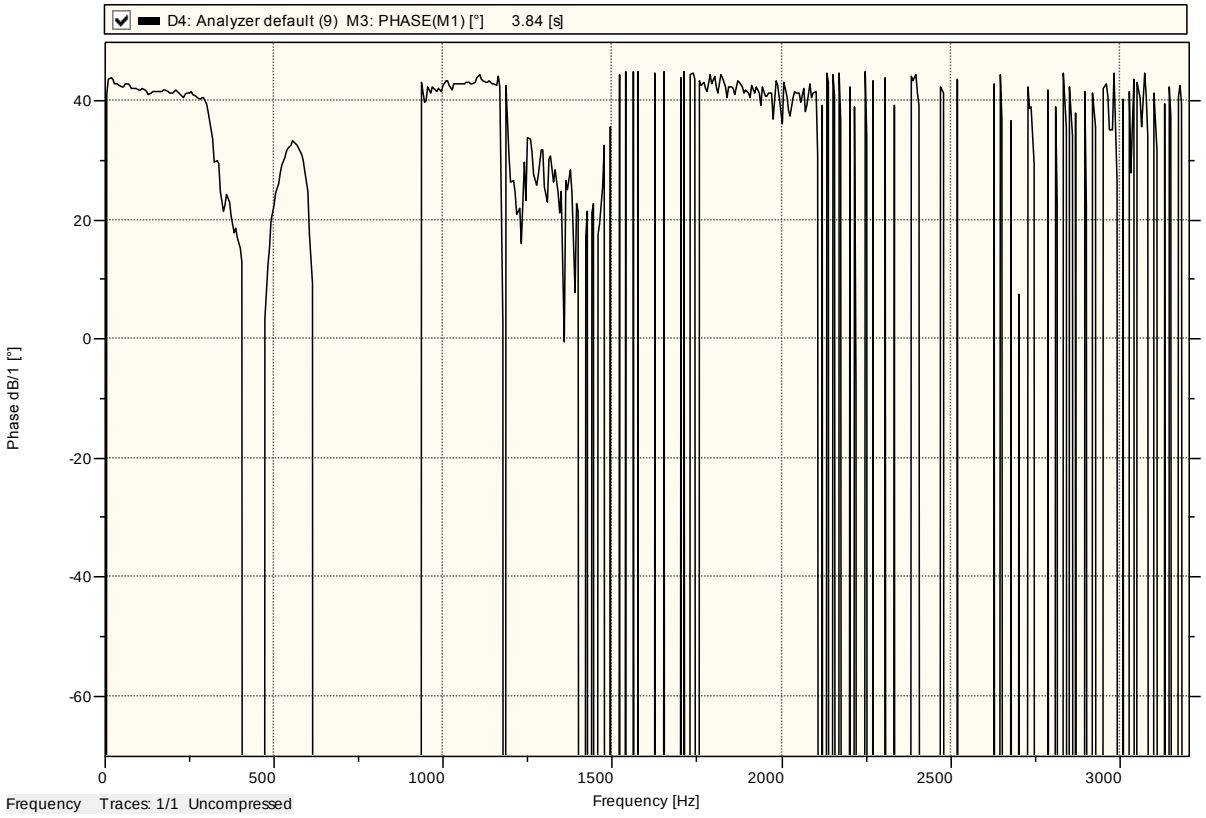

Figure 44 The phase plot of the FRF for sample 5

Table 15 Measured natural frequencies and calculated modulus of elasticity for sample 5

Mode	Natural Frequency (Hz)	Modulus of Elasticity (GPa)
1	325	0.92
2	925	0.98

The modulus of elasticity for the two modes of vibration has been found to be 920 MPa and 980 MPa. This is once again considerably lower than the value which was expected.

5.3.6 Sandwich Panel 6 – 20mm sample with fibreglass skins

Figure 45 shows the measured frequency response for sample 6, which is the second of the 20mm thick sample with fibreglass skins. This test was carried out over a sample bandwidth of 3200 Hz.

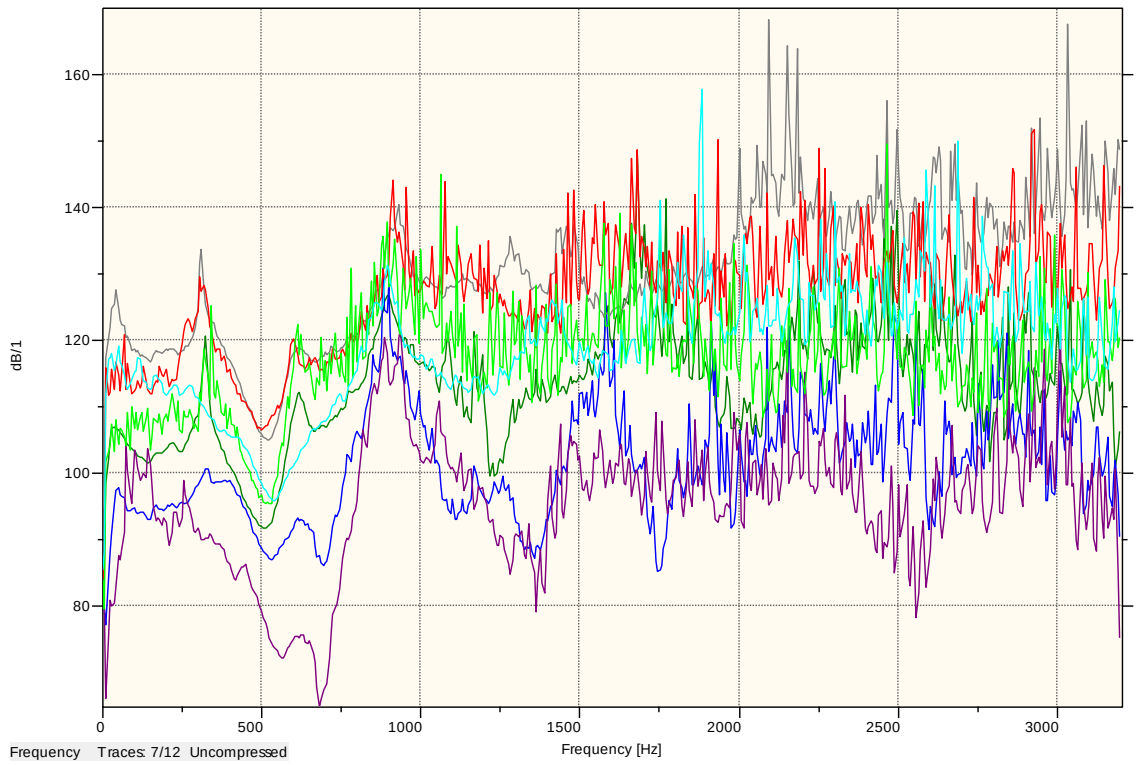

Figure 45 Frequency Response Function for sandwich panel 6 over a sample bandwidth of 3200 Hz.

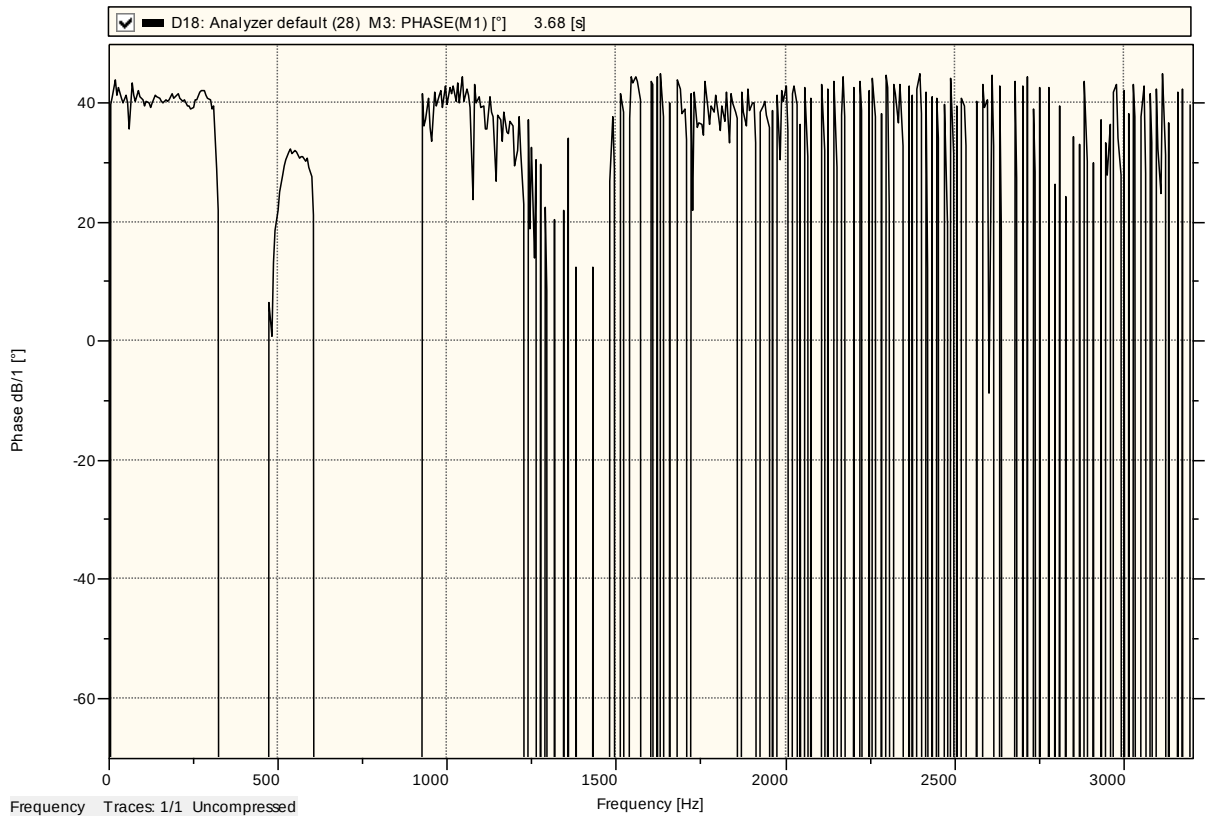

Figure 46 The phase plot of the FRF for sample 6

The first natural frequency has been identified at about 325 Hz, and this is consistent with the majority of the tests undertaken, however it has failed to be excited in a couple of the tests. There is then a small peak at about the 600 Hz mark, however this is not thought to be a natural frequency of the system. The second natural frequency of the system has been identified at approximately 900 Hz, and this has been very well excited in both the green and purple traces. It is once again fairly difficult to identify the third natural frequency of the system as the traces become quite noisy. Only the blue trace displays a distinct third peak at approximately 1650 Hz. The phase plot once again has changes of phase which correspond to the peaks identified in the frequency response graph, which suggests these are natural frequencies of the system.

Table 16 Measured natural frequencies and calculated modulus of elasticity for sample 6

Mode	Natural Frequency (Hz)	Modulus of Elasticity (GPa)
1	325	0.9
2	900	0.91
3	1650	0.8

Table 16 shows the average natural frequency taken from the graph, and the corresponding modulus of elasticity which has been calculated. The modulus of elasticity calculated from the three different modes give fairly consistent results of around 900 MPa. While this is once again considerably lower than the expected modulus of elasticity, it is very close to the measured modulus of elasticity for the geometrically similar sample 5. This suggests that the natural frequencies being measured are indeed natural frequencies of the system, however due to the weight of the accelerometer and possibly the tension in the chord, this has a considerable effect on the system and we are unable to identify the modulus of elasticity as was expected using the normal free-free conditions.

5.3.7 Sandwich Panel 7 – 40mm Sandwich Panel with Fibreglass skins

Initially sample 7 was tested with a sample bandwidth of 6400 Hz and the measured frequency response for these tests has been presented in Figure 47. It is difficult to identify any peaks in this graph, however it looks like there may be one around the 1250 Hz mark.

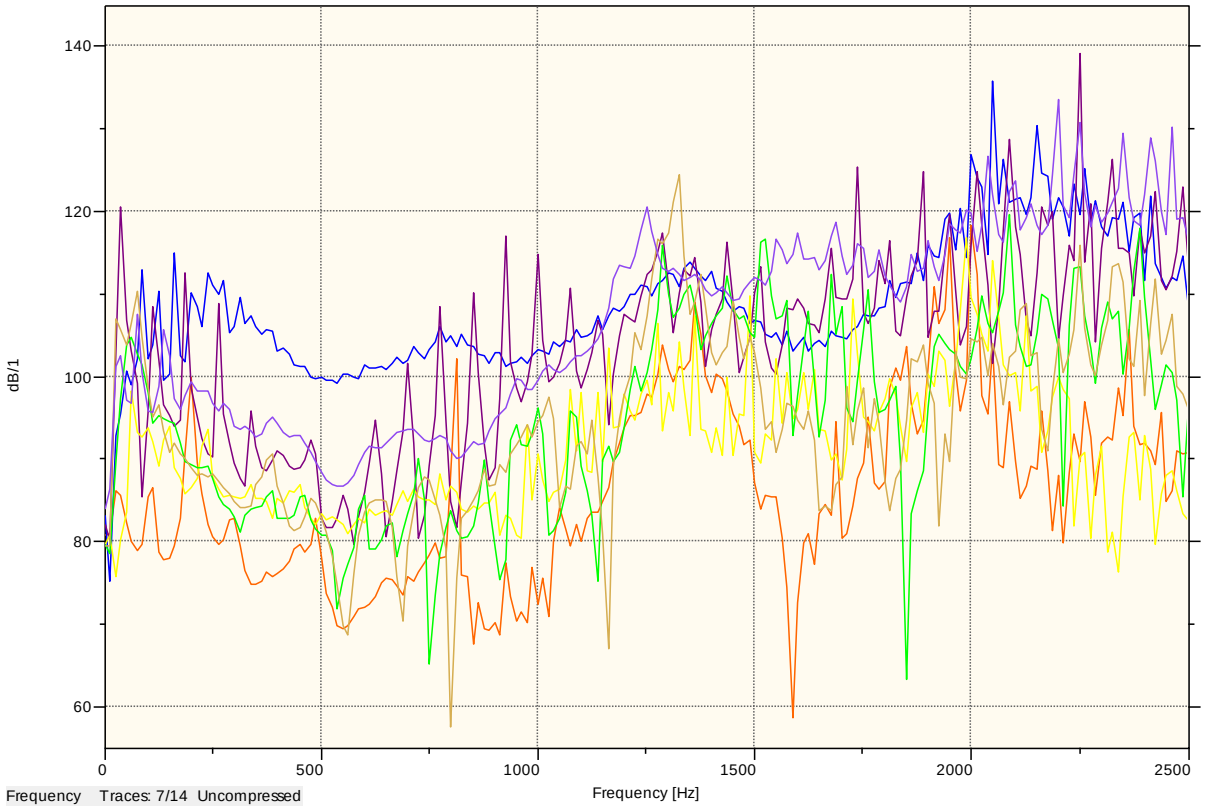

Figure 47 Frequency Response Function of sandwich panel 7 over a sample bandwidth of 6400 Hz. Only one natural frequency can be seen easily.

The sandwich panel was then tested using a sample bandwidth of 3200 Hz to improve the results and the measured frequency response has been presented in Figure 48. The first mode has been well excited, with the peak at around 300 Hz being consistently excited across all of the tests. There is then a small peak at around 600 Hz similar to that being excited in some of the other sandwich panels, however this has once again not been taken as a bending natural frequency. The second natural frequency has been excited between 850 Hz and 1100 Hz, and the peak varies across this range between tests. The average of these peaks has been calculated and the second natural frequency has been estimated to be at 1000 Hz. After this it is difficult to identify where the next peak is located, as the different tests have peaks in very different positions. The phase plot has again been included

in Figure 49 despite it having an unexpected range. However there are still changes in phase which correspond to the peaks which have been identified in Figure 48. The natural frequencies which have been estimated from Figure 48 and the corresponding modulus of elasticity for each mode have been presented in Table 17.

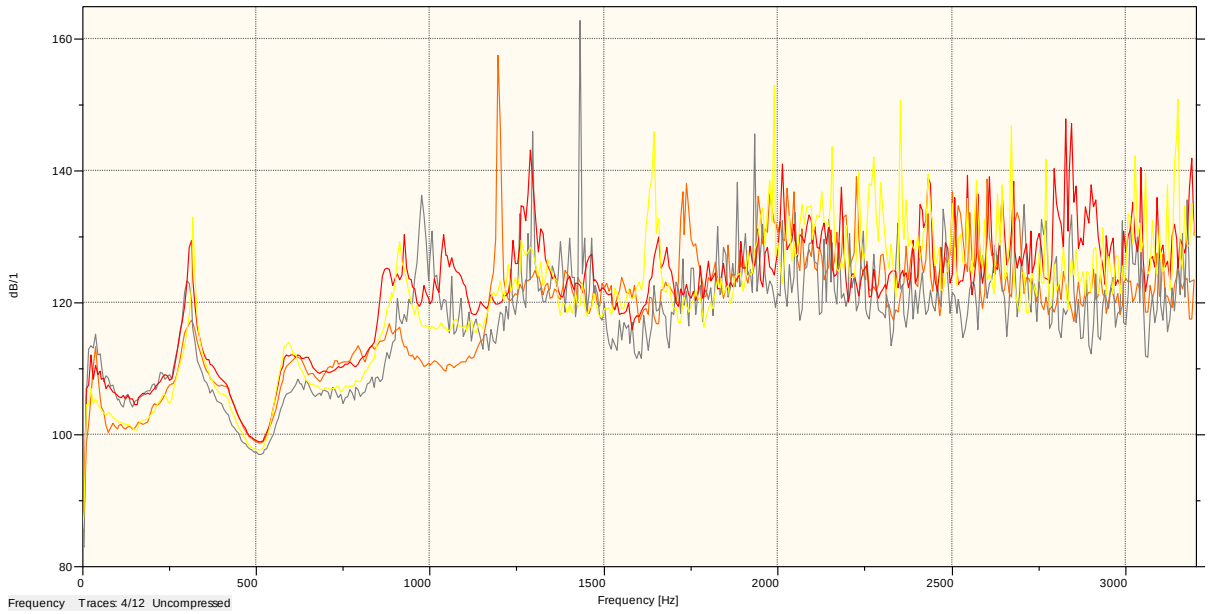

Figure 48 Frequency Response Function for sandwich panel 7 over a sample bandwidth of 3200 Hz.

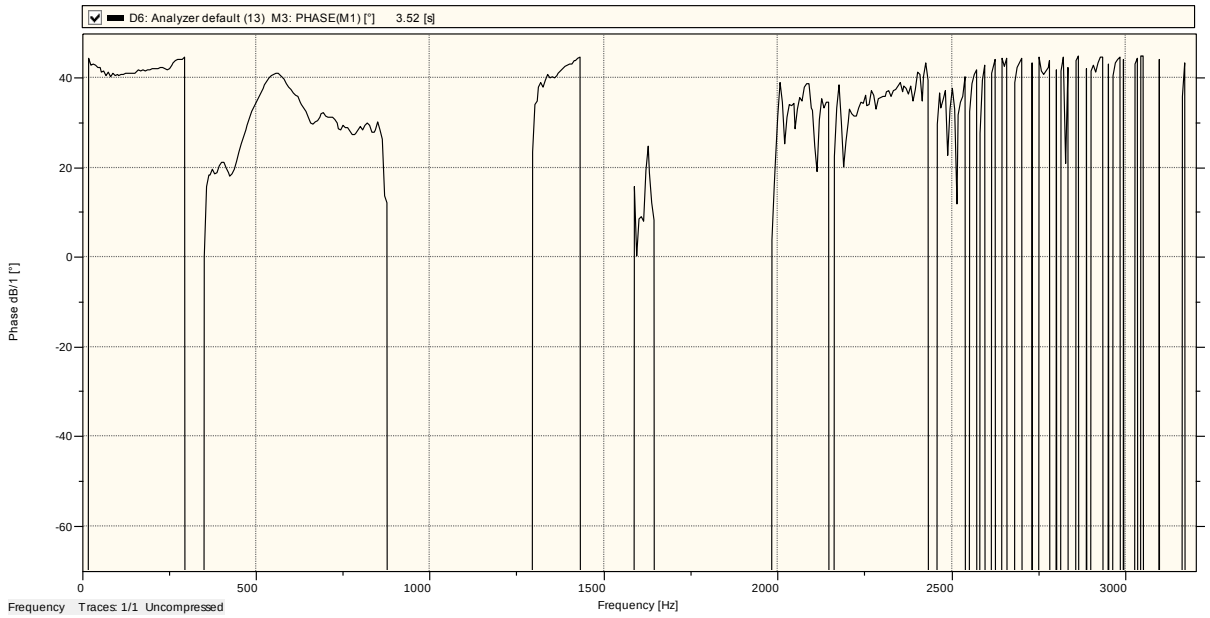

Figure 49 The phase plot of the FRF for sample 7

Table 17 Identified natural frequencies and calculated modulus of elasticity for sample 7

Mode	Natural Frequency (Hz)	Modulus of Elasticity (GPa)
1	300	0.26
2	1000	0.38

The modulus of elasticity for sample 7 has been calculated as ranging from 260 MPa to 380 MPa. The modulus of elasticity calculated for the three similar samples in the four point bending test was calculated as approximately 39 GPa. Once again the values calculated using Euler's equation for beams are considerably lower than those which were expected.

5.3.8 Sample 8 – 40mm Sample with fibreglass skins

Figure 50 shows the traces for sample 8 when tested over a sample bandwidth of 3200 Hz. The first natural frequency is not very distinct, however if the peaks from the green trace and the purple trace are taken these are fairly close. If these are taken as the first mode of vibration there is a natural frequency at around 200 Hz. There is then a small peak at around 700 Hz which is quite distinct in the blue trace but this is not really excited in the other traces. There is then a peak which is well excited at about 1300 Hz, however these differ over a range between tests.

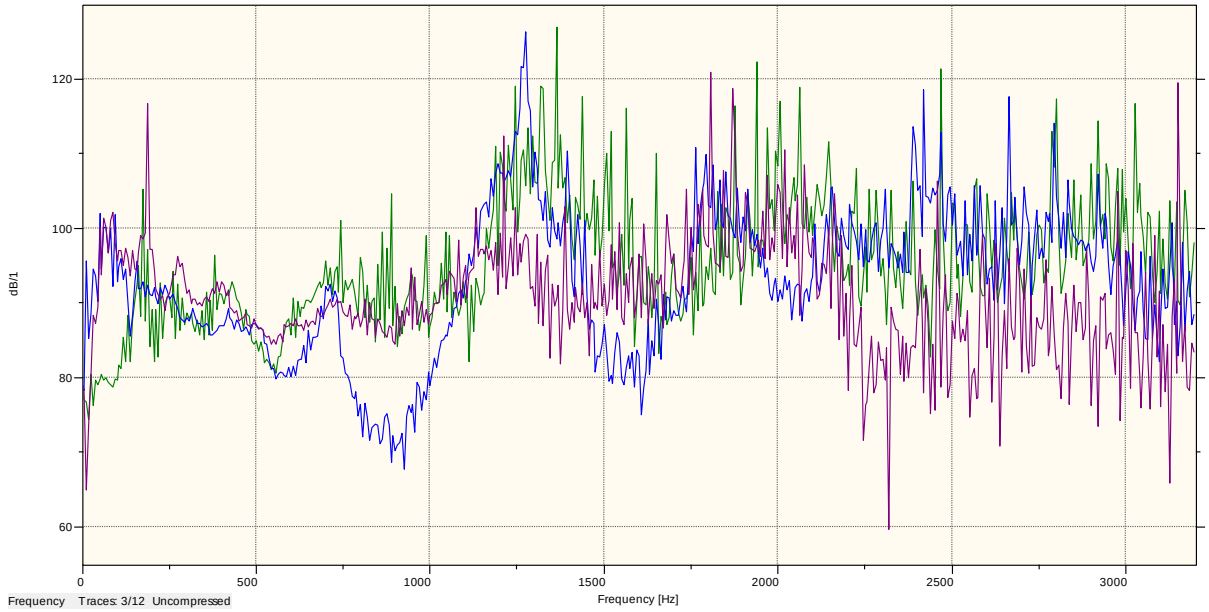

Figure 50 Frequency Response Function for sandwich panel 8 over a sample bandwidth of 3200 Hz.

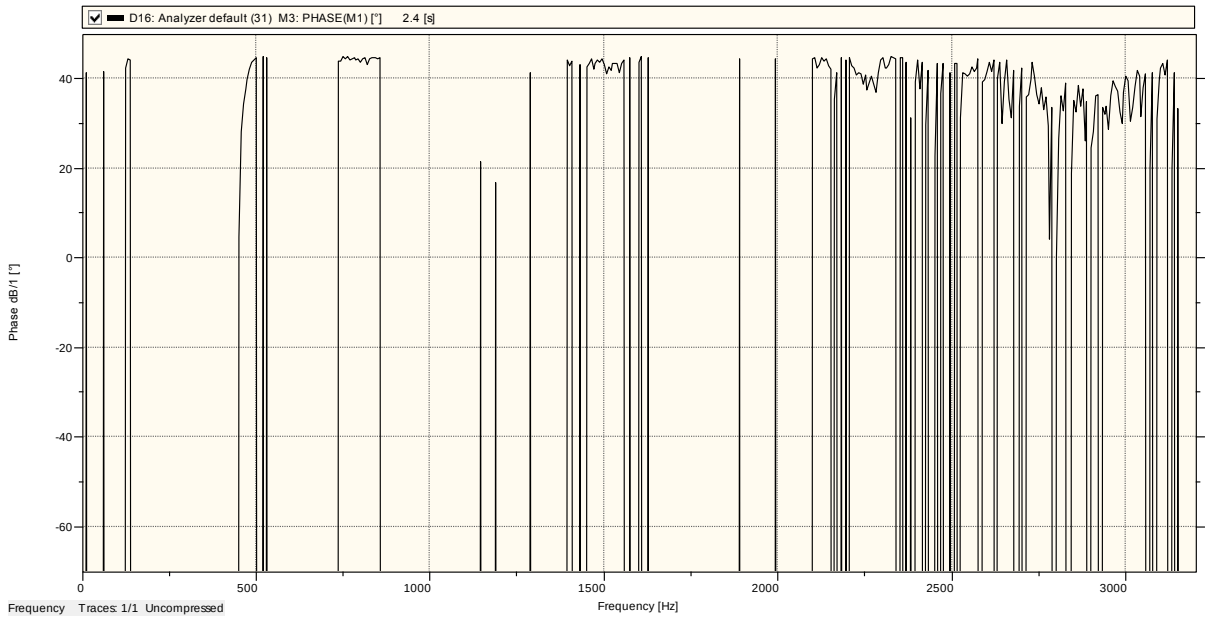

Figure 51 The phase plot of the FRF for sample 8

There is another group of tests which have peaks at different frequencies to those displayed in Figure 50. These traces are presented in Figure 52. It can be seen in Figure 52 that the first peak corresponding to a natural frequency occurs at approximately 400 to 500 Hz. This has been taken as 400 Hz. The second natural frequency has been excited quite well in both peaks and occurs at about 1200 Hz. The third natural frequency has not been excited in this test.

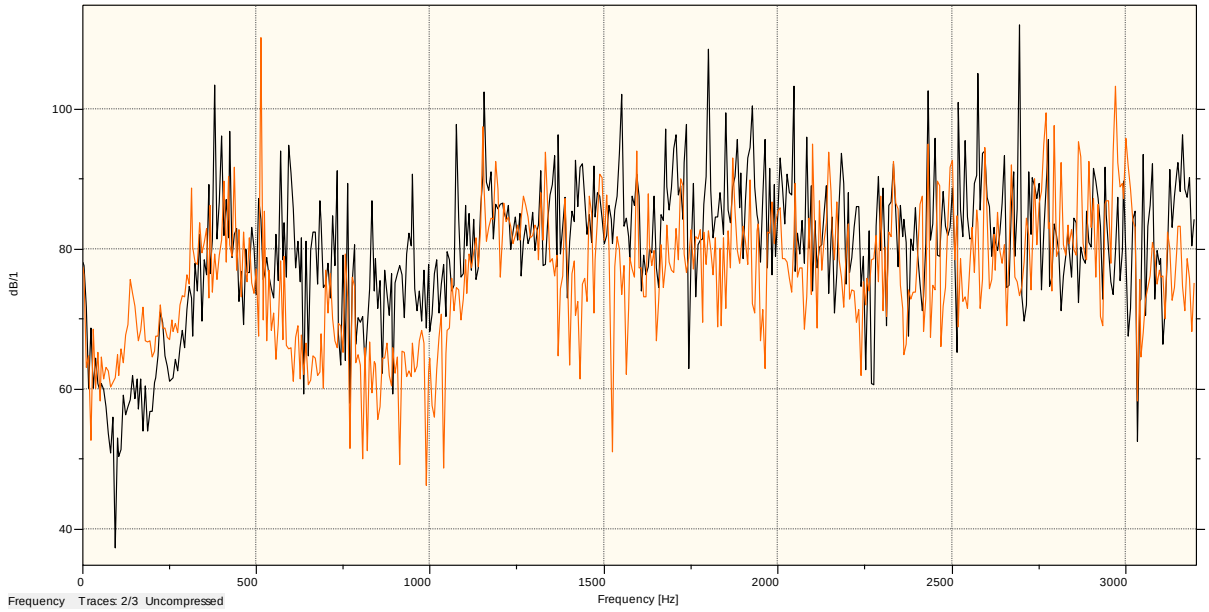

Figure 52 Alternate Frequency Response Function for sandwich panel 8 over a sample bandwidth of 3200 Hz.

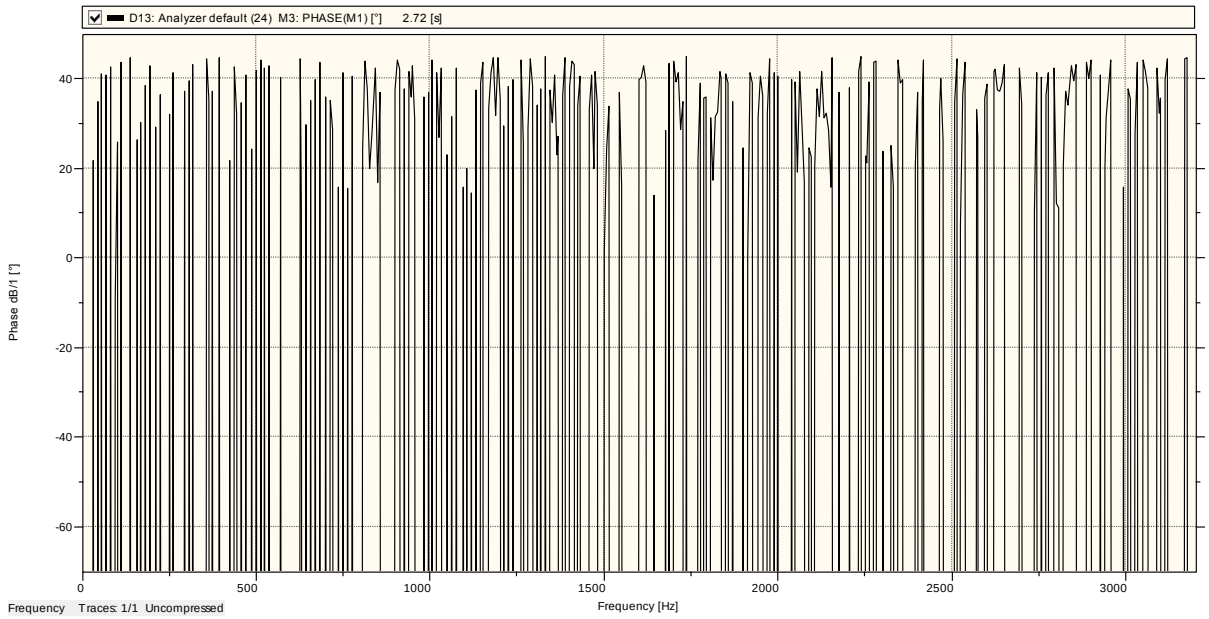

Figure 53 The phase plot of the FRF for sample 8

Table 18 Measured natural frequencies and calculated modulus of elasticity for sample 8

Mode 1	Figure 50		Figure 52	
	Natural Frequency (Hz)	Modulus of Elasticity (GPa)	Natural Frequency (Hz)	Modulus of Elasticity (GPa)
1	200	0.12	400	0.61
2	1300	0.67	1200	0.57

The fact that the modulus of elasticity calculated from the two different modes in Figure 52 are a lot closer than those derived from Figure 50 suggests that the traces in Figure 52 are more accurate representations of the frequency response function for the system. It is unclear what has caused the errors being obtained for the traces in Figure 50, however it is probably once again due to the weight of the accelerometer and the position of the chord connecting the accelerometer to the frontend system. Due to the lightweight of the sandwich panels this has the potential to have a large effect on the measured response. Poor hitting technique may also have contributed to these large errors being measured or quite simply poor impact as was the case for the different responses measured for sample 2.

5.4 Dynamic characterisation of honeycomb cores

5.4.1 Sample 9 – 40mm Nida core with no skins

The Nida core with no skins was the most difficult to excite due to the high damping properties of the material. Using the super soft red tip to excite the system produced the best results and the extender was used to impart more energy on the system. The extender works by adding more mass to the head of the hammer, and as force is a function of mass and acceleration, by increasing the mass of the head a greater impact force can be exerted on the sample. A sample bandwidth of 2000 Hz has been used as the natural frequency for this material was expected to be considerable lower than the sandwich panels or steel.

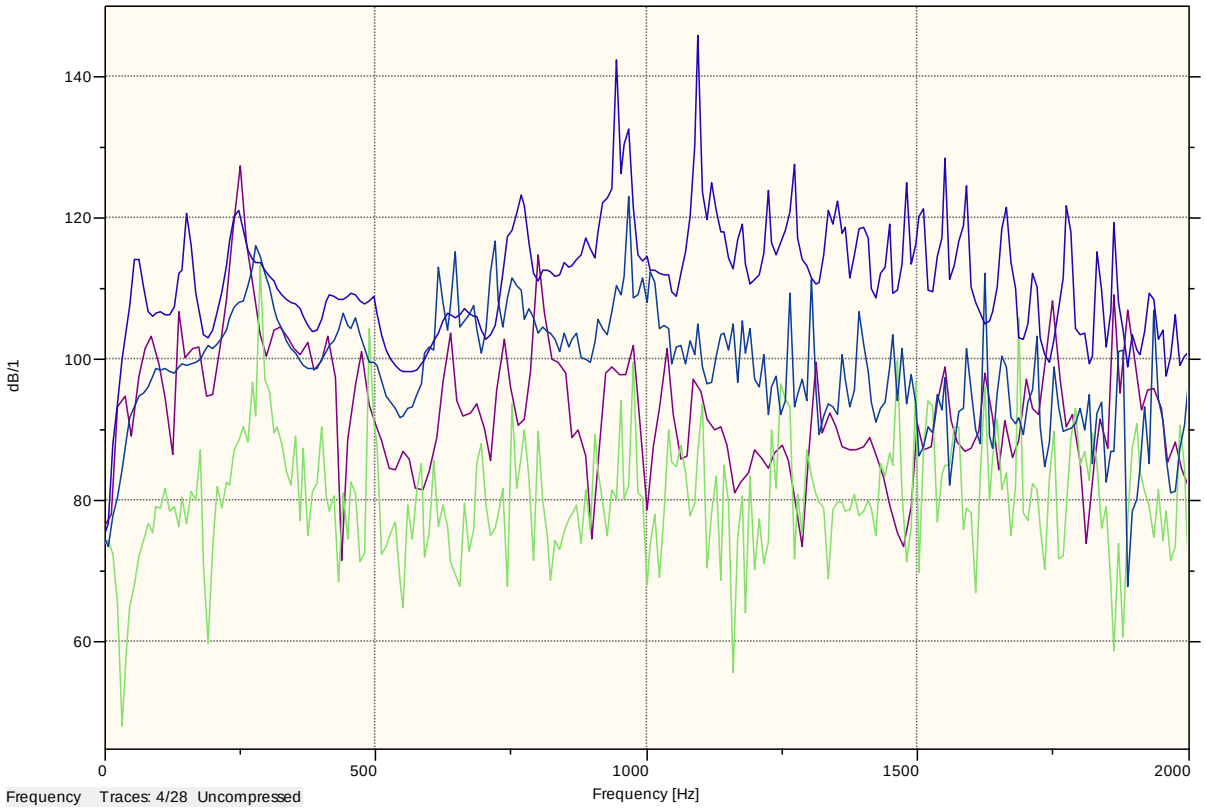

Figure 54 Frequency Response Function for Nida core sample 9 over a sample bandwidth of 2000 Hz.

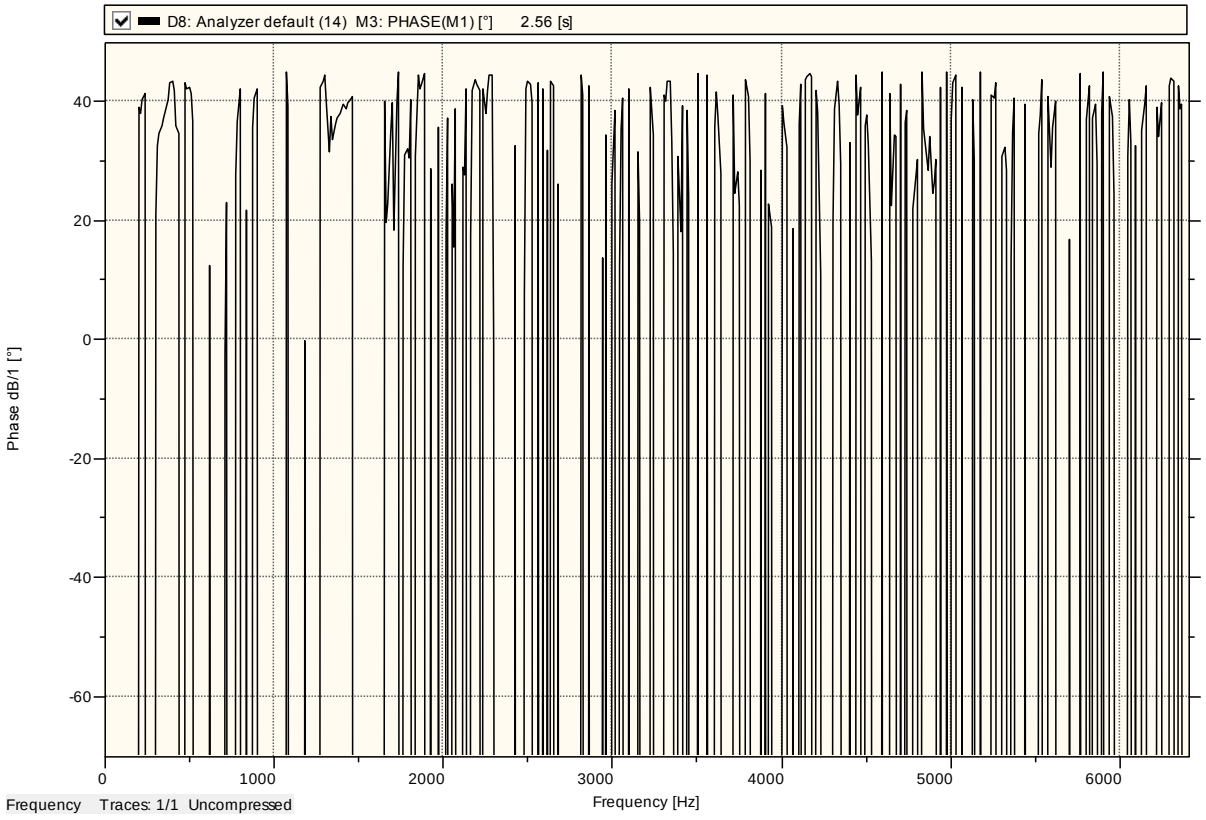

Figure 55 The phase plot of the FRF for sample 9

The measured frequency response has been presented in Figure 54. The first recorded peak occurs at approximately 275 Hz, and has been excited by all of the tests. It is considerably harder to identify the second peak as it is not distinct and the peaks occur at different locations for each trace. The average of all the traces was taken and the second natural frequency has been estimated to be at approximately 900 Hz. The blue trace then has a distinct peak at around 1100 Hz. This peak has not been excited in any of the other traces, and it was assumed that this peak corresponds to a torsional natural frequency. This was tested by shifting the accelerometer to the corner of the sample and exciting the sample at the corner. This peak was then excited very well which means it is probably a torsional natural frequency. After these peaks it is difficult to identify any distinct peaks.

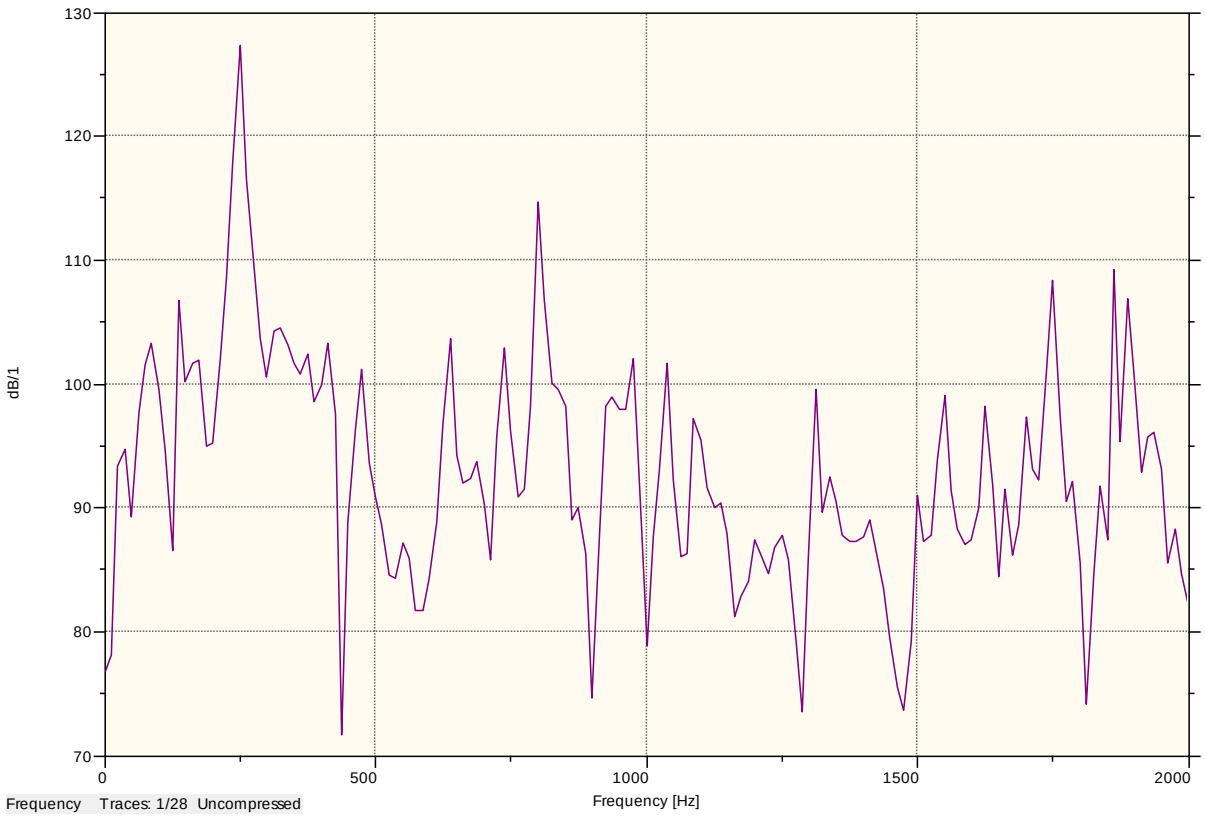

Figure 56 Frequency Response Function for 0ne trace of Nida core sample 9 over a sample bandwidth of 2000 Hz.

It was noticed that the third resonant frequency had been excited in one of the traces. This trace has therefore been graphed separately in Figure 56. When looking at this trace on its own the natural frequencies are in slightly different positions to those

when taking the average of the multiple traces. The first peak identified in Figure 56 can be seen at 250 Hz. The second peak is also very distinct and can be seen at the frequency of 800 Hz. The third peak is harder to locate, however due to the shape and position of the peak, the third natural frequency has been estimated to be the peak at 1300 Hz. Table 19 shows the natural frequencies identified for both Figure 54 and Figure 56, and the modulus of elasticity calculated for each of the modes of vibration.

Table 19 Measured natural frequencies and calculated modulus of elasticity for sample 9

Mode	Figure 54		Figure 56	
	Natural Frequency (Hz)	Modulus of Elasticity (GPa)	Natural Frequency (Hz)	Modulus of Elasticity (GPa)
1	275	0.01	250	0.01
2	900	0.02	800	0.02
3			1300	0.01

The calculated modulus of elasticity for sample 9 ranges from 10 to 20 MPa. The technical document for H8HP honeycomb core supplied by the manufacturer states that the core has a compressive modulus of 50 MPa. (Nidacore 2010) While this is not necessarily the answer for the bending modulus there is no other data available on what the bending modulus of the material is. If it is assumed that the compressive modulus is equal to the bending modulus then the recorded results are a lot closer to the expected results for the core with no skin than those for the sandwich panels. However the measured modulus of 10 to 20 MPa is still not very close to the expected modulus of 50 MPa. There are a number of reasons that may have caused these results to differ so much from the expected results. The first is the weight of the accelerometer in comparison to the core which will have an even bigger effect on the lightweight core than on the sandwich panel. There was also a defect detected in the two core samples tested which also may have an effect on the natural frequency of the material.

5.4.2 Sample 10 – 40mm Nida core with no skins

Figure 57 shows a number of traces for the second sample of the 40mm Nida core with no skins. The initial peaks are thought to be caused by the elasticity of the poly wire. The first peak has been excited in three out of the four traces at about 275 Hz. The second peak varies between each trace, however as they are all around the 750 Hz mark the average has been taken, and this peak has been identified as 725 Hz. It is then difficult to detect a distinct third peak due to the fact that the traces vary so much. Figure 58 shows the phase plot of the frequency response function, and once again it does not have the expected range from -180 to +180. This may be a problem with using the software and should be investigated. Table 20 shows the calculated modulus of elasticity for each of the two modes identified, and it can be seen that there is good agreement between results.

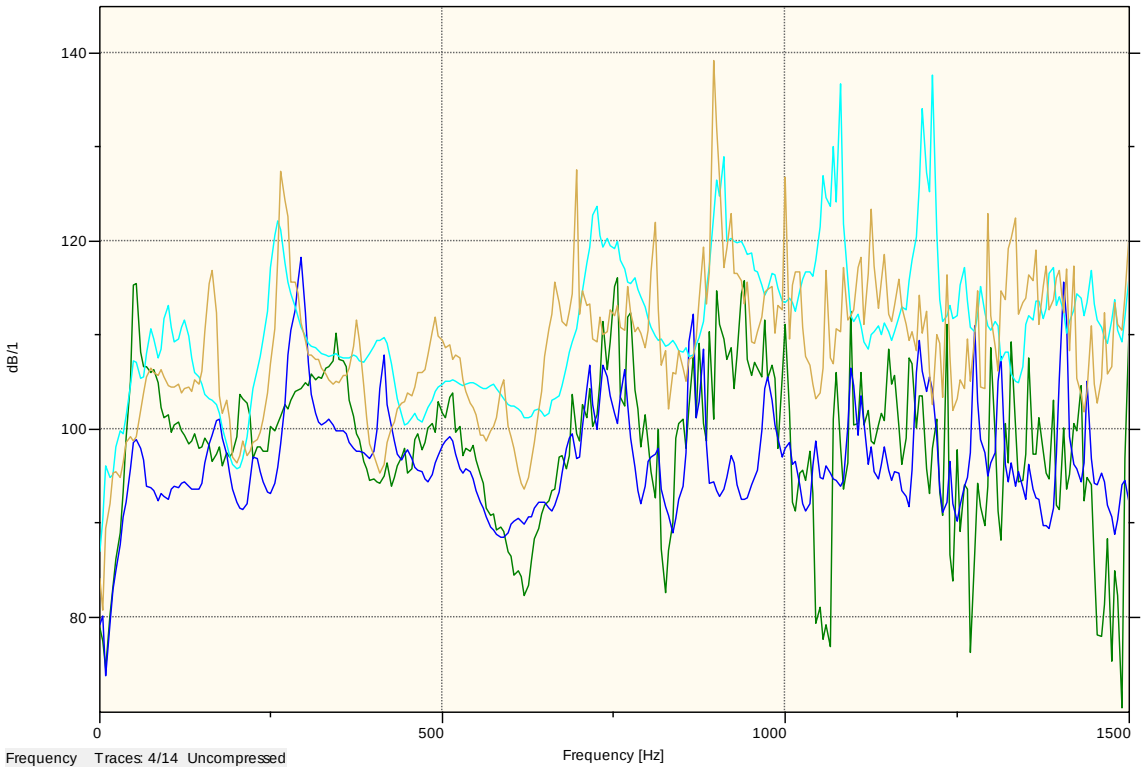

Figure 57 Frequency Response Function for Nida core sample 10 over a sample bandwidth of 2000 Hz.

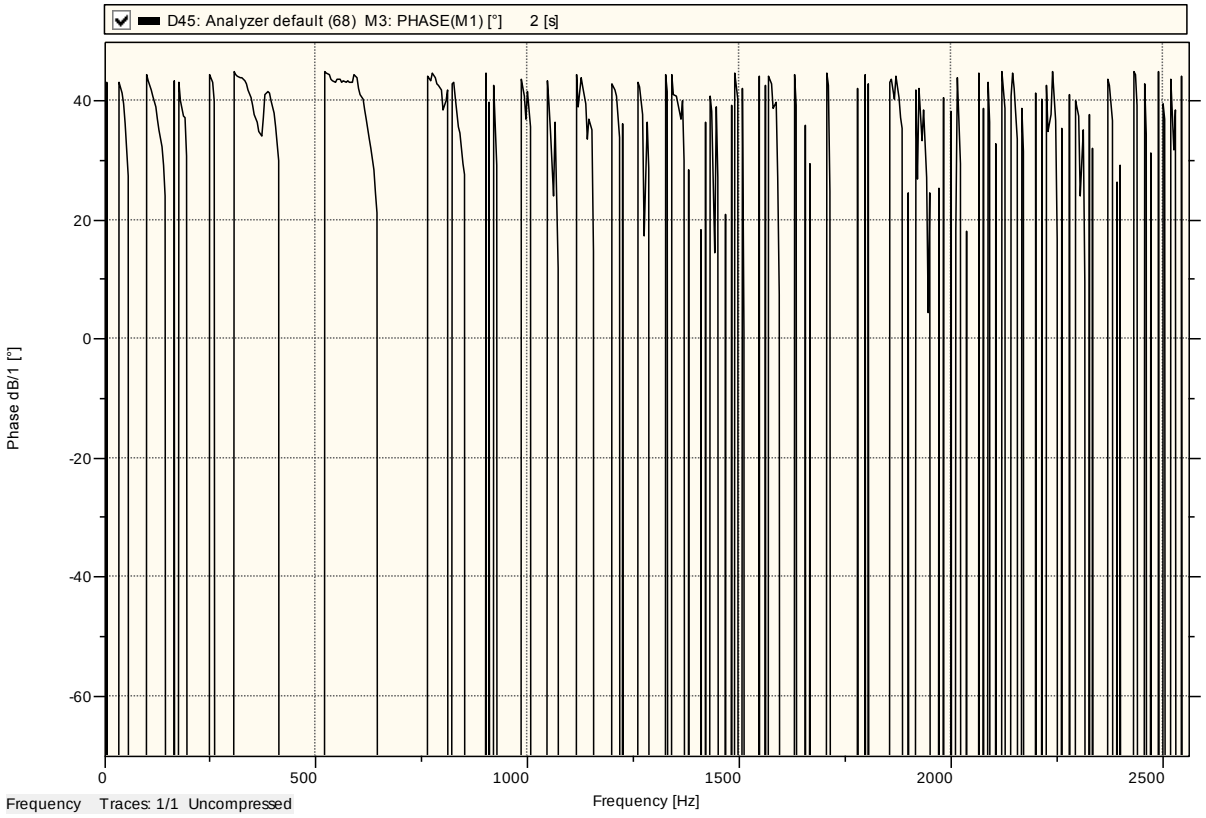

Figure 58 The phase plot of the FRF for sample 10

Table 20 Measured natural frequencies and calculated modulus of elasticity for sample 10

Mode	Natural Frequency (Hz)	Modulus of Elasticity (GPa)
1	275	0.01
2	725	0.01

The calculated modulus of elasticity for sample 10 is 10 MPa which is again similar to sample 9. This suggests that the natural frequency of the system has been successfully determined using this method, however, due to the weight of the accelerometer and potential tension in the chord attached to the accelerometer, the system being analysed is not an accurate free-free beam. Alterations need to be made to take into account the point load represented by the accelerometer, however this would prove to be quite complex. Another solution would be to use a measuring technique that eliminates this excess weight and contact with the material caused by the chord.

5.5 Alternate method of calculation

As a further check of the results the equation from the paper by Nilsson and Nilsson (2002) has also been used to check the results. These results have been presented in Table 21.

Table 21 Comparison of results using Euler's beam theory and Nilsson's equation

Sample Number	Modulus of Elasticity using Euler's Method (GPa)	Modulus of Elasticity using Nilsson's equation (GPa)
1	0.7	8.7
2	1	18
3	0.3	5.5
4	4	6
5	0.9	12
6	0.9	12
7	0.3	3
8	0.8	5.7

As can be seen this method gives a closer result to the expected result than the Euler's Method, however the results are still far lower than the expected modulus of elasticity. It was also planned to use Larsson's equation to find both the modulus of elasticity and the shear modulus, however as the modulus of elasticity has not been successfully identified this has not been completed.

5.6 Summary of Results

The results which have been obtained do not give very good results based on the results which were expected for the material which was tested. The main reason for this is assumed to be the weight of the accelerometer being used in comparison to the weight of the material. Better results would be achievable if non-contact measurements were able to be taken, such as using a laser vibrometer. By attaching the accelerometer to the beam this is essentially placing a point load on one end of the beam, which means that the assumed boundary conditions are not accurate.

The short lengths of the beam have made it difficult to pick up the natural frequencies. It can be seen from the results for the steel samples that it is considerably easier to test a longer sample as it has lower natural frequencies. This is especially true for the sandwich panels and honeycomb cores because due to their high damping properties it is very difficult to excite the higher natural frequencies.

The shape of the FFT for the hitting technique is not what was expected. In addition to this the shapes of the FRF and phase plots were also not what were expected. This may be an issue with the software, or may simply be caused by poor hitting technique. The FRF graphs were also very noisy which has lowered the level of confidence in the results being correct. The settings being used may need to be altered to achieve better results. Other methods such as windowing and the use of a signal conditioner may also aid in achieving better results.

6. Conclusion

The aim of this project set out to successfully identify the natural frequencies of the beams and use these to characterise the out-of-plane properties of the material. This involved conducting an impact hammer test to produce the frequency response functions for the material to determine the natural frequencies. These were then substituted into Euler's beam theory to calculate the modulus of elasticity for the material.

It has been proven that the modulus of elasticity for steel can be successfully determined using Euler's beam theory and the natural frequencies which have been obtained from a dynamic test with free-free boundary conditions. It has however been more difficult to successfully calculate the modulus of elasticity for sandwich panels or honeycomb cores using this method. The measured results for the sandwich panels and honeycomb cores were all considerably lower than the expected results based on the four point bending tests. The reason for this is expected to be due to the weight of the accelerometer as well as the effect of the chord attached to the accelerometer and the effect that these inconsistencies have on the vibration of the system.

The modulus of elasticity and shear modulus have been successfully calculated from the four point bending test for 40 mm Nida-core samples with both aluminium and fibreglass skins. These values have been checked against values in the literature and appear to be the expected values.

In conclusion it has been found that this method using the apparatus discussed is not suitable for performing dynamic characterisation of sandwich panels. A non-contact measuring technique should be used to record the vibration of sandwich panels and cellular cores due to their low mass density of the core material.

7. Future Work

As has been previously mentioned the main issue with this experiment has been the weight and contact of the accelerometer on the relatively light samples of nida-core and sandwich panels. With this in mind the experiment should be repeated using a non-contact form of measurement such as a laser vibrometer. When this is done longer samples of the sandwich panel and core material should be used as these will have lower natural frequencies which will be more easily excited.

8. References

'Advanced FRF based determination of structural inertia properties', *LMS International*, <http://www.lmsintl.com/advanced-FRF-based-determination-structural-inertia-properties>

ASTM 2011, C273 Standard Test Method for Shear Properties of Sandwich Core Materials, ASTM International.

ASTM C393 / C393M - 11e1, 2012, ASTM International, viewed 10th October, <http://www.astm.org/Standards/C393.htm>.

Gibson, RF 2000, 'Modal vibration response measurements for characterization of composite materials and structures', *Composites Science and Technology*, vol. 60, pp. 2769 - 80,

Larsson, P-O 1991, 'Determination of Young's and shear Moduli from flexural vibrations of beams', *Journal of Sound and Vibration*, vol. 146, no. 1, pp. 111-23,

Martinez-Agirre, ME, M.J. 2011, 'Dynamic characterisation of high-damping viscoelastic materials from vibration test data', *Journal of Sound and Vibration*, vol. 330, no. 3930-3943,

Model 086C04 SPECS 086C04 SERIES Installation and Operating Manual, 2010, PCB Piezotronics, Depew, United States. <http://www.pcb.com/contentstore/docs/PCB_Corporate/Vibration/products/Manuals/086C04.pdf>.

Mujika, F, Pujana, J & Olave, M 2011, 'On the determination of out-of-plane elastic properties of honeycomb sandwich panels', *Polymer Testing*, vol. 30, no. 2, pp. 222-8,

Nakamura, HM, K. Mutsuyoshi, H. and Suzukawa, K. 2007, *SHEAR DEFORMATION CHARACTERISTICS AND WEB-CRIPPLING OF NEW HYBRID COMPOSITE GIRDERS*, <http://www.iifc-hq.org/proceedings/APFIS_2007/Papers/V1-L3-APFIS-038-camera%20ready.pdf>.

Newland, DE 1993, *An introduction to random vibrations, spectral and wavelet analysis*, Third edn, Longman Scientific and Technical, Harlow.

Nidacore 2008, 'Nida core structural honeycomb materials, Rigid elastic technology',

Nidacore 2010, *Product Data Sheet: H8PP, H8HP*, Nidacore, Saint Lucie, <http://nida-core.com/pdfs/pds/nidacore/pds_H8PP-H11PP-8HP.pdf>.

Nilsson, EaN, A.C. 2002, 'Prediction and measurement of some dynamic properties of sandwich structures with honeycomb and foam cores', *Journal of Sound and Vibration*, vol. 251, no. 3, pp. 409-3,

Renault, AJ, L. & Sgard, F 2011, 'Characterization of elastic parameters of acoustical porous materials from beam bending vibrations', *Journal of Sound and Vibration*, vol. 330, pp. 1950-63,

Sadowski, T & Bęc, J 2011, 'Effective properties for sandwich plates with aluminium foil honeycomb core and polymer foam filling – Static and dynamic response', *Computational Materials Science*, vol. 50, no. 4, pp. 1269-75,

Schwingshackl, CW, Aglietti, GS & Cunningham, PR 2006, 'Determination of Honeycomb Material Properties: Existing Theories and an Alternative Dynamic Approach', *JOURNAL OF AEROSPACE ENGINEERING*, pp. 177-83,

Thompson, WT 1988, *Theory of Vibration with applications, Third Edition*, Prentice Hall, Englewood Cliffs.

Young, WC 1989, *ROARK'S Formulas for Stress & Strain 6th Edition*, McGraw Hill, Singapore.

Zenkert, D 1997, *Sandwich Construction*, EMAS Publishing, Worcestershire.

Appendix A

University of Southern Queensland

FACULTY OF ENGINEERING AND SURVEYING

ENG4111/4111 Research Project

PROJECT SPECIFICATION

FOR: HAYDN O'LEARY

TOPIC: DYNAMIC CHARACTERISATION OF CELLULAR CORES AND SANDWICH PANELS

SUPERVISOR: Dr. Sourish Banerjee

PROJECT AIM: This project seeks to determine the natural frequencies for cellular cores and sandwich panels, in an attempt to characterise their dynamic behaviour and calculate their elastic properties.

PROGRAMME: **Issue A, 21st March 2012**

1. Research the background information relating to the cellular cores and sandwich panels, and the dynamic characterisation of materials
2. Measure the out-of-plane dynamic properties of polymeric honeycomb and foam core materials
3. Measure dynamic characteristics of sandwich panels
4. Characterise the dynamic behaviour and calculate the elastic properties
5. Conduct four point bending test on sandwich panels.
6. Compare the results from dynamic test and four point bending test.

AGREED:

_____(Student)

_____(Examiner)

___ / ___ / ___ ___ / ___ / __